8

Model Evaluation

Co-ordinating Lead Author
B.J. McAvaney

Lead Authors
C. Covey, S. Joussaume, V. Kattsov, A. Kitoh, W. Ogana, A.J. Pitman, A.J. Weaver, R.A. Wood, Z.-C. Zhao

Contributing Authors
K. AchutaRao, A. Arking, A. Barnston, R. Betts, C. Bitz, G. Boer, P. Braconnot, A. Broccoli, F. Bryan, M. Claussen, R. Colman, P. Delecluse, A. Del Genio, K. Dixon, P. Duffy, L. Dümenil, M. England, T. Fichefet, G. Flato, J.C. Fyfe, N. Gedney, P. Gent, C. Genthon, J. Gregory, E. Guilyardi, S. Harrison, N. Hasegawa, G. Holland, M. Holland, Y. Jia, P.D. Jones, M. Kageyama, D. Keith, K. Kodera, J. Kutzbach, S. Lambert, S. Legutke, G. Madec, S. Maeda, M.E. Mann, G. Meehl, I. Mokhov, T. Motoi, T. Phillips, J. Polcher, G.L. Potter, V. Pope, C. Prentice, G. Roff, F. Semazzi, P. Sellers, D.J. Stensrud, T. Stockdale, R. Stouffer, K.E. Taylor, K. Trenberth, R. Tol, J. Walsh, M. Wild, D. Williamson, S.-P. Xie, X.-H. Zhang, F. Zwiers

Review Editors
Y. Qian, J. Stone

Contents

Executive Summary

This chapter evaluates the suitability of models (in particular coupled atmosphere-ocean general circulation models) for use in climate change projection and in detection and attribution studies. We concentrate on the variables and time-scales that are important for this task. Models are evaluated against observations and differences between models are explored using information from a number of systematic model intercomparisons. Even if a model is assessed as performing credibly when simulating the present climate, this does not necessarily guarantee that the response to a perturbation remains credible. Therefore, we also assess the performance of the models in simulating the climate over the 20th century and for selected palaeoclimates. Incremental improvements in the performance of coupled models have occurred since the IPCC WGI Second Assessment Report (IPCC, 1996) (hereafter SAR) resulting from advances in the modelling of the atmosphere, ocean, sea ice and land surface as well as improvements in the coupling of these components.

Highlights include:

- Coupled models can provide credible simulations of both the present annual mean climate and the climatological seasonal cycle over broad continental scales for most variables of interest for climate change. Clouds and humidity remain sources of significant uncertainty but there have been incremental improvements in simulations of these quantities.

- Confidence in model projections is increased by the improved performance of several models that do not use flux adjustment. These models now maintain stable, multi-century simulations of surface climate that are considered to be of sufficient quality to allow their use for climate change projections.

- There is no systematic difference between flux adjusted and non-flux adjusted models in the simulation of internal climate variability. This supports the use of both types of model in detection and attribution of climate change.

- Confidence in the ability of models to project future climates is increased by the ability of several models to reproduce the warming trend in 20th century surface air temperature when driven by radiative forcing due to increasing greenhouse gases and sulphate aerosols. However, only idealised scenarios of only sulphate aerosols have been used.

- Some modelling studies suggest that inclusion of additional forcings such as solar variability and volcanic aerosols may improve some aspects of the simulated climate variability of the 20th century.

- Confidence in simulating future climates has been enhanced following a systematic evaluation of models under a limited number of past climates.

- The performance of coupled models in simulating the El Niño-Southern Oscillation (ENSO) has improved; however, the region of maximum sea surface temperature variability associated with El Niño events is displaced westward and its strength is generally underestimated. When suitably initialised with an ocean data assimilation system, some coupled models have had a degree of success in predicting El Niño events.

- Other phenomena previously not well simulated in coupled models are now handled reasonably well, including monsoons and the North Atlantic Oscillation.

- Some palaeoclimate modelling studies, and some land-surface experiments (including deforestation, desertification and land cover change), have revealed the importance of vegetation feedbacks at sub-continental scales. Whether or not vegetation changes are important for future climate projections should be investigated.

- Analysis of, and confidence in, extreme events simulated within climate models is emerging, particularly for storm tracks and storm frequency. “Tropical cyclone-like” vortices are being simulated in climate models, although enough uncertainty remains over their interpretation to warrant caution in projections of tropical cyclone changes.

Final Assessment

Coupled models have evolved and improved significantly since the SAR. In general, they provide credible simulations of climate, at least down to sub-continental scales and over temporal scales from seasonal to decadal. The varying sets of strengths and weaknesses that models display lead us to conclude that no single model can be considered “best” and it is important to utilise results from a range of coupled models. We consider coupled models, as a class, to be suitable tools to provide useful projections of future climates.

8.1 Summary of Second Assessment Report

The systematic evaluation of coupled climate models was only beginning to emerge at the time of the IPCC WGI Second Assessment Report (IPCC, 1996) (hereafter SAR). Suitable formalisms for evaluating fully coupled models were in very early stages of development whereas considerable progress had been made in the evaluation of the performance of individual components (atmosphere, ocean, land surface and sea ice and their interactions).

The need for flux adjustment and the widely varying spin-up methodologies in coupled models were areas of concern and the need for a more systematic evaluation of these on the simulated climate was expressed. It was noted that, although flux adjustments were generally large in those models that used them, the absence of flux adjustment generally affected the realism of the simulated climate and could adversely affect the associated feedback processes. It was hoped that the need for flux adjustment would diminish as components were improved.

A new feature of coupled model evaluation was an analysis of the variability of the coupled system over a range of time-scales. The new opportunities that provided for more comprehensive evaluation were an important component of the overall assessment of coupled model capabilities.

Evaluation of the performance of individual components of the coupled system (especially for atmosphere-only models) was much more advanced than previously. Results from the first phase of the Atmospheric Model Intercomparison Project (AMIP) demonstrated that *"current atmospheric models generally provide a realistic portrayal of the phase and amplitude of the seasonal march of the large-scale distribution of temperature, pressure and circulation"*. The simulation of clouds and their seasonal variation was noted as the major source of uncertainty in atmospheric models. In general it was found that *"atmospheric models respond realistically to large-scale sea surface temperature (SST) patterns"* and hence can reproduce many facets of interannual variability. In the case of the land-surface component, however, it was noted that *"the general agreement found among the results of relatively simple land-surface schemes in 1990 has been reduced by the introduction of more complex parametrizations"*. Ocean and sea-ice models were found to *"portray the observed large-scale distribution of temperature, salinity and sea ice more accurately than in 1990"*, but some reservations were expressed regarding the possible adverse effects of the relatively coarse resolution of the ocean components of current coupled models.

The overall assessment of coupled models was that *"current models are now able to simulate many aspects of the observed climate with a useful level of skill"* and *"model simulations are most accurate at large space scales (e.g., hemispheric or continental); at regional scales skill is lower"*.

8.2 What is Meant by Evaluation?

8.2.1 The Approach: Mean State and Variability in Climate Models

In this chapter, we (as the authors of this chapter) have attempted a two-pronged approach to evaluation. As is traditional, we discuss how well models simulate the mean seasonal climate for a number of variables (i.e., the average for a given season taken over many simulated years). Since the characterisation of a climate state includes its variability, we also describe simulated climate variability over a range of time-scales. In addition, we discuss aspects of the variability in the behaviour of specific phenomena. Evaluation of the performance of global models in specific geographical regions is the subject of Chapter 10.

We use a wide range of "observations" in order to evaluate models. However, often the most useful source for a particular variable is a product of one of the reanalysis projects (most commonly that of the National Centers for Environmental Prediction (NCEP) (Kalnay *et al*., 1996) or from the European Centre for Medium-Range Weather Forecasts (ECMWF) (Gibson *et al*., 1997)). Although products from a data assimilation system are not direct "observations" (they are the outcome of a combination of observed and model data), the global grided nature and high time resolution of these products makes them extremely useful when their accuracy is not in question. Some additional useful products from reanalysis are not, in fact, the result of a direct combination of observed and model data but are in fact the outcome of model integration and hence must be used with caution. It is important to note that the various variables available are not all of the same quality and, especially for data-sparse regions, implicitly contain contributions from the errors in the underlying model (see also Chapter 2). The overall quality of reanalysis products is continually assessed at regular International Reanalysis Workshops.

8.2.2 The Basis

Recent discussions by Randall and Wielicki (1997), Shackley *et al.* (1998 and 1999), Henderson-Sellers and McGuffie (1999) and Petersen (2000) illustrate many of the confusions and uncertainties that accompany attempts to evaluate climate models especially when such models become very complex. We recognise that, unlike the classic concept of Popper (1982), our evaluation process is not as clear-cut as a simple search for "falsification". While we do not consider that the complexity of a climate model makes it impossible to ever prove such a model "false" in any absolute sense, it does make the task of evaluation extremely difficult and leaves room for a subjective component in any assessment. The very complexity of climate models means that there are severe limits placed on our ability to analyse and understand the model processes, interactions and uncertainties (Rind, 1999). It is always possible to find errors in simulations of particular variables or processes in a climate model. What is important to establish is whether such errors make a given model "unusable" in answering specific questions.

Two fundamentally different ways are followed to evaluate models. In the first, the important issues are the degree to which a model is physically based and the degree of realism with which essential physical and dynamical processes and their interactions have been modelled. This first type of evaluation is undertaken in Chapter 7. (We discuss the related aspects of the numerical formulation and numerical resolution in Section 8.9.) In the second, there are attempts to quantify model errors, to consider

the causes for those errors (where possible) and attempts to understand the nature of interactions within the model. We fully recognise that many of the evaluation statements we make contain a degree of subjective scientific perception and may contain much "community" or "personal" knowledge (Polanyi, 1958). For example, the very choice of model variables and model processes that are investigated are often based upon the subjective judgement and experience of the modelling community.

The aim of our evaluation process is to assess the ability of climate models to simulate the climate of the present and the past. Wherever possible we will be concentrating on coupled models, however, where necessary we will examine the individual model components. This assessment then acts as a guide to the capabilities of models used for projections of future climate.

8.2.3 Figures of Merit

There have been many attempts to obtain a "figure of merit" for climate models. Usually such quantification is only attempted for well-observed atmospheric variables and range from calculation of simple root mean square errors (r.m.s.) between a model variable and an observation, to more complex multi-variate calculations. Among the most promising attempts at generating skill scores deemed more suitable for climate models are: the normalised mean square error approach of Williamson (1995) that follows on, in part, from Murphy (1988); and the categorisation of models in terms of combination of the error in the time mean and the error in temporal variability along the lines suggested by Wigley and Santer (1990) (see Chapter 5, Section 5.3.1.1. of the SAR for an example). Other less widely used non-dimensional measures have also been devised (e.g., Watterson, 1996). Although a number of skill scoring methods have been devised and used for the seasonal prediction problem (e.g., Potts *et al*., 1996; linear error in probability space score – LEPS) these have not found general application in climate models. Attempts to derive measures of the goodness of fit between model results and data containing large uncertainties have been partially successful in the oceanographic community for a limited number of variables (Frankignoul *et al*., 1989; Braconnot and Frankignoul, 1993). Fuzzy logic techniques have been trialled by the palaeoclimatology community (Guiot *et al*., 1999). It is important to remember that the types of error measurement that have been discussed are restricted to relatively few variables. It has proved elusive to derive a fully comprehensive multi-dimensional "figure of merit" for climate models.

Since the SAR, Taylor (2000) has devised a very useful diagrammatic form (termed a "Taylor diagram" – see Section 8.5.1.2 for description) for conveying information about the pattern similarity between a model and observations. This same type of diagram can be used to illustrate the relative accuracy amongst a number of model variables or different observational data sets (see Section 8.5.1). One additional advantage of the "Taylor diagram" is that there is no restriction placed on the time or space domain considered.

While at times we use a figure of merit to intercompare models for some selected variables, we usually apply more subjective assessments in our overall evaluations; we do not believe it is objectively possible to state which model is "best overall" for climate projection, since models differ amongst themselves (and with available observations) in many different ways. Even if a model is assessed as performing credibly when simulating the present climate, we cannot be sure that the response of such a model to a perturbation remains credible. Hence we also rely on evaluating models in their performance with individual processes (see Chapter 7) as well as past climates as in Section 8.5.5.

8.3 Model Hierarchy

8.3.1 Why is a Hierarchy of Models Important?

The impact of anthropogenic perturbation on the climate system can be projected by calculating all the key processes operating in the climate system through a mathematical formulation which, due to its complexity, can only be implemented in a computer program, referred to as a climate model. If all our current understanding of the climate system were explicitly included, the model would be too complex to run on any existing computer; hence, for practical purposes, simplifications are made so that the system has reduced complexity and computing requirements. Since different levels of simplifications are possible, a hierarchy of models tends to develop (see Chapter 1 and Harvey *et al*., 1997).

The need to balance scientific understanding against computational efficiency and model realism often guides the choice of the particular class of models used. In addition, it is usually necessary to balance the relative level of detail in the representation, and the level of parametrization, within each component of the climate system.

8.3.2 Three-dimensional Climate Models

The most complex climate models, termed coupled atmosphere-ocean general circulation models (and abbreviated as AOGCM in this report), involve coupling comprehensive three-dimensional atmospheric general circulation models (AGCMs), with ocean general circulation models (OGCMs), with sea-ice models, and with models of land-surface processes, all of which are extensively reviewed in the SAR (Chapters 4 and 5). For AOGCMs, information about the state of the atmosphere and the ocean adjacent to, or at the sea surface, is used to compute exchanges of heat, moisture and momentum between the two components. Computational limitations mean that the majority of sub-grid scale processes are parametrized (see Randall and Wielicki, 1997 and Chapter 7). Occasionally atmospheric models with simple mixed-layer ocean models (much discussed and utilised in the SAR) are still used.

8.3.3 Simple Climate Models

Simplifications can be made so that the climate model has reduced complexity (e.g., a reduction in dimensionality to two or even zero). Simple models allow one to explore the potential

sensitivity of the climate to a particular process over a wide range of parameters. For example, Wigley (1998) used a modified version of the Wigley and Raper (1987, 1992) upwelling diffusion-energy climate model (see Kattenberg *et al.*, 1996; Raper *et al*., 1996) to evaluate Kyoto Protocol implications for increases in global mean temperatures and sea level. While such a simple climate model relies on climate sensitivity and ocean heat uptake parameters based on coupled atmosphere-ocean models and ice-melt parameters based upon more complex ice sheet and glacier models, it nevertheless allows for a first-order analysis of various post-Kyoto emission reductions. Simple climate models are also used within larger integrated assessment models to analyse the costs of emission reduction (Peck and Teisberg, 1996; Manne and Richels, 1999) and impacts of climate change (Nordhaus, 1994; Tol, 1999).

8.3.4 Earth System Models of Intermediate Complexity

Recently, significant advances have occurred in the development of Earth System Models of Intermediate Complexity (EMIC), which are designed to bridge the gap between the three-dimensional comprehensive models and simple models. The main characteristic of EMICs is that they describe most of the processes implicit in comprehensive models, albeit in a more reduced (i.e., more parametrized) form. They also explicitly simulate the interactions among several components of the climate system including biogeochemical cycles. On the other hand, EMICs are computationally efficient enough to allow for long-term climate simulations over several tens of thousands of years or a broad range of sensitivity experiments over several millennia. As for AOGCMs, but in contrast to simple models, the number of degrees of freedom of an EMIC exceeds the number of adjustable parameters by several orders of magnitude. Currently, there are several EMICs in operation such as: two-dimensional, zonally averaged ocean models coupled to a simple atmospheric module (e.g., Stocker *et al*., 1992; Marchal *et al*., 1998) or geostrophic two-dimensional (e.g., Gallee *et al*., 1991) or statistical-dynamical (e.g., Petoukhov *et al*., 2000) atmospheric modules; three-dimensional models with a statistical-dynamical atmospheric and oceanic modules (Petoukhov *et al.*, 1998; Handorf *et al*., 1999); reduced-form comprehensive models (e.g., Opsteegh *et al.*, 1998) and those that involve an energy-moisture balance model coupled to an OGCM and a sea-ice model (e.g., Fanning and Weaver, 1996). Some EMICs have been used to investigate both the climate of the last glacial maximum (see Section 8.5) as well as to investigate the cause of the collapse of the conveyor in global warming experiments (Stocker and Schmittner, 1997; Rahmstorf and Ganopolski, 1999) while others have been used to undertake a number of sensitivity studies including the role of sub-grid scale ocean mixing in global warming experiments (Wiebe and Weaver, 1999).

EMIC development involves the same evaluation procedure as AOGCMs use, albeit restricted due to the reduced complexity of some, or all, of the constituent sub-components. While EMIC evaluation is in its early stages, the nature of these models allows for a detailed comparison with both historical and proxy observational data. Initial analyses (referenced above) suggest that EMICs hold promise as exploratory tools to understand important processes, and their interactions and feedbacks within the climate system. However, they are not useful for assessing regional aspects of climate change.

8.4 Coupled Climate Models – Some Methodologies

8.4.1 Model Initialisation

In this chapter, we assess climate models on the basis of their ability to simulate present and past climates. What it means to simulate a particular climate state is linked to the question of model initialisation. Ideally, given a "perfect model", and "perfect knowledge" of the present climate state, one could simply initialise a climate model with the present state. Then, given perpetual present day forcing (from trace substances and solar radiation), one might expect the model to remain close to the present state, perhaps with some level of variability. However, in practice, this ideal is not achieved and a model initialised in this way adjusts from the initial state. This adjustment has been characterised by two time-scales (Bryan, 1998): in the initial "fast" adjustment, the atmosphere, land surface, ocean mixed layer and sea ice reach a state of near equilibrium, typically taking 5 to 50 years. Surface temperature error patterns (e.g., Figure 8.1a) are generally established on this time-scale, and persist over many centuries of integration, but there typically remain slight imbalances in the surface heat and fresh water fluxes. These imbalances drive a second, slower, adjustment phase (often called "climate drift") which takes place over centuries to millennia and involves adjustment of the deep ocean to the surface imbalances. This "climate drift" can make interpretation of transient climate change simulations difficult, so models are generally allowed to adjust to a state where such drifts have become acceptably slow, before starting climate change simulations. A number of techniques have been used to achieve this (see Stouffer and Dixon, 1998), but it is not possible, in general, to say which of these procedures gives "better" initial conditions for a climate change projection run.

A number of model runs have now been made which are forced by the historical record of natural and anthropogenic forcing from the mid-19th century to the present. As well as avoiding the "cold start" problem in climate projections (SAR Chapter 6, Section 6.2.4 and Chapter 9), these runs can be compared against historical observations and form a valuable model evaluation tool (Section 8.6.1).

8.4.2 Flux Adjustment and Energy Transports

Given present day greenhouse gas concentrations, most coupled models at the time of the SAR had difficulty in obtaining a stable climate near to the present day state. Therefore "flux adjustment" terms were often added to the surface fluxes of heat, water and (sometimes) momentum which were passed from the atmosphere to the ocean model. Flux adjustments are non-physical in that they cannot be related to any physical process in the climate system and do not *a priori* conserve heat and water across the

atmosphere-ocean interface. The flux adjustments were specifically chosen to give a stable and realistic simulation of present surface climate (especially the sea surface temperature and sea-ice cover), and were often as large as the annual mean model fluxes themselves. The need to use such adjustments was clearly a source of uncertainty: the approach inherently disguises sources of systematic error in the models, and may distort their sensitivity to changed radiative forcing. Models which did not use flux adjustment produced unrealistic simulations of fundamental aspects of the climate system such as the strength of the North Atlantic thermohaline circulation (SAR Chapter 5, Table 5.5).

Recently a number of coupled models have emerged with greatly improved surface climatologies without using flux adjustments. Figure 8.1a shows SST errors from one such model, about 100 years after initialisation. Errors are generally less than 2°C, and the error pattern shown is stable over several centuries of integration. However some larger errors are seen, in particular a cooling in the North Pacific, a warming in the eastern tropical ocean basins (probably due to a lack of stratocumulus cloud there), and a warming in the southern ocean. These errors appear to be common to a number of more recent non-flux adjusted models (Action de Recherche Petite Echelle Grand Echelle/Océan Parallélisé (ARPEGE/OPA1), Guilyardi and Madec 1997; Climate System Model (CSM 1.0), Boville and Gent 1998; Hadley Centre Coupled Model (HadCM3), Gordon *et al.*, 2000), but other models show different error patterns (ARPEGE/OPA2, Institut Pierre Simon Laplace/Coupled Atmosphere-Ocean-Vegetation Model (IPSL-CM2), Barthelet *et al.*, 1998a,b). The surface climatologies in several non-flux adjusted models are now considered good enough and stable enough to use those models for climate change projections. Typical flux adjusted models do show smaller SST errors, because the flux adjustments are chosen specifically to minimise those errors (Figure 8.1b). For comparison, Figure 8.1c shows the SST errors when the older, flux adjusted model was run in non-flux adjusted mode.

It appears that the success of the recent models which do not require heat flux adjustments is related to an improved ability to simulate the large-scale heat balances described in Chapter 7 (Weaver and Hughes, 1996; Guilyardi and Madec, 1997; Johns *et al.*, 1997; Bryan, 1998; Gordon *et al.*, 2000). Improvements to both atmospheric (Section 8.5.1.2.2) and oceanic (Section 8.5.2.2) components of the models have played a part in this advance. Such models have the advantage over flux-adjusted models that, provided the large-scale balances are obtained using a physically justifiable choice of model parameters, these models are physically self-consistent representations of the climate system. However, in some cases only very loose physical constraints can be placed on the model parameters.

The fresh water budget is more complex than the heat budget because of the effects of land surface processes, rivers and sea ice. Water budget errors are potentially far reaching because there is no direct feedback between surface salinity errors and the surface fresh water flux, for example, persistent freshening at high latitudes could lead to a collapse of the ocean thermohaline circulation (Manabe and Stouffer, 1997; see also Chapter 7, Section 7.6.2). Some aspects of the large-scale hydrological cycle

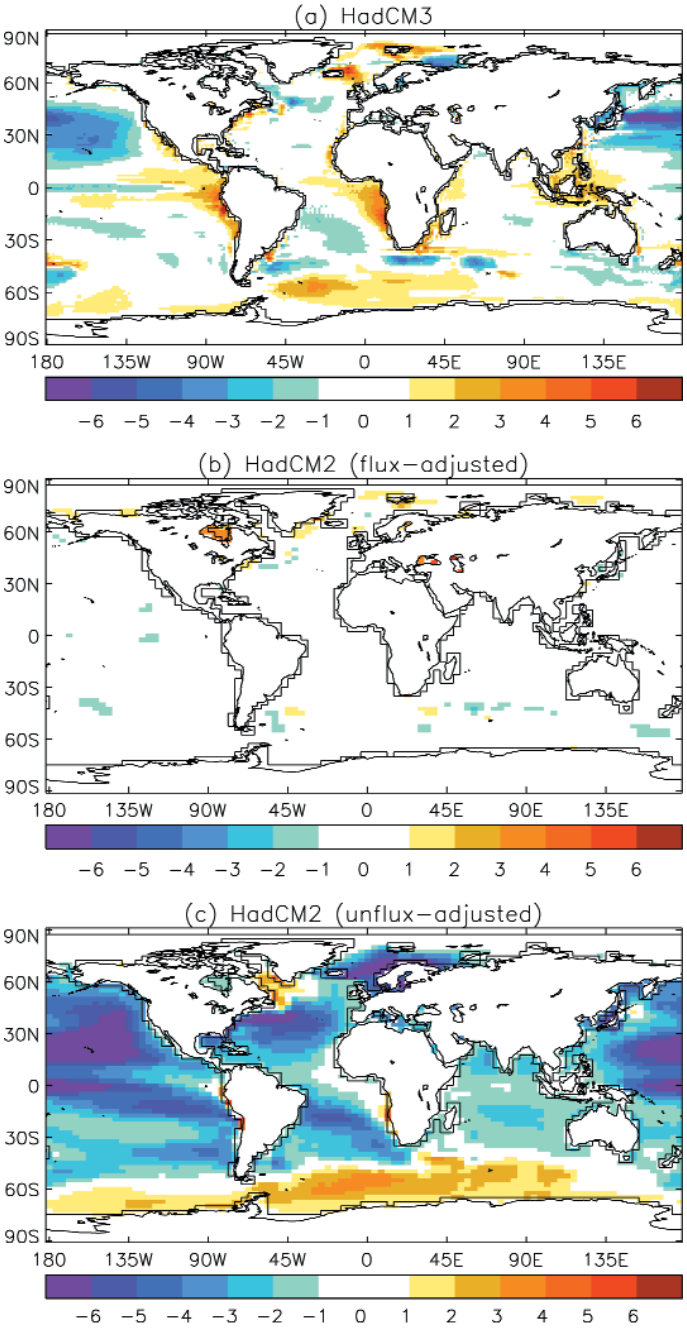

Figure 8.1: Decadal mean SST errors relative to the GISST climatology for (a) the non-flux adjusted model HadCM3 (Gordon *et al.*, 2000), (b) the previous generation, flux adjusted model HadCM2 (Johns *et al.* 1997), (c) the HadCM2 model when run without flux adjustments (Gregory and Mitchell, 1997). The figures are from representative periods after at least 100 years of each control run. Multi-century drifts in each run are much smaller than the differences between the runs. The errors are smallest in (b), because the flux adjustments were chosen specifically to minimise the errors. The errors in (c) result from a number of complex feedbacks. The model was designed to work in flux adjusted mode and it is possible that the non-flux adjusted SST errors could have been reduced by relatively minor "tuning" of the model.

Table 8.1: *Model control runs: a consolidated list of coupled AOGCMs that are assessed in Chapter 8 and used in other Chapters. The naming convention for the models is as agreed by all modelling groups involved. Under the heading CMIP: 1,2 indicate that the model control run is included in the Coupled Model Intercomparison Phase 1 and 2 (CMIP1 and 2) databases, respectively.*

	MODEL NAME	CENTRE	REFERENCE	CMIP	Ch 9	Ch 11	Ch 12	ATMOSPHERIC RESOLUTION	OCEAN RESOLUTION	LAND SURFACE	SEA ICE	FLUX ADJUST
1	ARPEGE/OPA1	CERFACS	Guilyardi and Madec, 1997	1	– – –			T21 (5.6 × 5.6) L30	2.0×2.0 L31*	C	(d)	–
2	ARPEGE/OPA2	CERFACS	Barthelet *et al.*, 1998a,b	2	C – –			T31(3.9 × 3.9) L19	2.0×2.0 L31*	C	T	–
3	BMRCa	BMRC	Power *et al.*, 1993	1	C – –			R21 (3.2 × 5.6) L9	3.2×5.6 L12	M,B	T	–
4	BMRCb	BMRC	Power *et al.*, 1998	2	– – –			R21 (3.2 × 5.6) L17	3.2×5.6 L12*	M,B	T	H,W
5	CCSR/NIES	CCSR/NIES	Emori *et al.*, 1999	1,2	C – D			T21 (5.6 × 5.6) L20	2.8×2.8 L17	M,BB	T	H,W
6	CGCM1	CCCma	Boer *et al.*, 2000; Flato *et al.*, 2000	1,2	C – D	*	*	T32 (3.8 × 3.8) L10	1.8×1.8 L29	M,BB	T	H,W
7	CGCM2	CCCma	Flato and Boer, 2001	–	– S –	*	*	T32 (3.8 × 3.8) L10	1.8×1.8 L29	M,BB	T,R	H,W
8	COLA1	COLA	Schneider *et al.*, 1997; Schneider and Zhu, 1998	1	– – –			R15 (4.5 × 7.5) L9	1.5×1.5 L20*	C	T	–
9	COLA2	COLA	Dewitt and Schneider, 1999	1	– – –			T30 (4 × 4) L18	3.0×3.0 L20*	C	T	–
10	CSIRO Mk2	CSIRO	Gordon and O'Farrell, 1997	1,2	C – D			R21 (3.2 x 5.6) L9	3.2×5.6 L21	C	T,R	H,W,M
11	CSM 1.0	NCAR	Boville and Gent, 1998	1,2	C – –			T42 (2.8 × 2.8) L18	2.0×2.4 L45*	C	T,R	–
12	CSM 1.3	NCAR	Boville *et al.*, 2001	–	– S D			T42 (2.8 × 2.8) L18	2.0×2.4 L45*	C	T,R	–
13	ECHAM1/LSG	DKRZ	Cubasch *et al.*, 1992; von Storch, 1994; von Storch *et al.*, 1997	1	– – –		*	T21 (5.6 × 5.6) L19	4.0×4.0 L11	C	T	H,W,M
14	ECHAM3/LSG	DKRZ	Cubasch et al 1997; Voss *et al.*, 1998	1,2	C – D		*	T21 (5.6 × 5.6) L19	4.0×4.0 L11	C	T	H,W,M
15	ECHAM4/OPYC3	DKRZ	Roeckner *et al*., 1996	1	C – D	*	*	T42 (2.8 × 2.8) L19	2.8×2.8 L11*	C	T,R	H,W(*)
16	GFDL_R15_a	GFDL	Manabe *et al.*, 1991; Manabe and Stouffer1996	1,2	C – D		*	R15 (4.5 × 7.5) L9	4.5×3.7 L12	B	T,F	H,W
17	GFDL_R15_b	GFDL	Dixon and Lanzante, 1999	–	C – –	*		R15 (4.5 × 7.5) L9	4.5×3.7 L12	B	T,F	H,W
18	GFDL_R30_c	GFDL	Knutson *et al.*, 1999	–	C S –	*	*	R30 (2.25 × 3.75)L14	1.875×2.25 L18	B	T,F	H,W
19	GISS1	GISS	Miller and Jiang, 1996	1	– – –			4.0 × 5.0 L9	4.0×5.0 L16	C	T	–
20	GISS2	GISS	Russell *et al.*, 1995	1,2	C – –			4.0 × 5.0 L9	4.0×5.0 L13	C	T	–
21	GOALS	IAP/LASG	Wu *et al.*, 1997; Zhang *et al.*, 2000	1,2	C – –			R15 (4.5 × 7.5) L9	4.0×5.0 L20	C	T	H,W,M
22	HadCM2	UKMO	Johns 1996; Johns *et al.*, 1997	1,2	C – D		*	2.5 × 3.75 L19	2.5×3.75 L20	C	T,F	H,W
23	HadCM3	UKMO	Gordon *et al.*, 2000	2	C S D		*	2.5 × 3.75 L19	1.25 × 1.25 L20	C	T,F	–
24	IPSL-CM1	IPSL/LMD	Braconnot *et al.*, 2000	1	– – –			5.6 × 3.8 L15	2.0×2.0 L31*	C	(d)	–
25	IPSL-CM2	IPSL/LMD	Laurent *et al.*, 1998;	2	C – –			5.6 × 3.8 L15	2.0×2.0 L31*	C	T	–
26	MRI1[a]	MRI	Tokioka *et al.*, 1996	1,(2)[a]	C – –			4.0 × 5.0 L15	2.0×2.5 L21(23)[a]*	M,B	T,F	H,W
27	MRI2	MRI	Yukimoto *et al.*, 2000	–	C S –	*		T42(2.8 × 2.8) L30	2.0×2.5 L23*	C	T,F	H,W,M
28	NCAR1	NCAR	Meehl and Washington, 1995; Washington and Meehl, 1996	1,2	– – –			R15 (4.5 × 7.5) L9	1.0×1.0 L20	B	T,R	–
29	NRL	NRL	Hogan and Li, 1997; Li and Hogan, 1999	1,2	– – –			T47 (2.5 × 2.5) L18	1.0 × 2.0 L25*	BB	T(p)	H,W(*)
30	DOE PCM	NCAR	Washington *et al*., 2000	2	C S D			T42 (2.8 × 2.8) L18	0.67 × 0.67 L32	C	T,R	–
31	CCSR/NIES2	CCSR/NIES	Nozawa *et al.*, 2000	–	C S –			T21 (5.6 × 5.6) L20	2.8 × 3.8 L17	M,BB	T	H,W
I1	BERN2D	PIUB	Stocker *et al.*, 1992; Schmittner & Stocker, 1999	–	– – –	*		10* × ZA L1	10* × ZA L15	–	T	–
I2	UVIC	UVIC	Fanning and Weaver, 1996; Weaver *et al.*, 1998	–	– – –	*		1.8 × 3.6 L1	1.8 × 3.6 L19	–	T,R	–
I3	CLIMBER	PIK	Petoukhov *et al.*, 2000	–	– – –	*		10 × 51 L2	10 × ZA L11	C	T,F	–

[a] Model MRI1 exists in two versions. At the time of writing, more complete assessment data was available for the earlier version, whose control run is in the CMIP1 database. This model is used in Chapter 8. The model used in Chapter 9 has two extra ocean levels and a modified ocean mixing scheme. Its control run is in the CMIP2 database. The equilibrium climate sensitivities and Transient Climate Responses (Chapter 9, Table 9.1) of the two models are the same.

CMIP: 1,2 indicate that the model control run is included in the CMIP1 and CMIP2 databases, respectively.
Ch 9: C indicates that a run or runs with the CMIP2 1% p.a. CO_2 increase scenario is used in Chapter 9 (irrespective of whether the data is included in the CMIP database). S indicates that SRES scenario runs (including at least A2 and B2) are used in Chapter 9. D indicates that model output is lodged at the IPCC Data Distribution Centre.
Ch 11, Ch 12: An asterisk indicates that the model has been used to make sea level projections (Chapter 11) or in detection/attribution studies (Chapter 12).
Atmospheric resolution: Horizontal and vertical resolution. The former is expressed either as degrees latitude × longitude or as a spectral truncation with a rough translation to degrees latitude × longitude. An asterisk indicates enhanced meridional resolution in midlatitudes. ZA indicates a zonally averaged model (360° zonal resolution). Vertical resolution is expressed as "Lmm", where mm is the number of vertical levels.
Ocean resolution: Horizontal and vertical resolution. The former is expressed as degrees latitude × longitude, while the latter is expressed as "Lmm", where mm is the number of vertical levels. An asterisk indicates enhanced horizontal resolution near the Equator. ZA indicates a zonally averaged model for each ocean basin. The following classification of ocean horizontal resolution is used throughout Chapters 7 to 9: Coarse: >2°, Medium: 2/3° to 2°, Eddy-permitting: 1/6° to 2/3°, Eddy-resolving: <1/6°.
Land surface scheme: B = standard bucket hydrology scheme; BB = modified bucket scheme with spatially varying soil moisture capacity and/or a surface resistance; M = multi-layer temperature scheme; C = a complex land surface scheme usually including multi-soil layers for temperature and soil moisture, and an explicit representation of canopy processes.
Sea ice model: T = thermodynamic ice model only; F = 'free drift' dynamics; R = ice rheology included; (d) = ice extent/thickness determined diagnostically from ocean surface temperature; (p) = ice extent prescribed.
Flux adjustment: H = heat flux; W = fresh water flux; M = momentum flux. An asterisk indicates annual mean flux adjustment only.

are subject to large observational uncertainty (Wijffels *et al*., 1992), and this has inhibited evaluation and improvements in the water budget. Nonetheless, some models are now able to produce stable multi-century runs without water flux adjustments

8.4.2.1 Does the use of flux adjustments in a model have a significant impact on climate change projections?

Marotzke and Stone (1995) show that using flux adjustment to correct surface errors in the control climate does not necessarily correct errors in processes which control the climate change response. Flux adjustments can also result in spurious multiple equilibrium states of the tropical (Neelin and Dijkstra, 1995) and thermohaline (Dijkstra and Neelin, 1999) ocean circulation. On the other hand, a good representation of, say, sea-ice extent may be important to produce the correct magnitude of ice-albedo feedback under climate change, and it may be preferable to use flux adjustments to give a good sea-ice distribution than to omit the flux adjustments but to have a poorer sea-ice extent. Overall, differences have been seen in the climate change response of flux adjusted and equivalent non-flux adjusted models (Fanning and Weaver, 1997b; Gregory and Mitchell, 1997), but it is not clear whether the differences are due to the flux adjustment itself, or to the systematic errors in the non-flux adjusted model. The only practical way to resolve this issue may be to continue the progress which has been made towards models which achieve good surface climatology without flux adjustment, whereupon the effect of flux adjustments will cease to be of concern.

8.5 Coupled Climate Models – Means

8.5.1 Atmospheric Component

8.5.1.1 Development since the SAR

The model evaluation chapter of the IPCC Second Assessment Report (Gates *et al.*, 1996) found that "large-scale features of the current climate are well simulated on average by current coupled models." However, two major points of concern were noted. Firstly, the SAR found that simulation of clouds and related processes "remains a major source of uncertainty in atmospheric models". As discussed in Chapter 7, these processes continue to account for most of the uncertainty in predicting human-induced climate change. Secondly, the SAR noted an unsatisfactory situation involving flux adjustments (Section 8.4.2): they "are relatively large in the models that use them, but their absence affects the realism of the control climate and the associated feedback processes". Improvements in coupled climate models since the SAR have addressed both points of concern. For the atmospheric (as well as the oceanic) component, these improvements have included higher horizontal resolution (which means less numerical diffusion and better representation of topography), and advances in parametrizations. In addition, the advent of the Coupled Model Intercomparison Program (CMIP; see Meehl *et al.*, 2000a) since the SAR has provided an additional database for evaluating AOGCMs. Some basic details of models evaluated in this chapter and used elsewhere in this report are presented in Table 8.1.

8.5.1.2 Tropospheric climate

8.5.1.2.1 Surface quantities

The SAR's evaluation of coupled-model simulations focused on surface air temperature, sea level pressure and precipitation. The SAR concluded that model simulations of surface air temperature were "very similar" to observations. Simulations of the other two quantities were found to be less accurate but nevertheless reasonable: the SAR concluded that coupled models represented "the observed large-scale geographical distribution" of sea level pressure "rather well", and that they were "generally successful in simulating the broad-scale structure of the observed precipitation".

Figures 8.2 and 8.3 (reproduced from Lambert and Boer, 2001) update this assessment using coupled model output from the CMIP1 database. For each quantity, the figures show both a map of the average over all fifteen models ("model mean") and

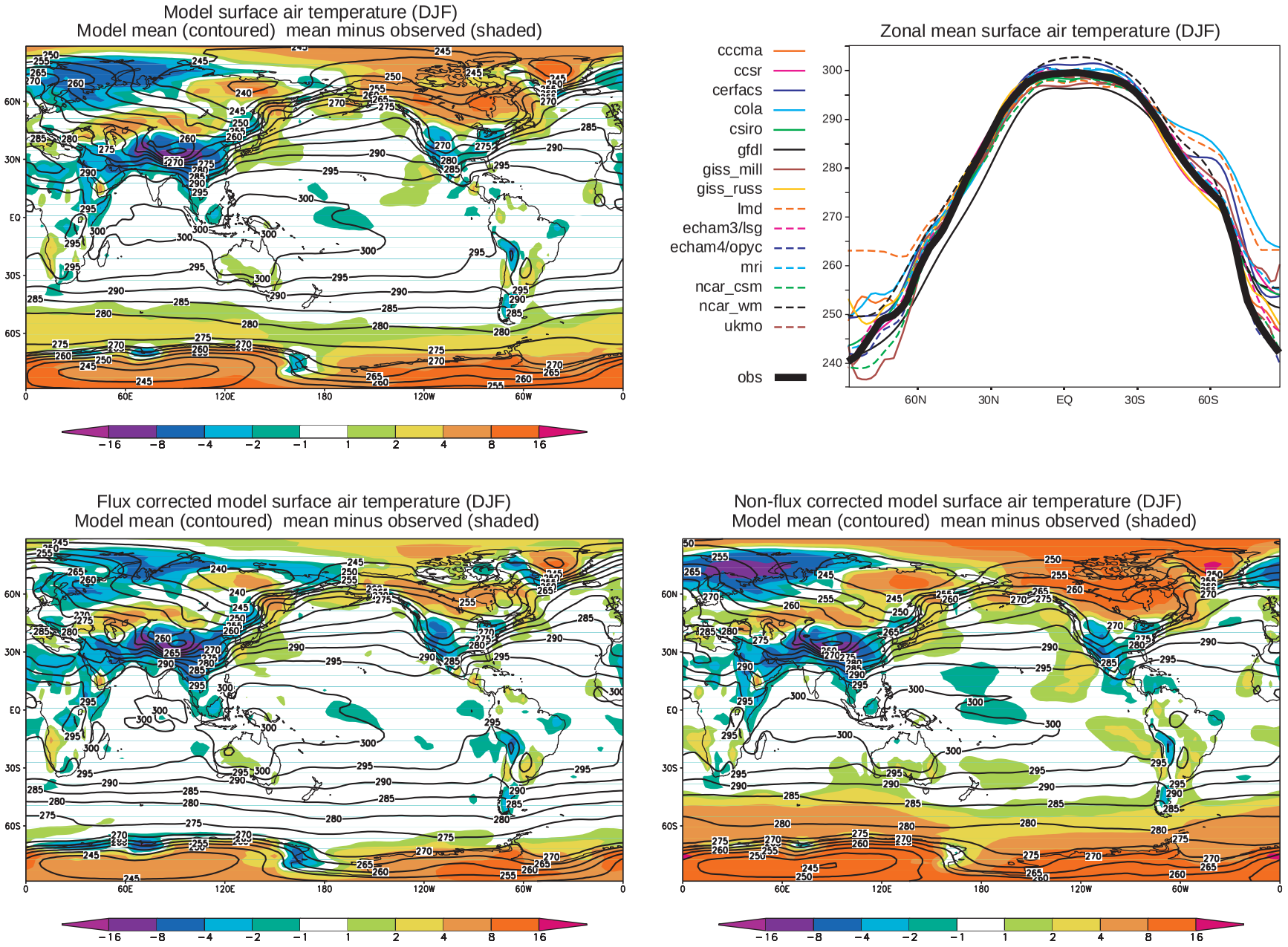

Figure 8.2: December-January-February climatological surface air temperature in K simulated by the CMIP1 model control runs. Averages over all models (upper left), over all flux adjusted models (lower left) and over all non-flux adjusted models (lower right) are shown together with zonal mean values for individual models (upper right). Observed value is shown in the zonal mean plot (thick solid line), and the difference between "average model" and observation is shown on the longitude-latitude maps. From Lambert and Boer (2001).

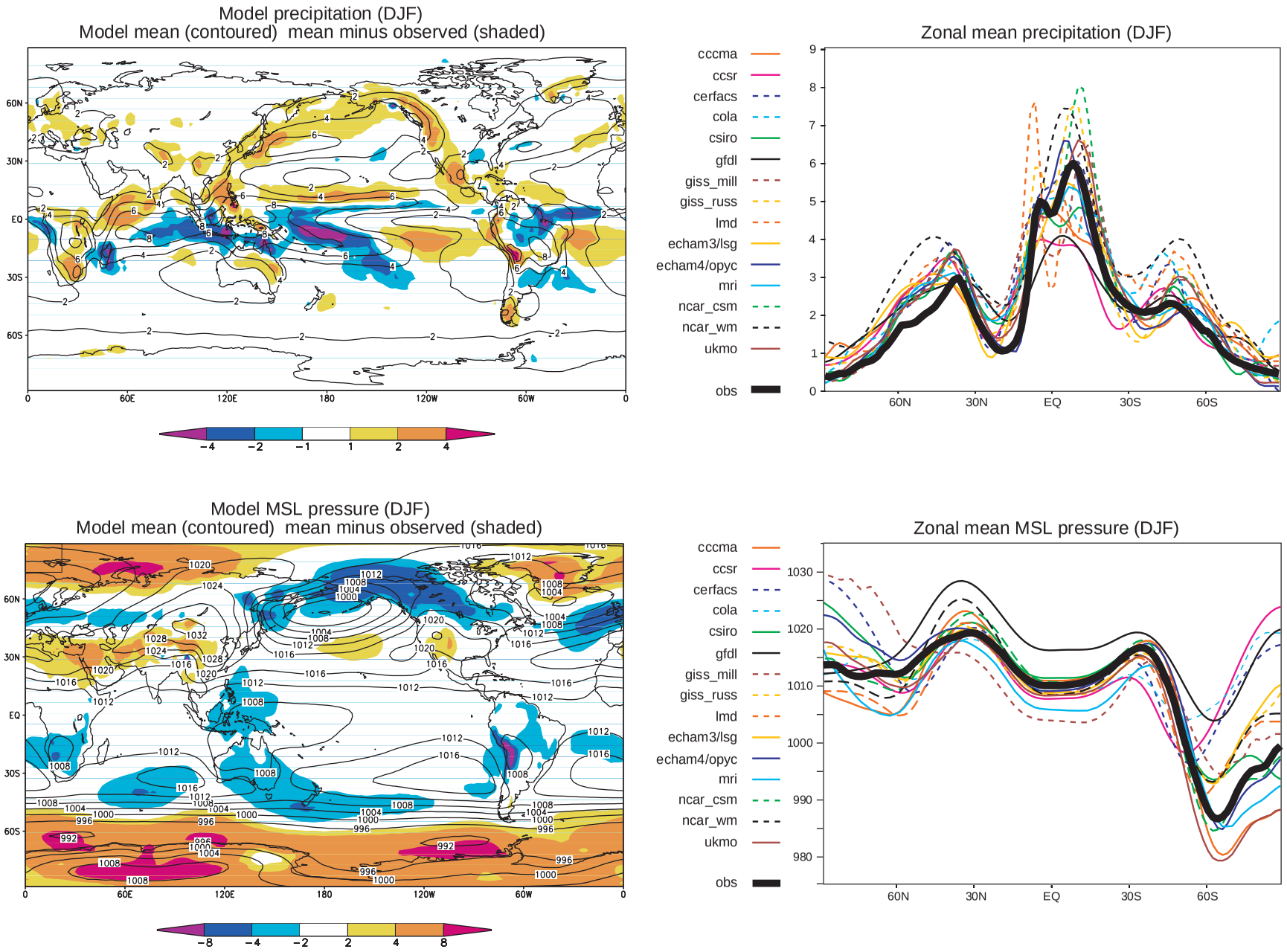

Figure 8.3: December-January-February climatological precipitation in mm per day (top) and mean sea level pressure in hPa (bottom) simulated by CMIP1 model control runs. Averages over all models are shown at left and zonal mean values for individual models are shown at right. Observed values are shown on the zonal mean plot (thick solid line) and the difference between an "average model" and the observations is shown by shading on the longitude-latitude maps. From Lambert and Boer (2001).

zonal means for all individual fifteen models. Lambert and Boer (2001) demonstrate that the model mean exhibits good agreement with observations, often better than any of the individual models. Inspection of these portions of the figures reaffirms the SAR conclusions summarised above. The errors in model-mean surface air temperature rarely exceed 1°C over the oceans and 5°C over the continents; precipitation and sea level pressure errors are relatively greater but the magnitudes and patterns of these quantities are recognisably similar to observations. The bottom portion of Figure 8.2 shows maps of the model mean taken separately over all flux adjusted models (lower left) and all non-flux adjusted models (lower right). Flux adjusted models are generally more similar to the observations – and to each other – than are non-flux adjusted models. However, errors in the non-flux adjusted model mean are not grossly larger than errors in the flux adjusted model mean (except in polar regions). This result from the "inter-model" CMIP database suggests that the SAR was correct in anticipating that the need for flux adjustments would diminish as coupled models improve. It is reinforced by "intra-model ensembles", i.e., by the experience that improvements to individual models can reduce the need for flux adjustments (e.g., Boville and Gent, 1998).

The foregoing points are made in a more quantitative fashion by Figures 8.4 to 8.6 (reproduced from Covey *et al*., 2000b). Figure 8.4 gives the standard deviation and correlation with observations of the total spatial and temporal variability (including the seasonal cycle, but omitting the global mean) for surface air temperature, sea level pressure and precipitation in the CMIP2 simulations. The standard deviation is normalised to its observed value and the correlation ranges from zero along an upward vertical line to unity along a line pointing to the right. Consequently, the observed behaviour of the climate is represented by a point on the horizontal axis a unit distance from the origin. In this coordinate system, the linear distance between each model's point and the "observed" point is proportional to the r.m.s. model error (Taylor, 2000; see also Box 8.1). Surface air temperature is particularly well simulated, with nearly all models closely matching the observed magnitude of variance and exhibiting a correlation > 0.95 with the observations. Sea level pressure and precipitation are simulated less well, but the simulated variance is still within ±25% of observed and the correlation with observations is noticeably positive (about 0.7 to 0.8 for sea level pressure and 0.4 to 0.6 for precipitation).

Observational uncertainties are indicated in Figure 8.4 by including extra observational data sets as additional points, as if they were models. These additional points exhibit greater agreement with the baseline observations as expected. It is noteworthy, however, that the differences between alternate sets of observations are not much smaller than the differences between models and the baseline observations. This result implies that in terms of variance and space-time pattern correlation, the models nearly agree with observations to within the observational uncertainty.

Figures 8.5 and 8.6 show global mean errors ("bias") and root mean square (r.m.s.) errors normalised by standard deviations for surface air temperature and precipitation in

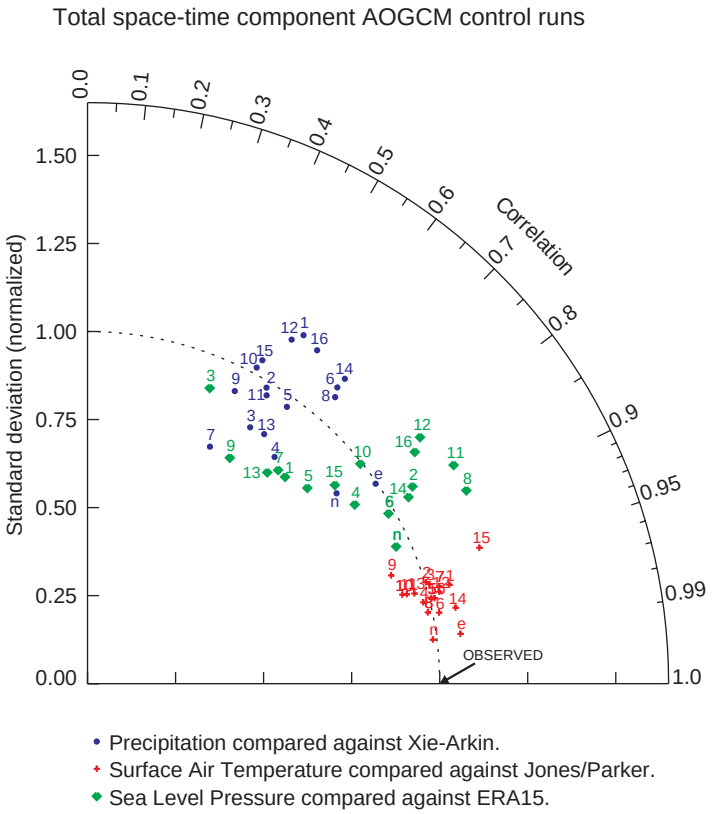

Figure 8.4: Second-order statistics of surface air temperature, sea level pressure and precipitation simulated by CMIP2 model control runs. The radial co-ordinate gives the magnitude of total standard deviation, normalised by the observed value, and the angular co-ordinate gives the correlation with observations. It follows that the distance between the OBSERVED point and any model's point is proportional to the r.m.s model error (see Section 8.2). Numbers indicate models counting from left to right in the following two figures. Letters indicate alternate observationally based data sets compared with the baseline observations: e = 15-year ECMWF reanalysis ("ERA"); n = NCAR/NCEP reanalysis. From Covey *et al*. (2000b).

CMIP2 model simulations. Both the r.m.s. errors and the background standard deviations are calculated from the full spatial and temporal variability of the fields. The r.m.s. errors are divided into a number of components such as zonal mean vs. deviations and annual mean vs. seasonal cycle. For nearly all models the r.m.s. error in zonal- and annual-mean surface air temperature is small compared with its natural variability. The errors in the other components of surface air temperature, and in zonal mean precipitation, are relatively larger but generally not excessive compared with natural variability.

In Figures 8.5 and 8.6, models are divided into flux adjusted and non-flux adjusted classes. Slight differences between the two may be discerned, but it is not obvious that these are statistically significant if the two classes are considered as random samples from a large population of potential climate models. The same conclusion was reached in a detailed study of the seasonal cycle of surface air temperature in the CMIP models (Covey *et al*.,

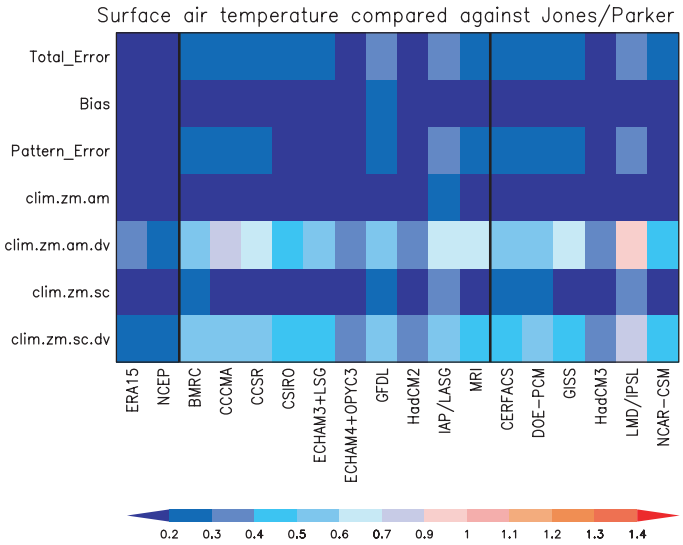

Figure 8.5: Components of space-time errors of surface air temperature (climatological annual cycle) simulated by CMIP2 model control runs. Shown are the total errors, the global and annual mean error ("bias"), the total r.m.s ("pattern") error, and the following components of the climatological r.m.s. error: zonal and annual mean ("clim.zm.am"); annual mean deviations from the zonal mean ("clim.zm.am.dv"), seasonal cycle of the zonal mean ("clim.zm.sc"); and seasonal cycle of deviations from the zonal mean ("clim.zm.sc.dv"). For each component, errors are normalised by the component's observed standard deviation. The two left-most columns represent alternate observationally based data sets, ECMWF and NCAR/NCEP reanalyses, compared with the baseline observations (Jones *et al*., 1999). Remaining columns give model results: the ten models to the left of the second thick vertical line are flux adjusted and the six models to the right are not. From Covey *et al*. (2000b).

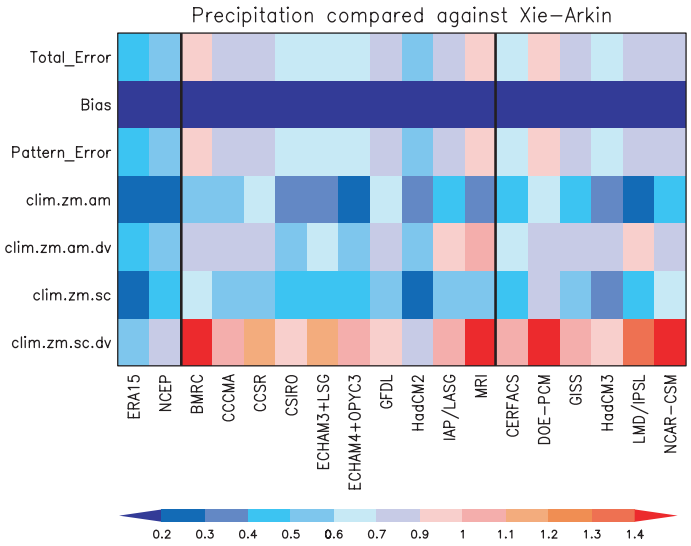

Figure 8.6: As in the Figure 8.5, for precipitation. The two left-most columns represent alternate observationally based data sets, 15-year ECMWF reanalysis ("ECMWF") and NCAR/NCEP reanalysis ("NCEP"), compared with the baseline observations (Xie and Arkin, 1996). From Covey *et al*. (2000b).

Box 8.1: Taylor diagrams

To quantify how well models simulate an observed climate field, it is useful to rely on three non-dimensional statistics: the ratio of the variances of the two fields:

$$\gamma^2 = \delta^2_{\text{mod}} / \delta^2_{\text{obs}}$$

the correlation between the two fields (R, which is computed after removing the overall means), and the r.m.s difference between the two fields (E, which is normalised by the standard deviation of the observed field). The ratio of variance indicates the relative amplitude of the simulated and observed variations, whereas the correlation indicates whether the fields have similar patterns of variation, regardless of amplitude. The normalised r.m.s error can be resolved into a part due to differences in the overall means (E_0), and a part due to errors in the pattern of variations (E').

These statistics provide complementary, but not completely independent, information. Often the overall differences in means (E_0) is reported separately from the three pattern statistics (E', γ, and R), but they are in fact related by the following equation:

$$E'^2 = E^2 - E_0^2 = 1 + \gamma^2 - 2\gamma R$$

This relationship makes it possible to display the three pattern statistics on a two-dimensional plot like that in Figure 8.4. The plot is constructed based on the Law of Cosines. The observed field is represented by a point at unit distance from the origin along the abscissa. All other points, which represent simulated fields, are positioned such that γ is the radial distance from the origin, R is the cosine of the azimuthal angle, and E' is the distance to the observed point. When the distance to the point representing the observed field is relatively short, good agreement is found between the simulated and observed fields. In the limit of perfect agreement (which is, however, generally not achievable because there are fundamental limits to the predictability of climate), E' would approach zero, and γ and R would approach unity.

2000a). (That study, however, also noted that many of the non-flux adjusted models suffered from unrealistic "climate drift" up to about 1°C / century in global mean surface temperature.) The relatively small differences between flux adjusted and non-flux adjusted models noted above suggest that flux adjustments could be – indeed, are being – dispensed with at acceptable cost in many climate models, at least for the century time-scale integrations of interest in detecting and predicting anthropogenic climate change. In recent models that omit flux adjustment, the representation of atmospheric fields has in some cases actually improved, compared with older, flux-adjusted versions of the models. Examples include the HadCM3 model and the CSM 1.0 model. In CSM 1.0, atmospheric temperature, precipitation and atmospheric circulation are close to values simulated when the atmospheric component of the CSM 1.0 model is driven by observed sea surface temperatures (Boville and Hurrell, 1998).

8.5.1.2.2 Surface and top of atmosphere (TOA) fluxes

In this and the following two sub-sections we discuss simulations by AGCMs that are provided observed sea surface temperatures and sea-ice distributions as input boundary conditions. AOGCM control runs have not yet been thoroughly examined in studies of surface boundary fluxes or mid-tropospheric and stratospheric quantities.

Satellite observations over the past quarter of a century have provided estimates of top of atmosphere (TOA) flux that are considered reliable. Any discrepancies between models and observations are usually attributed to the inadequate modelling of clouds, since they are difficult to specify and accurately model, and account for most of the variability.

Unfortunately, there are no global estimates of surface flux that do not rely heavily on models. The best model-independent estimates come from the Global Energy Balance Archive (GEBA), a compilation of observations from more than 1,000 stations (Gilgen *et al*., 1998). Compared with GEBA observations, surface solar insolation is overestimated in most AGCMs (Betts *et al*., 1993; Garratt, 1994; Wild *et al*., 1997, 1998; Garratt *et al*., 1998). Downwelling long wave radiation, on the other hand, is underestimated (Garratt and Prata, 1996; Wild *et al*., 1997). The shortwave discrepancy is of more concern: it is more than a factor of two larger than the long-wave discrepancy, and could be due to missing absorption processes in the atmosphere.

The observations indicate that about 25% of the incident solar flux at the TOA is absorbed in the atmosphere, but most models underestimate this quantity by 5 to 8% of the of the incident solar flux (Arking, 1996, 1999; Li *et al*., 1997). The extent and the source (or sources) of this discrepancy have been intensely debated over the past five years, with investigations yielding contradictory results on whether the discrepancy is associated with clouds, aerosols, water vapour, or is an artefact of the instrumentation and/or the methods by which sensors are calibrated and deployed.

This discrepancy is important for climate modelling because it affects the partitioning of solar energy between the atmosphere and the surface. If the observations are correct, then improving the models will reduce the energy available for surface evaporation by 10 to 20% with a corresponding reduction in precipitation (Kiehl *et al*., 1995) and a general weakening of the hydrological cycle.

8.5.1.2.3 Mid-tropospheric variables

The SAR concluded that although atmospheric models adequately simulate the three-dimensional temperature distribution and wind patterns, "current models portray the large-scale latitudinal structure and seasonal change of the observed total cloud cover with only fair accuracy". Subsequent studies have confirmed both the good and bad aspects of model simulations. Throughout most of the troposphere, errors in AMIP1 ensemble simulations of temperature and zonal wind are small compared with either inter-model scatter or the observed spatial standard deviation (Gates *et al*., 1999). (See Section 8.8 for brief discussion of storm tracks.) On the other hand, discrepancies between models and observations that substantially exceed the observational uncertainty are evident for both clouds (Mokhov and Love, 1995; Weare *et al*., 1995, 1996; Weare, 2000a, 2000b) and upper tropospheric humidity (see Chapter 7).

Although solutions to these problems have proved elusive, incremental improvements have been noted since publication of the SAR. For total cloudiness, a revised subset of AMIP models exhibits noticeably less inter-model variation and significantly less average r.m.s error (Gates *et al*., 1999; Figure 8.7), compared with the original versions of the models. Several models adequately simulate seasonal changes in cloud radiative forcing (Cess *et al.*, 1997). Model intercomparisons organised under the Global Energy and Water cycle Experiment (GEWEX) Cloud System Study (Stewart *et al.*, 1998) will provide further information for improving cloud simulation. For tropospheric humidity, improved agreement with observations may result from improved numerical techniques (Section 8.9). Furthermore, even though the seasonal mean amounts of clouds and upper tropospheric water vapour are not well simulated in current climate models, *variations* of these quantities may be more important than absolute amounts for predicting climate changes. For example, Del Genio *et al*. (1994) noted that, in mid-latitudes, the seasonal cycle of upper tropospheric humidity can be simulated reasonably well by climate models. They argued that this variation provides a surrogate for decadal climate change in mid-latitudes because both are characterised by combined temperature increase and latitudinal temperature-gradient decrease, and thus both have similar effects on storms.

Examination of monsoons in climate models provides another measure of their ability to simulate hydrologic variations. Developments since publication of the SAR have been encouraging. Sperber and Palmer (1996) found that about half the original AMIP models obtained a realistic dependence of monsoon circulation on location and season. A follow-up study reveals that nearly all the revised AMIP models do so (Sperber *et al*., 1999; see Section 8.7.3).

8.5.1.3 Stratospheric climate

Simulation of the stratosphere in coupled climate models is advancing rapidly as the atmospheric components of these models enhance their vertical resolution in the upper part of their domain. Since publication of the SAR, it has become increas-

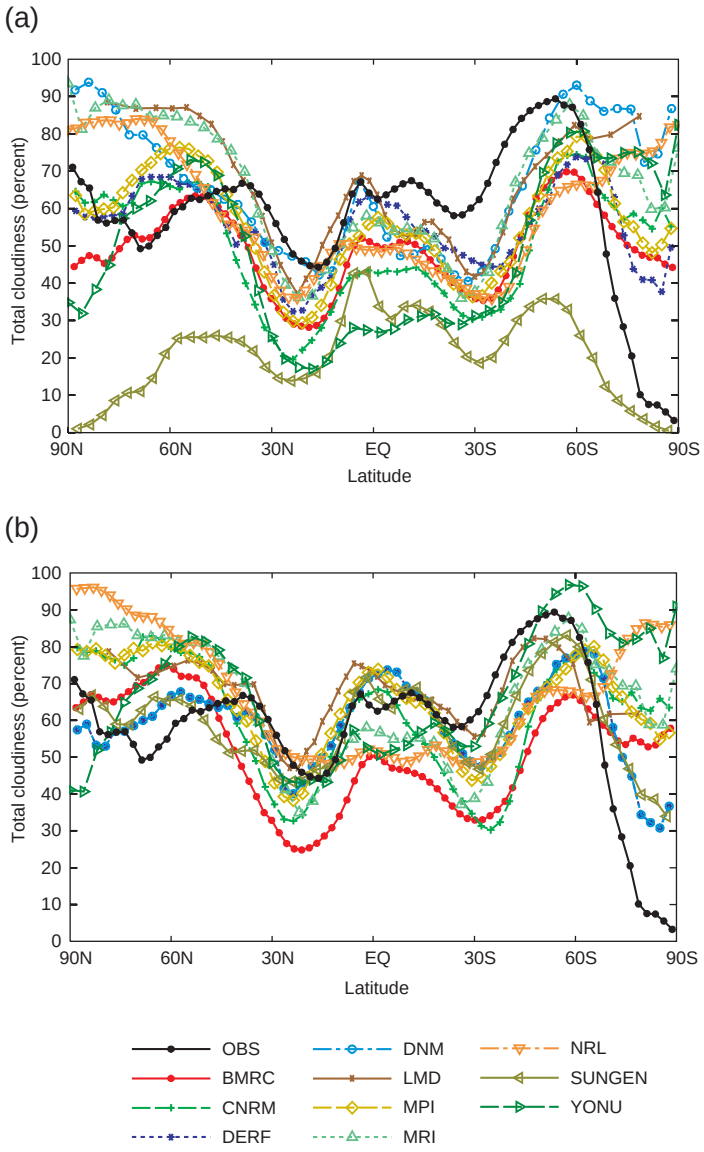

Figure 8.7: Zonally averaged December-January-February total cloudiness simulated by ten AMIP1 models (a) and by revised versions of the same ten models (b). The solid black line gives observed data from the International Satellite Cloud Climatology Project (ISCCP). From Gates *et al.* (1999).

ingly apparent that comparison between model simulations and observations of the stratosphere play an important role in detection and attribution of climate change (see Chapter 12).

An intercomparison of stratospheric climate simulations (Pawson *et al.*, 2000) shows that all models reproduce to some extent the zonally averaged latitudinal and vertical structure of the observed atmosphere, although several deficiencies are apparent. There is a tendency for the models to show a global mean cold bias at all levels (Figure 8.8a). The latitudinal distribution shows that almost all models are too cold in both hemispheres of the extra-tropical lower stratosphere (Figure 8.8b). There also is a large scatter in the tropical temperatures. Another common model deficiency is in the strengths and

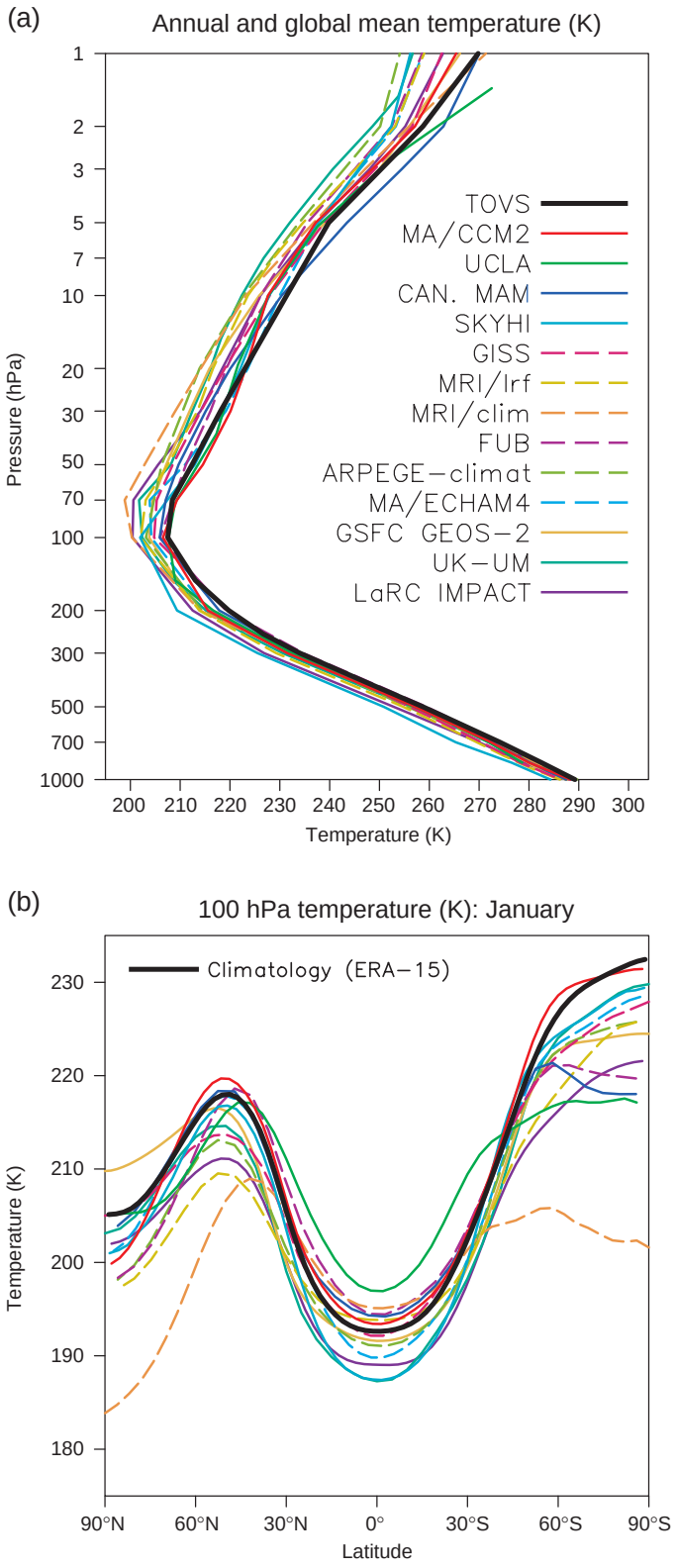

Figure 8.8: (a) Vertical structure of the annual-mean, globally averaged temperature (K) from observations and the thirteen models. (b) Latitudinal structure of January temperature at 100 hPa. From Pawson *et al.* (2000).

locations of the jets. The polar night jets in most models are inclined poleward with height, in noticeable contrast to an equatorward inclination of the observed jet. There is also a differing degree of separation in the models between the winter sub-tropical jet and the polar night jet.

Proper accounting of the role of gravity waves can improve stratospheric modelling. An orographic gravity wave scheme has been shown to improve the cold pole problem. Recent work with non-orographic gravity wave schemes show that waves of non-zero phase speed result in equatorward inclined jet through larger deceleration of westerly winds in polar regions (Manzini and McFarlane, 1998; Medvedev *et al*., 1998). Nevertheless, all models have shortcomings in their simulations of the present day climate of the stratosphere, which might limit the accuracy of predictions of future climate change (Shindell *et al*., 1999).

8.5.1.4 Summary

Coupled climate models simulate mean atmospheric fields with reasonable accuracy, with the exception of clouds and some related hydrological processes (in particular those involving upper tropospheric humidity). Since publication of the SAR, the models have continued to simulate most fields reasonably well while relying less on arbitrary flux adjustments. Problems in the simulation of clouds and upper tropospheric humidity, however, remain worrisome because the associated processes account for most of the uncertainty in climate model simulations of anthropogenic change. Incremental improvements in these aspects of model simulation are being made.

8.5.2 Ocean Component

8.5.2.1 Developments since the SAR

There have been a number of important developments in the ocean components of climate models since the SAR. Many climate models now being used for climate projections have ocean resolution of order 1 to 2° (Table 8.1), whereas at the time of the SAR most models used in projections had ocean resolution of order 3 to 5° (SAR Tables 5.1 and 6.3). The improved resolution may contribute to better representation of poleward heat transport (Section 8.5.2.2.2), although some key processes are still not resolved (see Sections 8.5.2.3, 8.9.2). Coupled models with even finer resolution are under development at the time of writing, but their computational expense makes their use in climate change projections impractical at present. Advances in the parametrization of sub-grid scale mixing (Chapter 7, Section 7.3.4) have also led to improved heat transports (Section 8.5.2.2.2). Some models have also adopted more advanced parametrizations of the surface mixed layer (Guilyardi and Madec, 1997; Gent *et al*., 1998; see Chapter 7, Section 7.3.1)

A formal comparison project of a wide range of ocean-climate models has not yet been set up. This is largely because the specification of surface forcing for the ocean, and the long spinup time-scale, make a co-ordinated experimental design more difficult to achieve than for the atmosphere. Nonetheless, a number of smaller, focused projects have provided valuable information about the performance of different model types and the importance of specific processes (Chassignet *et al*., 1996; Roberts *et al*., 1996; DYNAMO group 1997). Also, the Ocean Carbon Cycle Intercomparison Project (OCMIP) has compared the ocean circulation in a number of models (Sarmiento *et al.*, 2000; Orr *et al.,* 2001), and some comparisons have been made of the ocean components of coupled models under CMIP (see, e.g., Table 8.2; Jia, 2000)

The observational phase of the World Ocean Circulation Experiment (WOCE) was completed in 1997. Much analysis of the data to date has concentrated on individual sections or regions, and some of this analysis has been used in the assessment of climate models (e.g., Banks, 2000). Some initial attempts to put sections together into a consistent global picture also appear promising (MacDonald, 1998; de las Heras and Schlitzer, 1999). Such a global picture is an important baseline against which models can be tested (Gent *et al*., 1998; Gordon *et al*., 2000; see also Chapter 7, Section 7.6).

8.5.2.2 Present climate

8.5.2.2.1 Wind driven circulation

The wind-driven dynamics of the interior of the ocean basins are largely a linear response to the wind, and are generally well represented in current models, although there is still some observational debate over the reality of the classical Sverdrup balance (Wunsch and Roemmich, 1985). The main errors can usually be traced back to errors in the driving winds from the atmospheric model. The same can be said of surface Ekman transport, which makes an important contribution to poleward heat transport in the tropics (Danabasoglu, 1998). However, the western boundary currents and inertial recirculations which close the wind-driven gyres are generally poorly resolved by current models, and this may lead to an underestimate of the heat transport by this component of the system at higher latitudes (Fanning and Weaver, 1997a; Bryan and Smith 1998).

8.5.2.2.2 Heat transport and thermohaline circulation

Section 8.4.2 and Chapter 7, Section 7.6 discuss the fundamental importance of poleward heat transport in modelling the climate system. Ocean heat transport is greatly improved in some more recent models, compared with the models in use at the time of the SAR (see, e.g., Table 8.2; Chapter 7, Section 7.6). Increased horizontal resolution (Fanning and Weaver, 1997a; Gordon *et al*., 2000) and improved parametrization of sub-grid scale mixing (Danabasoglu and McWilliams, 1996; Visbeck *et al*., 1997; Gordon *et al*., 2000) have been important factors in this. The fresh water transports of coupled models have not been widely evaluated (see Section 8.4.2 and Chapter 7, Section 7.6). Bryan (1998) shows how fresh water imbalances can lead to long-term drifts in deep ocean properties.

The thermohaline circulation (THC) plays an important role in poleward heat transport, especially in the North Atlantic. Table 8.2 shows the strength of North Atlantic THC for various models. In contrast to the SAR, some non-flux adjusted models are now able to produce a THC with a realistic strength of around 20 Sv, which is stable for many centuries. A common systematic error at the time of the SAR was a model thermocline that was too deep and diffusive, resulting in deficient heat transport because the

Table 8.2: *Diagnostics of the ocean circulation from a number of coupled model control runs (see Table 8.1 for the specification of models).*

MODEL NAME	OVERTURNING ATLANTIC 25°N (Sv)	TEMPERATURE CONTRAST ATLANTIC 25°N (°C)	HEAT TRANSPORT ATLANTIC 25°N (PW)	HEAT TRANSPORT PACIFIC 25°N (PW)	HEAT TRANSPORT ATLANTIC 30°S (PW)	HEAT TRANSPORT INDO-PACIFIC 30°S (PW)	ACC TRANSPORT (Sv)	NIÑO 3 SST STD DEV (°C)	NIÑO 4 SST STD DEV (°C)
ARPEGE/OPA1	16.0	12.4	0.74	0.83	0.20	–0.79	60		
ARPEGE/OPA2	12.6	15.9	0.77	0.64	0.33	–0.69	143		
CCSR/NIES*	20.8	10.0	0.73	0.32	–0.06	–2.44	200	0.8	0.6
CGCM1*	18.3	9.0	0.72	0.40	0.22	–0.97	62	0.2	0.3
COLA1	16.4	11.0	0.38	0.55	–0.13	–0.48	10		
CSIRO Mk 2*	13.0	12.1	0.81	0.43	0.21	–1.31	103		
CSM 1.0	24.6	14.0	1.30	0.74	0.54	–1.14	236	0.5	0.5
CSM 1.3	22		1.15	0.8	0.45	–1.10	178		
ECHAM1/LSG*	30						100		
ECHAM3/LSG*	28.1	9.9	0.76	0.26	0.09	–1.98	112	0.2	0.3
ECHAM4/OPYC3*	22.9	7.3	0.59	0.49	–0.19	–2.31	122	0.8	0.5
GFDL_R15_a*	15.0	9.9	0.59	0.34	0.08	–1.09	70	0.5	0.4
GISS1	18.6	12.3	1.01	0.76	0.37	–0.72	75		
GISS2	7.9	21.5	0.56	0.67	0.07	–0.60			
GOALS			0.68	0.44	0.05	–1.56	74		
HadCM2*	16.8	11.9	0.82	0.34	0.40	–0.93	216		
HadCM3	18.1	14.8	1.10	0.51	0.55	–1.25	204	1.1	1.0
IPSL-CM1	11.2	15.2	0.61	0.61	0.27	–0.81	66	0.3	0.2
IPSL-CM2	22.7	11.1	0.90	0.66	0.26	–1.48	164		
MRI1*	1.6		–0.29	0.82	–1.00	–1.08	50	0.4	0.7
MRI2*	17.0		0.86	0.78	0.26	–1.21	83	1.9	1.7
NCAR1	35.8	10.3	0.58	0.32	0.80	1.00	79	0.5	0.4
NRL*	3.1		0.43	0.72	-0.10	–0.77	66		
DOE PCM	27.2	12.7	1.13	0.77	0.40	–0.73			
BMRCa							39	0.4	0.4
COLA2								0.7	0.5
GFDL_R30_c*								0.4	0.6
OBSERVED	19.3[a]	14.1[a]	1.15[b]	0.76[c]	0.50[d]	–1.34[d]	123[e]	0.7[f]	0.5[f]

Positive heat transport values indicate northward transport. An asterisk indicates flux adjusted models. Cells are left blank where particular data items are unavailable.

Temperature contrast Atlantic 25°N: The difference between the mean temperatures of the northward flowing surface water and the southward flowing North Atlantic Deep Water at 25°N (Jia 2000).

NIÑO3/4 SST Std Dev: standard deviation of the sea surface temperature in the NIÑO3 and NIÑO4 regions of the tropical Pacific.

References:

[a] Hall and Bryden, 1982

[b] Trenberth, 1998a (see Chapter 7, Section 7.6)

[c] Bryden *et al.*, 1991

[d] MacDonald, 1998

[e] Whitworth and Petersen, 1985

[f] Parker *et al.*, 1995

temperature contrast between cold, southward and warm, northward flows was too weak. The models with realistic North Atlantic heat transports generally maintain a realistic temperature contrast (Table 8.2). Some models also show improved realism in the spatial structure of the THC, with separate deep water sources in the Nordic Seas and in the Labrador Sea (Wood *et al*., 1999).

Interior diapycnal mixing plays a critical role in the thermohaline circulation. Recent process studies (part of WOCE) have confirmed that such mixing is highly localised in the deep ocean (Polzin *et al*., 1997; Munk and Wunsch, 1998). This mixing is very crudely represented in climate models, and it is not known whether this deficiency has a significant effect on the model thermohaline circulations (Marotzke, 1997).

Although overall heat transports are now better represented in some models, the partition of the heat transport between different components of the circulation may not agree so well

with observational estimates (Gordon *et al.*, 2000). How important such discrepancies may be in modelling the transient climate change response is not well understood.

The deep western boundary current, which carries much of the deep branch of the North Atlantic THC, contains a number of strong recirculating gyres (e.g., Hogg, 1983). These recirculations may act as a buffer, delaying the response of the THC to climate anomalies. The representation of these recirculations in climate models, and their importance in transient climate response, have not been evaluated.

8.5.2.2.3 Antarctic circumpolar current (ACC)

Many current models produce rather poor estimates of the volume transport of the Antarctic circumpolar current (ACC) (Table 8.2). The reason for this is not fully understood. Thermohaline as well as wind-driven processes are believed to be important (Cox 1989; Bryan 1998). The problem is shared by some eddy-permitting ocean models, so insufficient horizontal resolution does not seem to be the only factor. The path of the ACC is largely controlled by topography, and errors in the path can lead to significant local sea surface temperature errors. The Atlantic and Indian sectors of the southern ocean appear to be particularly susceptible (e.g., Figure 8.1b; Gent *et al.*, 1998; Gordon *et al.*, 2000). However, it is not clear how, or whether, the transport and SST errors impact on the atmospheric climate or on the climate change response of the models.

8.5.2.2.4 Water mass formation

At high latitudes, deep convection and subsequent spreading of dense water form the deep water masses that fill most of the volume of the ocean. At mid-latitudes, the processes of mode water formation and thermocline ventilation are the means by which surface changes are propagated into the thermocline (Chapter 7, Section 7.3.1). These processes play an important role in determining the effective rate of heat uptake by the ocean in response to climate change (see Chapter 9, Section 9.3.4.2), and in the response of the THC (see Chapter 9, Section 9.3.4.3). Water mass formation processes can be evaluated directly from model fields (Guilyardi, 1997; Doney *et al.*, 1998), or indirectly using model simulations of the ocean uptake of anthropogenic tracers such as CFCs and carbon 14 (Robitaille and Weaver,

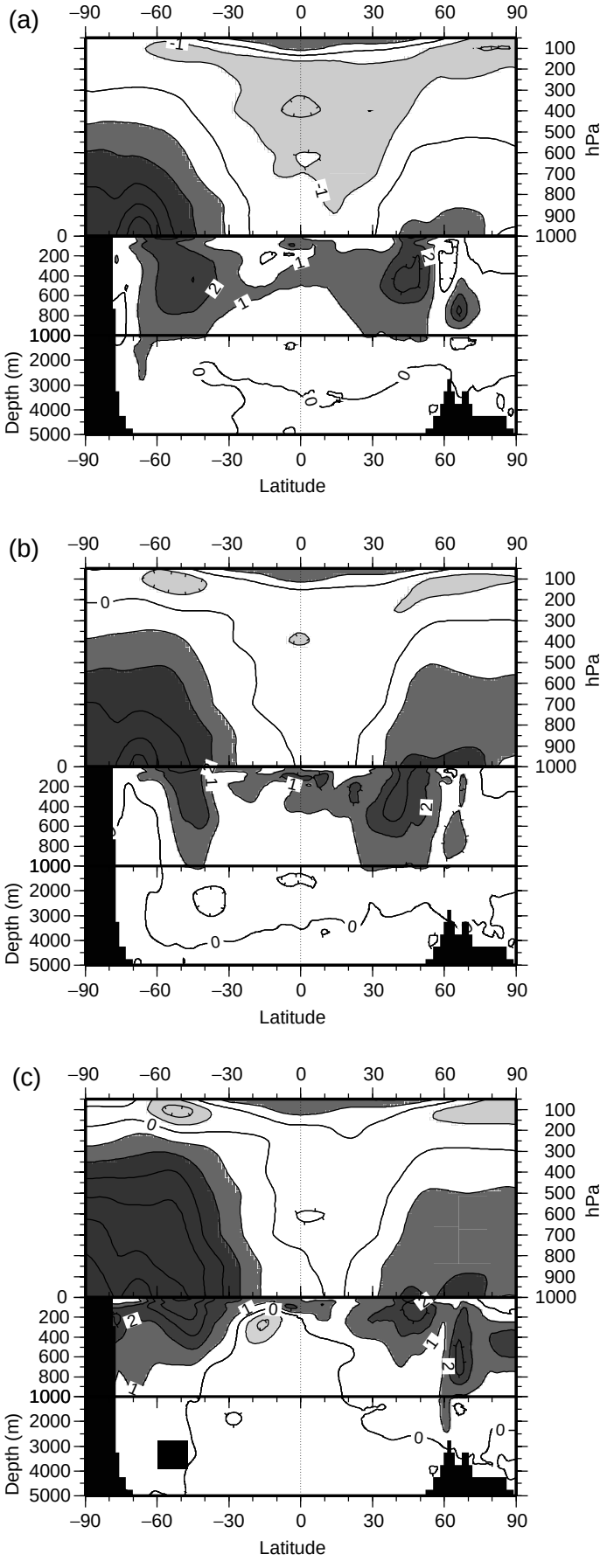

Figure 8.9: Zonal mean air and sea temperature "errors" in °C (defined here as the difference from the initial model state, which was derived from observations), for three different coupled models. The models are all versions of the ARPEGE/OPA model, with T31 atmospheric resolution, and differ only in the parametrization of lateral mixing used in the ocean component ((a) lateral diffusion, (b) isopycnal diffusion, (c) the scheme of Gent and McWilliams (1990)). The different mixing schemes produce different rates of heat transport between middle and high latitudes, especially in the Southern Hemisphere. The atmosphere must adjust in order to radiate the correct amount of heat to space at high latitudes (Chapter 7, Section 7.6 and Section 8.4.1), and this adjustment results in temperature differences at all levels of the atmosphere. From Guilyardi (1997).

Table 8.3: *Coupled model simulations (CMIP1) for December, January, February (DJF) and June, July, August (JJA) of sea-ice cover (columns 2 to 5) and snow cover (10^6 km^2) columns 6 and 7). Model names (column 1) are supplemented with ordinal numbers (in brackets) which refers to the models listed in Table 8.1. The observed sea-ice extent is from Gloersen et al. (1992) and the climatological observed snow is from Foster and Davy (1988).*

Model name	Sea-ice cover (10^6 km^2)				Snow cover (10^6 km^2)	
	Northern Hemisphere		Southern Hemisphere		Northern Hemisphere	
	DJF (winter)	JJA (summer)	JJA (winter)	DJF (summer)	DJF (winter)	JJA (summer)
ARPEGE/OPA1 (1)	10.1	8.8	2.5	1.9	50.6	19.2
BMRCa (3)	13.7	12.0	0.0	0.0	42.4	2.2
CCSR/NIES (5)	13.0	9.3	16.7	8.6	46.2	12.0
CGCM1 (6)	8.6	7.0	12.3	8.2	47.5	13.9
COLA1 (8)	9.4	5.9	0.0	0.0	58.7	2.5
CSIRO Mk2 (10)	14.3	14.1	14.2	13.6	48.8	18.9
CSM 1.0 (11)	18.6	13.1	22.8	10.0	43.7	4.7
ECHAM3/LSG (14)	12.5	10.4	11.1	7.3	35.8	9.1
ECHAM4/OPYC3 (15)	10.5	9.1	21.0	13.4		
GFDL_R15_a (16)	10.6	8.8	13.2	6.5	56.9	2.4
GISS1 (19)	15.3	14.6	8.7	7.1		
GISS2 (20)	15.7	15.2	10.9	9.5	43.2	9.3
HadCM2 (22)	12.0	10.1	24.7	11.8	45.0	8.2
IPSL-CM1 (24)					44.2	11.2
MRI1 (26)	19.4	18.3	14.5	4.1	60.2	11.6
NCAR1 (28)	11.6	10.6	20.8	16.4	38.9	3.6
Observed	14.5	11.5	16.0	7.0	49.3	3.7

1995; Dixon *et al*., 1996; England and Rahmstorf, 1999; Goosse *et al*., 1999; England and Maier-Reimer, 2001). A conclusion from many of these studies is that, while the models clearly show some skill in this area, ventilation processes are sensitive to the details of the ocean mixing parametrization used. Wiebe and Weaver (1999) show that the efficiency of ocean heat uptake is also sensitive to these parametrizations.

8.5.2.3 Summary

Considerable progress has been made since the SAR in the realism of the ocean component of climate models. Models now exist which simultaneously maintain realistic poleward heat transports, surface temperatures and thermocline structure, and this has been a vital contributor to the improvement in non-flux adjusted models. However, there are still a number of processes which are poorly resolved or represented, for example western boundary currents (see Chapter 7, Section 7.3.6), convection (Chapter 7, Section 7.3.2), overflows (Chapter 7, Section 7.3.5), Indonesian through flow, eddies (including Agulhas eddies which travel long distances and may be hard to treat by a local parametrization; Chapter 7, Section 7.3.4), Antarctic Bottom Water formation (Chapter 7, Section 7.3.2) and interior diapycnal mixing (Chapter 7, Section 7.3.3). In many cases, the importance of these processes in controlling transient climate change has not been evaluated. Over the next few years there is likely to be a further move to finer resolution models, and a wider range of model types; these developments are likely to reduce further some of these uncertainties. Finally, there is still only patchy understanding of the effects of sub-grid scale parametrizations in the context of coupled models. Valuable understanding can be gained from sensitivity studies using ocean or atmosphere models alone, but Figure 8.9 shows the inherently coupled nature of the climate system – changes in ocean parametrizations can have a significant impact throughout the depth of the atmosphere (the reverse is also true). Further sensitivity studies in the coupled model context will help to quantify and reduce uncertainty in this area.

8.5.3 Sea Ice Component

While the important role of sea ice in projections of future climate has been widely recognised (Chapter 7, Section 7.5.2), results of systematic intercomparisons or sensitivity studies of AOGCM sea-ice components remain very limited. The sea-ice simulations of fifteen global coupled models contributed to CMIP1 are summarised in Table 8.3. (All these models are also presented in Table 8.1, where the last two columns indicate whether an ice dynamics scheme is included, and whether the model is flux adjusted.) Sea-ice thermodynamic formulations of the coupled models are mostly based on simplified schemes: few employ a multi-layer representation of heat transfer through the ice, while the rest assume a linear temperature profile. In addition, roughly half of the models ignore leads and polynyas in the ice although these account for principal thermodynamic coupling of the atmosphere and ocean. Some models also ignore the thermodynamic effects of snow on sea ice. Despite the rather mature status of sea-ice dynamics modelling (e.g., the Sea Ice Model Intercomparison Project (SIMIP), Lemke *et al*., 1997),

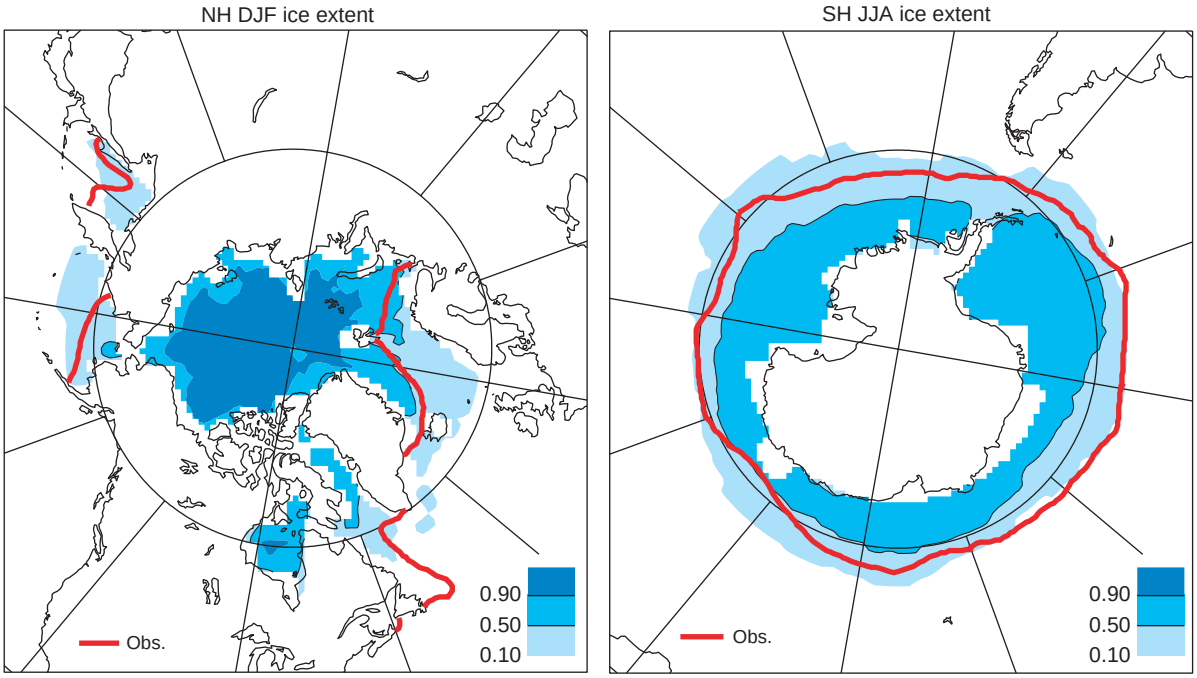

Figure 8.10: Illustration of the range of sea-ice extent in CMIP1 model simulations listed in Table 8.3: Northern Hemisphere, DJF (left) and Southern Hemisphere, JJA (right). For each model listed in Table 8.3, a 1/0 mask is produced to indicate presence or absence of ice. The fifteen masks were averaged for each hemisphere and season. The 0.5 contour therefore delineates the region for which at least half of the models produced sea ice. The 0.1 contour indicates the region outside of which only 10% of models produced ice, while the 0.9 contour indicates that region inside of which only 10% of models did not produce ice. The observed boundaries are based on GISST_2.2 (Rayner *et al.*, 1996) averaged over 1961 to 1990.

only two of the fifteen models include a physically based ice dynamics component. Three of the fifteen models allow ice to be advected with the ocean currents (the so-called 'free drift' scheme), and the remainder assume a motionless ice cover. Overall, this highlights the slow adoption, within coupled climate models, of advances in stand-alone sea ice and coupled sea-ice/ocean models (Chapter 7, Section 7.5.2).

Table 8.3 provides a comparison of ice extent, defined as the area enclosed by the ice edge (which is in turn defined as the 0.1 m thickness contour or the 15% concentration contour, depending on the data provided), for winter and summer seasons in each hemisphere. The last row of the table provides an observed estimate based on satellite data (Gloersen *et al.*, 1992) covering the period 1978 to 1987. It should be noted that assessment of sea-ice model performance continues to be hampered by observational problems. For the satellite period (1970s onward) the accuracy of observations of sea-ice concentration and extent is fair, however observational estimates of sea-ice thickness and velocity are far from satisfactory.

Figure 8.10 provides a visual presentation of the range in simulated ice extent, and was constructed as follows. For each model listed in Table 8.3, a 1/0 mask was produced to indicate presence or absence of ice. The fifteen masks were averaged for each hemisphere and season and the percentage of models that had sea ice at each grid point was calculated.

There is a large range in the ability of models to simulate the position of the ice edge and its seasonal cycle, particularly in the Southern Hemisphere. Models that employ flux adjustment tend, on average, to produce smaller ice extent errors, but there is no obvious connection between fidelity of simulated ice extent and the inclusion of an ice dynamics scheme. The latter finding probably reflects the additional impact of errors in the simulated wind field and surface heat fluxes that offset, to a great extent, any improvements due to including more realistic parametrizations of the physics of ice motion. In turn this partially explains the relative slowness in the inclusion of sophisticated sea ice models with AOGCMs. However, even with quite simple formulations of sea ice, in transient simulations, some AOGCMs demonstrate ability to realistically reproduce observed annual trend in the Arctic sea ice extent during several past decades of the 20th century (see Chapter 2, Section 2.2.5.2), which adds some more confidence in the use of AOGCM for future climate projections (Vinnikov *et al.*, 1999)

8.5.4 Land Surface Component (including the Terrestrial Cryosphere)

8.5.4.1 Introduction

The role of the land surface (soil, vegetation, snow, permafrost and land ice) was discussed in detail in the SAR. The SAR noted that improvements had occurred in our ability to model land-surface processes but that there was a wide disparity among current land-surface schemes when forced by observed meteorology. Our physical understanding of the role of land-surface processes within the climate system was discussed in Chapter 7, Section 7.4.1.

8.5.4.2 Developments since the SAR

Most of the effort in trying to reduce the disparity in land-surface scheme performance has been performed in offline intercomparisons under the auspices of International Geosphere Biosphere Programme (IGBP) and the World Climate Research Programme (WCRP). Due to the difficulties in coupling multiple land-surface schemes into climate models (see Section 8.5.4.3) specific endeavours have been: the Project for the Intercomparison of Land-surface Parametrization Schemes (PILPS), the Global Soil Wetness Project (GSWP), the International Satellite Land Surface Climatology Project (ISLSCP), and the Biological Aspects of the Hydrological Cycle (BAHC) (e.g., Henderson-Sellers *et al.*, 1995; Polcher *et al.*, 1996; Dirmeyer *et al.*, 1999; Schlosser *et al.*, 2000). In comparisons between offline simulation results and observations, difficulties in partitioning available energy between sensible and latent heat and partitioning of available water between evaporation and runoff were highlighted (e.g., Chen *et al.*, 1997; Schlosser *et al.*, 2000). While we are far from a complete understanding of why land surface models differ by such a large degree, some progress has been made (e.g., Koster and Milly, 1997; Desborough, 1999). Significant progress has also been made in adding physical processes into land-surface models (see Chapter 7, Section 7.4). Where some observations exist (e.g., for incoming solar radiation, net radiation and soil moisture), an evaluation of the ability of current climate models to simulate these quantities suggests that significant problems remain (Wild *et al.*, 1997; Garratt *et al.*, 1998; Robock *et al.*, 1998). The evaluation of surface processes in climate models tends to focus on monthly and, less commonly, daily quantities. An evaluation of the ability of climate models to simulate land-surface quantities at the diurnal scale has yet to be performed systematically, although some efforts have been initiated since the SAR (e.g., Watterson, 1997).

Work since the SAR has also focused on trying to identify the relative significance of land-surface processes in comparison with other components of climate models. The sophistication in the representation of the land surface in coupled models is varied (see Chapter 7 and Table 8.1). The addition of more realistic plant physiology in some land-surface models (e.g., Bonan, 1995; Sellers *et al.*, 1996 (See Chapter 7, Section 7.4)) which permits the simulation of carbon dioxide (CO_2) and gas isotope fluxes, provides the opportunity to compare these quantities with local scale, regional scale and global scale observations from flux towers and satellites.

Snow, and the snow albedo feedback, are important components of the land surface. Current climate models incorporate snow in varying degrees of sophistication and there is currently major uncertainty in the ability of land-surface schemes to simulate snow mass or cover (see Chapter 7, Section 7.5). Frei and Robinson (1998) evaluated the simulation of monthly mean snow extent from 27 AMIP AGCMs and found weaknesses in the simulation of the seasonal cycle of snow extent and a general underestimation in interannual variability. These weaknesses limit confidence in the simulation of mid- and high latitude changes simulated by current climate models, since a failure to simulate snow accurately tends to impact significantly on albedo, surface roughness length and soil moisture (and therefore precipitation on subsequent seasons).

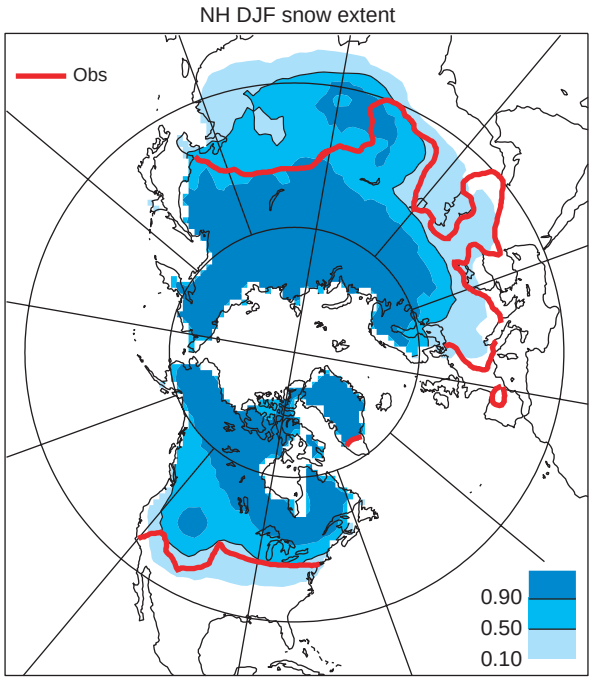

Figure 8.11: Illustration of the range of snow cover extent in CMIP1 model simulations listed in Table 8.3: Northern Hemisphere, DJF. The figure is constructed similarly to Figure 8.10 based on the prescribed 1 cm cutoff. The observed boundary is based on Foster and Davy (1988).

The Northern Hemisphere snow simulations of fourteen global coupled models contributed to CMIP are summarised in Figure 8.11 and Table 8.3. Figure 8.11 (constructed similarly to Figure 8.10) provides a visual presentation of the range in simulated (land only) snow extent. The relative error in simulated snow extent is larger in summer than in winter. There is no obvious connection between either flux adjustment or land-surface scheme and the quality of the simulated snow extent.

Other components of the land surface potentially important to climate change include lateral water flows from the continents into the ocean, permafrost, land-based ice and ice sheets. Some land-surface schemes now include river routing (e.g., Sausen *et al.*, 1994; Hagemann and Dümenil, 1998) in order to simulate the annual cycle of river discharge into the ocean. This appears to improve the modelling of runoff from some large drainage basins (Dümenil *et al.*, 1997), although water storage and runoff in regions of frozen soil moisture remain outstanding problems (Arpe *et al.*, 1997; Pitman *et al.*, 1999). River routing is also useful in diagnosing the representation of the hydrological cycle in models (e.g., Kattsov *et al.*, 2000). There has been limited progress towards developing a permafrost model for use in climate models (e.g., Malevsky-Malevich *et al.*, 1999) although existing simple models appear to approximate the observed range in permafrost reasonably well (e.g., Volodin and Lykosov, 1998). The dynamics of ice sheets and calving are not presently represented in coupled climate models. To close the fresh water budget for the coupled system, fresh water which accumulates on Greenland and Antarctica is usually uniformly distributed either

over the entire ocean or just in the vicinity of the ice sheets (e.g., Legutke and Voss, 1999; Gordon *et al.*, 2000). The impact of these limitations has yet to be investigated.

8.5.4.3 Does uncertainty in land surface models contribute to uncertainties in climate prediction?

Uncertainty in climate simulations resulting from the land surface has traditionally been deduced from offline experiments (see Chapter 7 and Section 8.5.4.2) due to difficulties associated with comparing land-surface schemes when forced by different climate models (e.g., Polcher *et al.*, 1998b). Some work since the SAR has focused on the sensitivity of land-surface schemes to uncertainties in parameters (e.g., Milly, 1997) and on whether different land-surface schemes, coupled to climate models, lead to different climate simulations or different sensitivity to increasing CO_2 (Henderson-Sellers *et al.*, 1995).

Polcher *et al.* (1998a) used four different climate models, each coupled to two different land-surface schemes to explore the role of the land surface under $1\times CO_2$ and $2\times CO_2$. The modification to the land-surface scheme tended to focus on aspects of the soil-hydrology and vegetation/soil-moisture interactions (Gedney *et al.*, 2000). To measure the uncertainty associated with surface processes, the variance of anomalies caused by the changes to the surface scheme in the four climate models was computed. The uncertainty in climate models was computed by using the variance of annual anomalies relative to a consensus (the average of all models). This measure takes into account the differences between climate models, as well as the internal variance of the atmosphere. With these two variances, a ratio was constructed to evaluate the relative importance of the uncertainty linked to surface processes in comparison to the uncertainty linked to other aspects of the climate model (Crossley *et al.*, 2000). In Figure 8.12a this diagnostic is applied to zonal mean values over land for the $1\times CO_2$ experiments. The highest values, indicating a large contribution of surface processes to the uncertainty, were obtained for evaporation, the variable most affected by surface processes (the asterisk indicates significance at the 95% of this measure). Surface air temperature was strongly dependent on surface processes in the tropics but at high latitudes its uncertainty was dominated by atmospheric processes. In the high latitudes, the hydrological cycle (characterised by precipitation and cloud cover) was partly controlled by the surface as indicated by high values of the ratio. Overall, Figure 8.12 shows that the contribution to total uncertainty in the simulation of climate resulting from the land surface may be large and varies geographically.

Figure 8.12b displays the same diagnostic but for the anomalies resulting from a doubling of CO_2. The maximum uncertainty is concentrated in the tropics and the variables most affected are cloud cover and temperature. The uncertainty in evaporation changes is large but does not dominate as in the control climate. In the Northern Hemisphere a secondary peak was found for cloud cover and to some extent for precipitation, indicating that a significant part of the uncertainties in the impact of climate change on the hydrological cycle originates from land-surface processes. The shapes of these curves are very different in the two figures, indicating that different processes are responsible for the uncertainties in the control simulation and the climate change anomalies. This implies that the sensitivity of land-surface schemes to climate change needs to be evaluated and that it can not be deduced from results obtained for present day conditions. Gedney *et al.* (2000) analysed these results regionally and found that the simulations differ markedly in terms of their predicted changes in evapotranspiration and soil moisture. They conclude that uncertainty in the predicted changes in surface hydrology is more dependent on gross features of the runoff versus soil moisture relationship than on the detailed treatment of evapotranspiration. The importance of hydrology was also demonstrated by Ducharne *et al.* (1998) and Milly (1997).

Other work has involved using global climate fields provided by GCM analyses to force land-surface models offline (see Dirmeyer *et al.*, 1999). In this study, different land-surface models use the same atmospheric forcings, and the same soil and

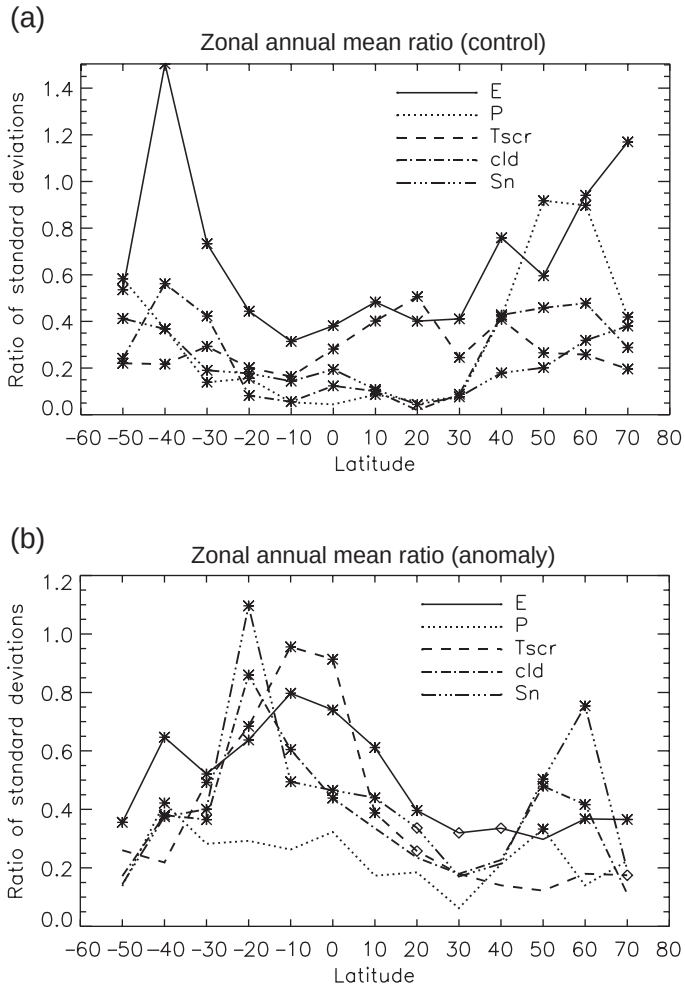

Figure 8.12: An uncertainty ratio for 10-degree latitude bands; (a) control simulations; (b) difference between the control and doubled greenhouse gas simulations. *E* is evaporation, *P* is precipitation, *Tscr* is screen temperature, *cld* is the percentage cloud cover and *Sn* is the net short-wave radiation at the surface. The units on the Y-axis are dimensionless. An asterisk means the value is statistically significant at 95% and a diamond at 90% (see Crossley *et al.*, 2000).

vegetation data sets. Model outputs are compared with regional runoff and soil moisture data sets and, where available, to observations from large-scale field experiments. To date, results highlight the differences between land-surface model treatments of large-scale hydrology and snow processes; it is anticipated that these and other trials will lead to significant improvements in these problem areas in the near future.

Uncertainty in land-surface processes, coupled with uncertainty in parameter data combines, at this time, to limit the confidence we have in the simulated regional impacts of increasing CO_2. In general, the evidence suggests that the uncertainty is largely restricted to surface quantities (i.e., the large-scale climate changes simulated by coupled climate models are probably relatively insensitive to land-surface processes). Our uncertainty derives from difficulties in the modelling of snow, evapotranspiration and below-ground processes. Overall, at regional scales, and if land-surface quantities are considered (soil moisture, evaporation, runoff, etc.), uncertainties in our understanding and simulation of land-surface processes limit the reliability of predicted changes in surface quantities.

8.5.5 Past Climates

Accurate simulation of current climate does not guarantee the ability of a model to simulate climate change correctly. Climate models now have some skill in simulating changes in climate since 1850 (see Section 8.6.1), but these changes are fairly small compared with many projections of climate change into the 21st century. An important motivation for attempting to simulate the climatic conditions of the past is that such experiments provide opportunities for evaluating how models respond to large changes in forcing. Following the pioneering work of the Co-operative Holocene Mapping Project (COHMAP-Members, 1988), the Paleoclimate Modeling Intercomparison Project (PMIP) (Joussaume and Taylor, 1995; PMIP, 2000) has fostered the more systematic evaluation of climate models under conditions during the relatively well-documented past 20,000 years. The mid-Holocene (6,000 years BP) was chosen to test the response of climate models to orbital forcing with CO_2 at pre-industrial concentration and present ice sheets. The orbital configuration intensifies (weakens) the seasonal distribution of the incoming solar radiation in the Northern (Southern) Hemisphere, by about 5% (e.g., 20 Wm^{-2} in the boreal summer). The last glacial maximum (21,000 years BP) was chosen to test the response to extreme cold conditions

8.5.5.1 Mid-Holocene

Atmosphere alone simulations

Within PMIP, eighteen different atmospheric general circulation models using different resolutions and parametrizations have been run under the same mid-Holocene conditions, assuming present-day conditions over the oceans (Joussaume *et al*., 1999). In summer, all of the models simulate an increase and northward expansion of the African monsoon; conditions warmer than present in high northern latitudes, and drier than present in the interior of the northern continents. Palaeo-data do not support drying in interior Eurasia (Harrison *et al*., 1996; Yu and Harrison, 1996; Tarasov *et al*., 1998), but they clearly show an expanded monsoon in northern Africa (Street-Perrott and Perrott 1993; Hoelzmann *et al*., 1998; Jolly *et al*., 1998a, 1998b), warming in the Arctic (Texier *et al*., 1997), and drying in interior North America (Webb *et al*., 1993).

Vegetation changes reconstructed from pollen data in the BIOME 6000 project (Jolly *et al*., 1998b; Prentice and Webb III, 1998) provide a quantitative model-data comparison in northern Africa. The PMIP simulations produce a northward displacement of the desert-steppe transition, qualitatively consistent with biomes, but strongly underestimated in extent (Harrison *et al*., 1998). At least an additional 100 mm/yr of precipitation would be required for most models to sustain grassland at 23°N, i.e., more than twice as much as simulated in this area (Joussaume *et al*., 1999) (Figure 8.13). The increased area of lakes in the Sahara has also been quantified (Hoelzmann *et al*., 1998) and, although the PMIP simulations do produce an increase, this latter is not large enough (Coe and Harrison, 2000). A similar underestimation is obtained at high latitudes over northern Eurasia, where PMIP simulations produce a northward shift of the Arctic tree-line in agreement with observed shifts (Tarasov *et al*., 1998) but strongly underestimated in extent (Kutzbach *et al*., 1996b; Texier *et al*., 1997; Harrison *et al*., 1998). Model-data discrepancies may, however, be due to missing feedbacks in the simplified PMIP experimental design.

Ocean feedbacks

Recent experiments with asynchronous (Kutzbach and Liu 1997; Liu *et al*., 1999) and synchronous (Hewitt and Mitchell, 1998; Braconnot *et al*., 2000) coupling of atmospheric models to full dynamical ocean models have been performed for the mid-Holocene. They all produce a larger enhancement of the African monsoon than shown in their PMIP atmosphere only experiments, resulting from the ocean thermal inertia and changes in the meridional ocean heat transport (Braconnot *et al*., 2000). However, the changes are not sufficient to reproduce the observed changes in biome shifts over northern Africa.

Coupled models are also beginning to address the issue of changes in interannual to inter-decadal variability under conditions of large differences in the basic climate. Some palaeo-environmental evidence has suggested that short-term climate variability associated with El Niño-Southern Oscillation (ENSO) was reduced during the early to mid-Holocene (Sandweiss *et al*., 1996; Rodbell, 1999). Up to now, ENSO variability has only been analysed in the CSM simulation, exhibiting no significant change at the mid-Holocene (Otto-Bliesner, 1999).

Land-surface feedbacks

Land-surface changes also provide an additional important feedback. During the mid-Holocene, vegetation changes over northern Africa have indeed favoured a larger increase in monsoon precipitation as shown through sensitivity experiments (Kutzbach *et al*., 1996a; Brostrom *et al*., 1998; Texier *et al*., 2000) as well as through coupled atmosphere-vegetation experiments (Claussen and Gayler, 1997; Texier *et al*., 1997; Pollard *et al*., 1998; Doherty *et al*., 2000; de Noblet *et al*., 2000). Including

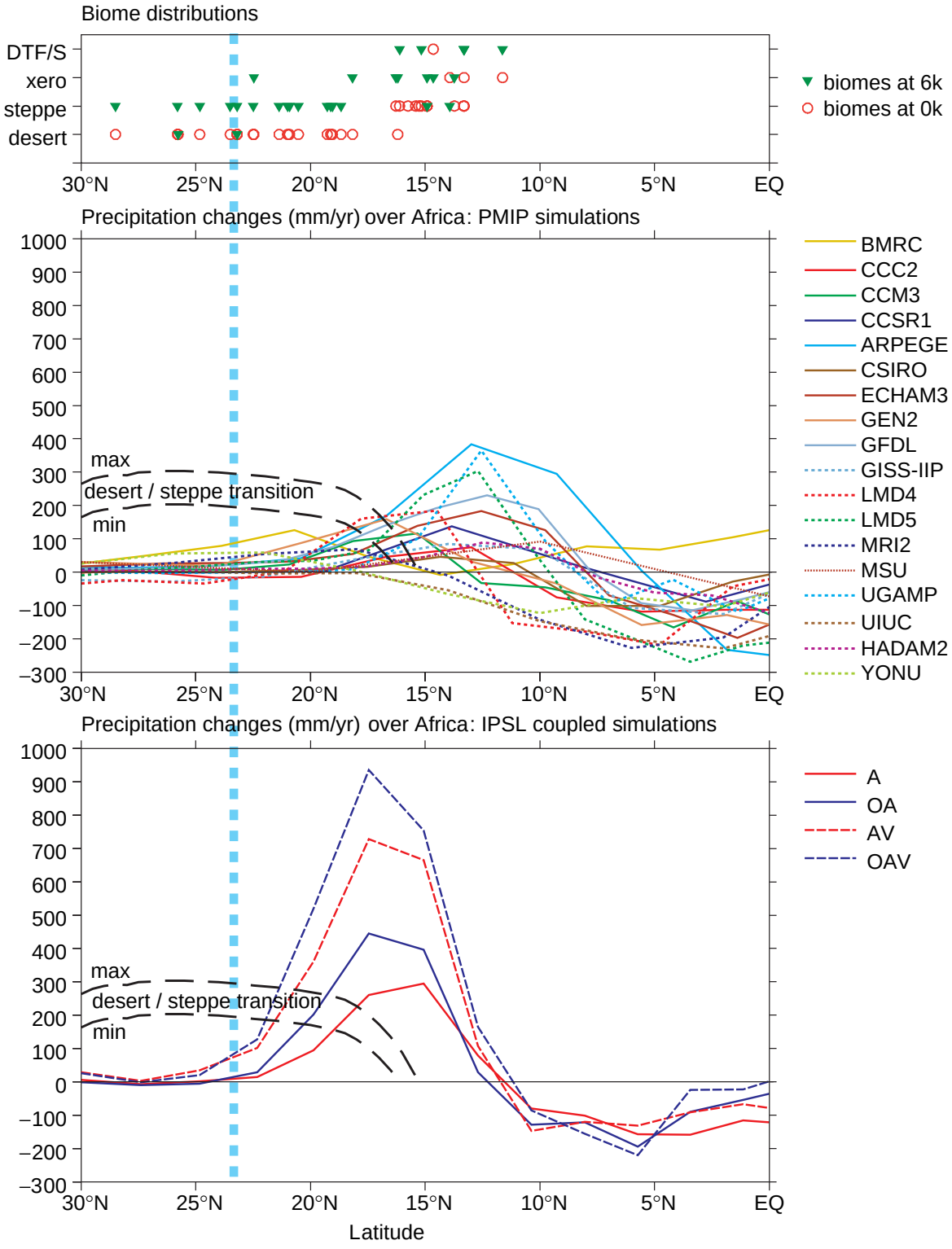

Figure 8.13: Annual mean precipitation changes (mm/yr) over Africa (20°W to 30°E) for the mid-Holocene climate: (upper panel) Biome distributions (desert, steppe, xerophytic and dry tropical forest/savannah (DTF/S)) as a function of latitude for present (red circles) and 6,000 yr BP (green triangles), showing that steppe vegetation replaces desert at 6,000 yr BP as far north as 23°N (vertical blue dashed line); (middle panel) 6000 yr BP minus present changes as simulated by the PMIP models. The black hatched lines are estimated upper and lower bounds for the excess precipitation required to support grassland, based on present climatic limits of desert and grassland taxa in palaeo-ecological records, the intersection with the blue vertical line indicates that an increase of 200 to 300 mm/yr is required to sustain steppe vegetation at 23°N at 6,000 yr BP (redrawn from Joussaume *et al.*, 1999); (lower panel) same changes for the IPSL atmosphere-alone (A), i.e., PMIP simulation, the coupled atmosphere-ocean (OA), the atmosphere-alone with vegetation changes from OA (AV) and the coupled atmosphere-ocean-vegetation (OAV) simulations performed with the IPSL coupled climate model. The comparison between AV and OAV emphasises the synergism between ocean and land feedbacks (redrawn from Braconnot *et al.*, 1999).

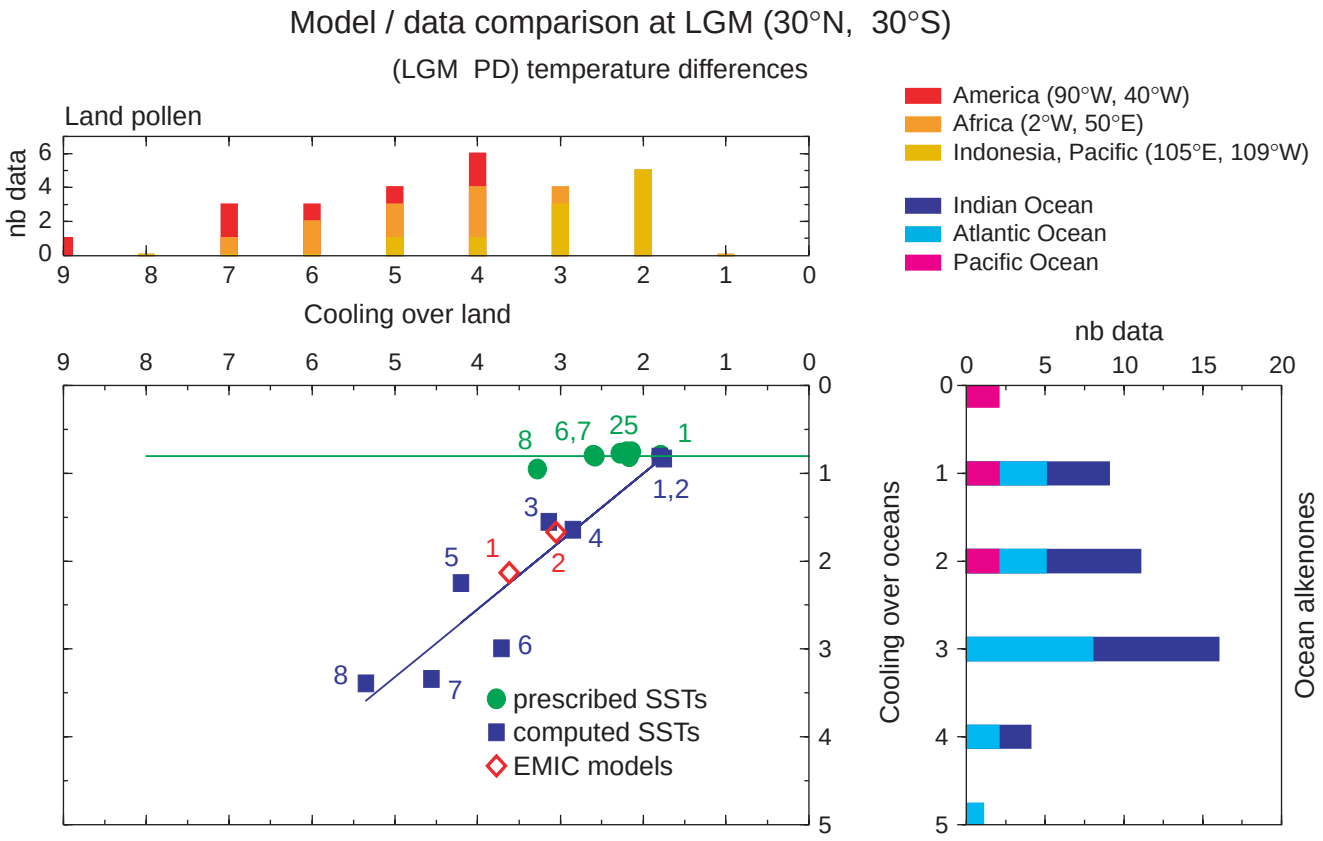

Figure 8.14: Annual mean tropical cooling at the last glacial maximum: comparison between model results and palaeo-data. (Centre panel) simulated surface air temperature changes over land are displayed as a function of surface temperature changes over the oceans, both averaged in the 30°S to 30°N latitudinal band, for all the PMIP simulations: models with prescribed CLIMAP SSTs (circles) and coupled atmosphere-mixed layer ocean models (squares) (from Pinot *et al*., 1999). Numbers refer to different models: circles, 1: LMD4, 2-5: MRI2, ECHAM3, UGAMP, LMD5 (higher resolution), 6-7: CCSR/NIES1, LMD5, 8: GEN2. Squares : 1: LMD4,2: UGAMP, 3: GEN2, 4: GFDL, 5: HADAM2, 6: MRI2, 7: CCM1, 8: CCC2 (names refer to Tables 8.1 and 8.5). Results from two EMIC models including a dynamical ocean model have also been displayed (diamonds): 1-UVIC (Weaver *et al*., 1998), 2-CLIMBER-2 (Petoukhov *et al*., 2000).
The comparison with palaeo-data: (upper panel) over land is with estimates from various pollen data for altitudes below 1,500m (the label "*nb data*" refers to the number of data points in three different regions corresponding to the temperature change estimate plotted in the abscissa) from (Farrera, *et al*., 1999); (right panel) the distribution of SST changes estimated from alkenones in the tropics from the Sea Surface Temperature Evolution Mapping Project based on Alkenone Stratigraphy (TEMPUS) (Rosell-Melé, *et al*., 1998) (*nb data*: same as upper panel, number of data points for each temperature change). Caution: in this figure, model results are averaged over the whole tropical domain and not over proxy-data locations, which may bias the comparison (e.g., Broccoli and Marciniak, 1996). For example, for the pollen data, extreme values are obtained for specific regions: weakest values over the Indonesia-Pacific region and coldest values over South America.

the observed occurrence of large lakes and wetlands (Coe and Bonan, 1997; Brostrom *et al*., 1998) also intensifies monsoon rains. Vegetation feedbacks also amplify the effects of orbital forcing at high latitudes where they led to greater and more realistic shifts of vegetation cover over northern Eurasia (Foley *et al*., 1994; Kutzbach *et al*., 1996b; Texier *et al*., 1997). The importance of land-surface feedbacks has further been emphasised in the IPSL AOGCM coupled to a vegetation model (Braconnot *et al*., 1999). The IPSL simulation shows that combined feedbacks between land and ocean lead to a closer agreement with palaeo-data (Figure 8.13). The ocean feedback increases the supply of water vapour, while the vegetation feedback increases local moisture recycling and the length of the monsoon season. The importance of land-surface feedbacks has also been shown by an EMIC (Ganopolski *et al*., 1998a), further emphasising that vegetation feedbacks may explain abrupt changes in Saharan vegetation in the mid-Holocene (Claussen *et al*., 1999).

8.5.5.2 *The last glacial maximum*

Results from the PMIP experiments

The Last Glacial Maximum (LGM) climate involves large changes in ice sheet extent and height, SSTs, albedo, sea level and CO_2 (200 ppm), but only minor changes in solar radiation. Over the oceans, two sets of experiments have been performed within PMIP using several atmospheric models, either prescribing SSTs estimated from macrofossil transfer functions (CLIMAP, 1981) or computing SSTs from a mixed-layer ocean

model. An annual mean global cooling of about –4°C is obtained by all models forced by the Climate: Long-range Investigation, Mapping and Prediction (CLIMAP) SSTs, whereas the range of cooling is larger when using computed SSTs, from –6 to –2°C. This range of 4°C arises both from differences in the simulated radiative forcing associated primarily with different ice albedo values, and from differences in model climate sensitivity (see Chapter 9, Section 9.2.1).

Evaluating the consistency between the simulated climate and that reconstructed from palaeo-data can potentially provide an independent check that model sensitivity is neither too large nor too small. A detailed analysis of a subset of the PMIP models (Taylor *et al*., 2000), shows that their forcing estimates for the LGM vary from about –4 to –6 Wm^{-2} and that their global climate sensitivity, given relatively to a doubling of CO_2, ranges from 3.2 to 3.9°C (assuming that climate sensitivity is independent of the type of forcing, although one model study shows a slightly stronger sensitivity at the LGM than for a CO_2 doubling (Hewitt and Mitchell, 1997)). A direct evaluation of climate sensitivity is, however, very difficult since global temperature changes are poorly known. Hoffert and Covey (1992) estimated a global cooling of –3 ± 0.6°C from CLIMAP (1981) SST data which would, using the simulated range of forcing, yield to a global climate sensitivity for a doubling of CO_2 ranging from 1.4 to 3.2°C, which probably gives a lower estimate of climate sensitivity since CLIMAP SSTs tend to be relatively too warm in the tropics (see below).

An alternative approach to evaluating climate sensitivity is provided by the detailed comparison of model results with proxy-data over different regions. The amplitude of the tropical cooling at LGM has long been disputed (Rind and Peteet, 1985; Guilderson *et al*., 1994). Compared to a new synthesis of terrestrial data (Farrera *et al*., 1999), PMIP simulations with prescribed CLIMAP sea-surface conditions produce land temperatures that are too warm (Pinot *et al*., 1999) (Figure 8.14), which may be due to too-warm prescribed SSTs, as indicated by new marine data based on alkenone palaeo-thermometry (Rosell-Melé *et al*., 1998) (Figure 8.14). Some mixed-layer ocean models have produced more realistic sea and land temperature cooling (Pinot *et al*., 1999), enhancing our confidence in using such models to estimate climate sensitivity (see Chapter 9, Section 9.3.4) (Figure 8.14). The same conclusion is derived by Broccoli (2000) when accounting for uncertainties in both the forcing and reconstructed climate from various proxy data. Over Eurasia, all the models simulate a cooling in fairly good agreement with proxy data estimates, except over western Europe (Kageyama *et al*., 2001), where they all underestimate the winter cooling shown from pollen data (Peyron *et al*., 1998). However, such simulations have an important caveat since they prescribe present day ocean heat transport whereas changes in the North Atlantic deep water circulation shown by two EMIC models (Ganopolski *et al*., 1998b; Weaver *et al*., 1998) and also inferred by palaeo-oceanographic data (e.g., Duplessy *et al*., 1988) may further decrease temperatures over Europe.

Land-surface feedbacks

Vegetation feedbacks at the LGM could have been due to climate-induced shifts in biomes, CO_2-induced changes in vegetation structure (Jolly and Haxeltine, 1997; Street-Perrot *et al*., 1997; Cowling, 1999), and CO_2-induced changes in leaf conductance (see Chapter 7, Section 7.4.2). Sensitivity experiments (Crowley and Baum, 1997; Levis *et al*., 1999) suggest that the first two types dominated. Over much of Eurasia, forests were replaced by tundra or steppe (Prentice *et al*., 1998) which may have contributed to the observed cooling over Europe (Crowley and Baum, 1997; Kubatzki and Claussen, 1998; Levis *et al*., 1999). Permafrost may also have to be accounted for (Renssen *et al*., 2000). In the tropics though, there is yet no systematic improvement of the simulated cooling, since the models find large areas of warming due to the simulated deforestation (Crowley and Baum, 1997; Levis *et al*., 1999). However, land-surface feedbacks may also have affected climate through mineral aerosol (dust) concentrations (Mahowald *et al*., 1999).

8.5.5.3 Summary

Mid-Holocene

Through PMIP experiments, it is now well-established that all atmospheric models are able to simulate several robust large-scale features of the Holocene climate but also that they all underestimate these changes. Several complementary simulations have shown that ocean and vegetation processes introduce important feedbacks which are necessary to explain the observed monsoon changes. These results urge for a systematic evaluation of coupled atmosphere-ocean-vegetation models for the mid-Holocene and for an investigation of the impact of vegetation changes, such as climate-induced density and land-use cover changes (see Chapter 7, Section 7.4.2), on future climate change projections.

Last Glacial Maximum

The more systematic evaluation of atmosphere alone models conducted within PMIP confirms that the LGM SST as estimated by CLIMAP (1981) need to be revised. Some simulations with atmospheric models coupled to mixed-layer models produce realistic results, especially in the tropics, and enhance our confidence in the estimates of climate sensitivity used in future climate change studies. However, such models neglect changes in ocean heat transport as well as land-surface feedbacks. Moreover, an evaluation of coupled AOGCMs is still needed at the LGM.

8.6 20th Century Climate and Climate Variability

8.6.1 20th Century Coupled Model Integrations Including Greenhouse Gases and Sulphate Aerosols

Since the pioneer experiments conducted at the Hadley Centre for Climate Prediction and Research (Mitchell *et al.* 1995) and at the Deutsche Klimarechenzentrum (DKRZ) (Hasselmann *et al.* 1995), reported in the SAR, a number of other groups internationally have reproduced the trend in the surface air temperature instrumental record over the 20th century. These include the Canadian Center for Climate Modelling and Analysis (CCCma) (Boer *et al.* 2000), Centre for Climate System Research/National Institute for

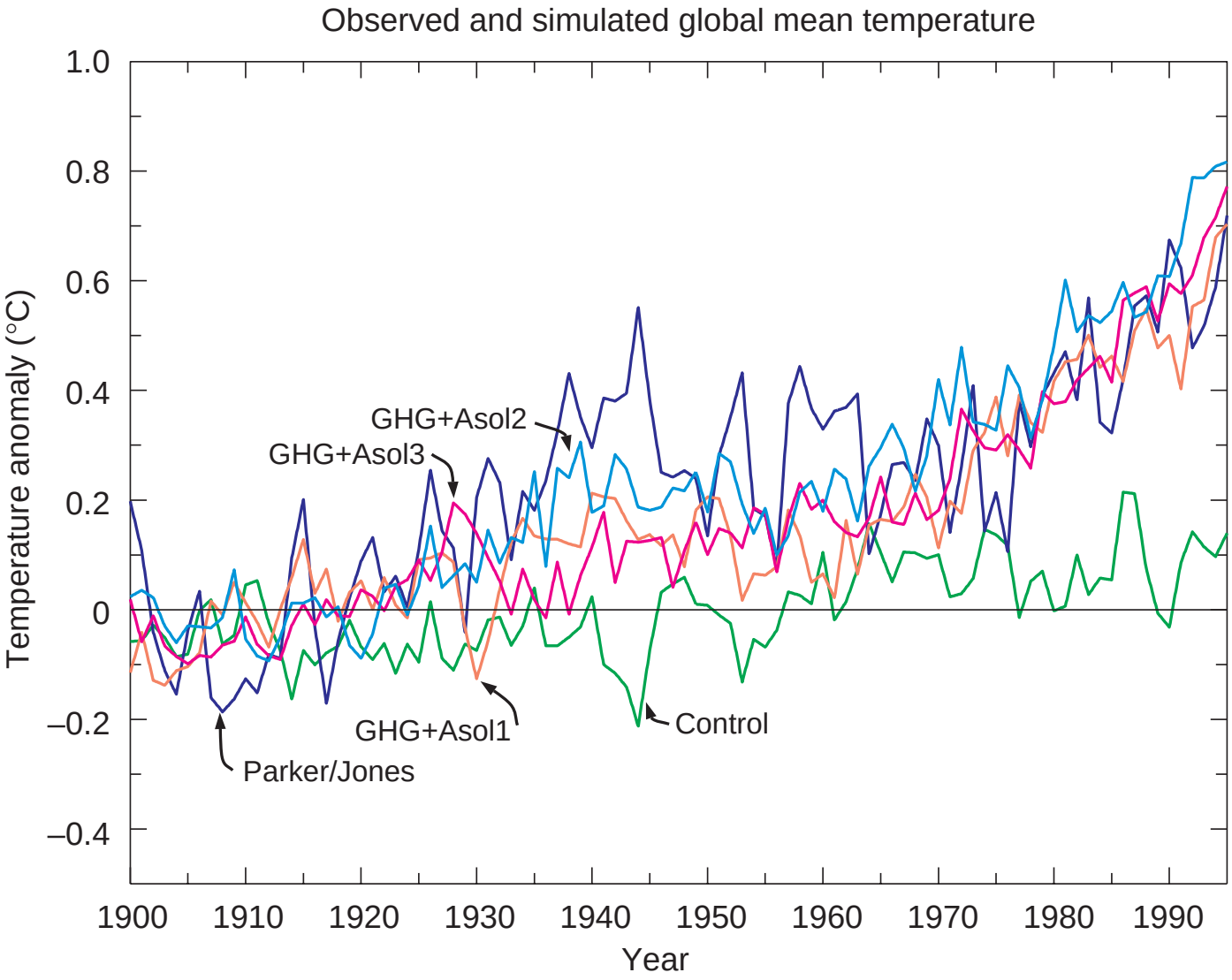

Figure 8.15: Observed (Parker/Jones) and modelled global annual mean temperature anomalies (°C) from the 1901 to 1930 climatological average. The control and three independent simulations with the same greenhouse gas plus aerosol forcing and slightly different initial conditions are shown from CGCM1 (Boer *et al*., 2000). The greenhouse gas alone simulation is labelled GHG. The three greenhouse gas plus aerosol simulations are labelled GHG+Asol1, GHG+Asol2 and GHG+Asol3, respectively.

Environmental Studies (CCSR/NIES) (Emori *et al*. 1999), Commonwealth Scientific and Industrial Research Organization (CSIRO), Geophysical Fluid Dynamics Laboratory (GFDL) (Haywood *et al*. 1997) and the National Center for Atmospheric Research (NCAR) (Meehl *et al*. 2000b). Many of these new contributions, including recent experiments at the Hadley Centre and DKRZ, include an ensemble of projections over the 20th century (e.g., Figure 8.15). Such an ensemble allows for an estimate of intra-model variability, which in the case of the CCCma model (Figure 8.15), is larger than the possible anthropogenic signal through the early part of the 20th century (cf., inter-model variability shown in Figure 9.3).

Coupled models that have been used to simulate changes over the 20th century have all started with "control model" levels of atmospheric CO_2 (typically 330 ppm). This initial condition is then referred to as the "pre-industrial" initial condition. Changes in radiative forcing are then calculated by taking the observed atmospheric equivalent CO_2 level over the 20th century as a difference relative to the actual pre-industrial level (280 ppm), and adding this as a perturbation to the control model levels. Implicit in this approach is the assumption that the climate system responds linearly to small perturbations away from the present climate. Haywood *et al*. (1997) demonstrated the near linear response of the GFDL-coupled model to changes in radiative forcing associated with increases in atmospheric greenhouse gases and sulphate aerosols. When added together, experiments which included aerosol and greenhouse gas increases separately over the 20th century yielded a similar transient response (in terms of globally averaged and geographical distribution of surface air temperature and precipitation) to

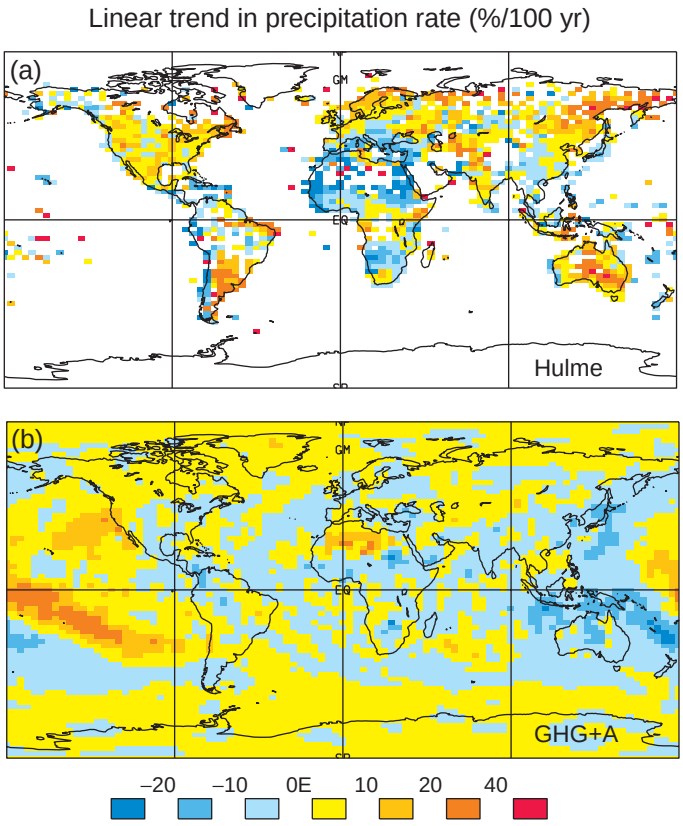

Figure 8.16: The geographical distribution of the linear trend in annual-mean precipitation (%/100 yr) for (a) the observations of Hulme (1992, 1994); (b) the ensemble of three greenhouse gas + aerosol integrations using the CCCma model. Taken from Boer *et al.* (2000).

an experiment which included both aerosol and greenhouse gas increases. This analysis is particularly important as it validates the methodological approach used in coupled model simulations of the 20th century climate.

As noted in the SAR, the inclusion of the direct effect of sulphate aerosols is important since the radiative forcing associated with 20th century greenhouse gas increase alone tends to overestimate the 20th century warming in most models. Groups that have included a representation of the direct effects of sulphate aerosols have found that their model generally reproduces the observed trend in the instrumental surface air temperature warming, thereby suggesting that their combination of model climate sensitivity and oceanic heat uptake is not unrealistic (see Chapter 9, Section 9.2.1 and Figure 9.7). These same models have more difficulty representing variability observed within the 20th century instrumental record (Sections 8.6.2, 8.6.3). As mentioned in Section 8.6.3, some modelling studies suggest that the inclusion of additional forcings from solar variability and volcanic aerosols may improve aspects of this simulated variability. Delworth and Knutson (2000), on the other hand, note that one of their six 20th century integrations (using GFDL_R30_c) bears a striking resemblance to the observed 20th century warming which occurs primarily in two distinct periods (from 1925 to 1944 and from 1978 to the present), without the need for additional external forcing. In addition, all coupled models have shown a trend towards increasing global precipitation, with an intensification of the signal at the high northern latitudes, consistent with the observational record (Figure 8.16). Nevertheless, AOGCM simulations have yet to be systematically analysed for the occurrence of other key observed trends, such as the reduction in diurnal temperature range over the 20th century and the associated increase in cloud coverage.

The aforementioned studies all prescribed the temporal and geographical distribution of sulphate aerosols and included their radiative effects by perturbing the surface albedo according to the amount of sulphate loading in the atmospheric column above the surface (see Chapter 6, Sections 6.7, 6.8 and 6.14). This approach both ignores the indirect effect of these aerosols (i.e., their effects on cloud formation) as well as weather affects on aerosol redistribution and removal. Roeckner *et al.* (1999) made a major step forward by incorporating a sulphur cycle model into the ECHAM4(ECMWF/MPI AGCM)/OPYC3(Ocean isoPYCnal GCM) AOGCM to eliminate these shortcomings. In addition, they included the radiative forcing due to anthropogenic changes in tropospheric ozone by prescribing ozone levels obtained from an offline tropospheric chemistry model coupled to ECHAM4. The simulation of the 20th century climate obtained from this model (Bengtsson *et al.* 1999), which includes the indirect effect of aerosols, shows a good agreement with the general 20th century trend in warming (see Chapter 12, Section 12.4.3.3). The results of this study also suggest that the agreement between model and observed 20th century warming trends, achieved without the inclusion of the indirect aerosol effect, was probably accomplished with an overestimated direct effect or an overestimated transient oceanic heat uptake. Alternatively, since these studies include only idealised scenarios of sulphate radiative forcing alone (direct and/or indirect) that do not include the apparent effects of other aerosol types (Chapter 6), one might view the sulphate treatment as a surrogate, albeit with large uncertainty, for the radiative forcing associated with all anthropogenic aerosols.

As noted in Chapter 2, Sections 2.2.2 and 2.2.3, land surface temperatures show a greater rate of warming than do lower tropospheric air temperatures over the last 20 years (see also discussion in Chapter 2, Section 2.2.4). While noting uncertainties in the observational records (Chapter 2, Sections 2.2.2 and 2.2.3), the National Research Council (NRC) (2000) pointed out that models, which tend not to show such a differential trend, need to better capture the vertical and temporal profiles of the radiative forcing especially associated with water vapour and tropospheric and stratospheric ozone and aerosols, and the effects of the latter on clouds. Santer *et al.* (2000) provide further evidence to support this notion from integrations conducted with the ECHAM4/OPYC3 AOGCM (Bengtsson *et al.* 1999; Roeckner *et al.*, 1999) that includes a representation of the direct and indirect effects of sulphate aerosols, as well as changes in tropospheric ozone. They showed that the further inclusion of stratospheric ozone depletion and stratospheric aerosols associated with the Pinatubo eruption lead to a better agreement with observed tropospheric temperature changes since 1979, although discrepancies still remain (see Chapter 12, Section 12.3.2 and Figure 12.4).

8.6.2 Coupled Model Variability

8.6.2.1 Comparison with the instrumental record

Barnett (1999) concatenated the annual mean near-surface temperature anomaly fields from the first 100 years of integration of eleven CMIP control experiments to produce common empirical orthogonal functions (EOFs) for the eleven AOGCMs. By projecting the Global Sea Ice and Sea Surface Temperature (GISST) annual mean temperature anomaly data set (Rayner *et al*. 1996) onto these common EOFs, he was able to estimate to what extent model variability represented the observed variability. An analysis of the partial eigenvalue spectrum for the different models (Figure 8.17a) suggests that there is considerable disparity between the estimates of variability within the coupled models. Some of this disparity arises from model drift and other low-frequency variability. Intra-model disparity was much lower than inter-model disparity as demonstrated by a similar common EOF analysis obtained from ten 100 year segments in the 1,000 year GFDL_R15_a control run (Figure 8.17b). While the highest two modes were substantially underestimated in the GFDL_R15_a model, the higher modes agreed better with observations. Error bars on the observational data are large and when this is taken into account, model disagreement with observations may not be significant. As Barnett (1999) did not remove the trend over the 20th century in the GISST data set, the observations also contain responses to both natural and anthropogenic forcing. One would therefore expect control integrations from coupled climate models to underestimate the observed spectrum at low frequencies (e.g., Folland *et al*., 1999).

An analogous study by Stouffer *et al*. (2000) compared the surface air temperature variability from three long 1,000-year CMIP integrations (GFDL_R15_a, HadCM2, ECHAM3/LSG (Large-Scale Geostrophic ocean model)) to the variability found in the same observational data set (Jones and Briffa, 1992; Jones 1994). They argued that, over the instrumental period, the simulated variability on annual to decadal time-scales was fairly realistic both in terms of the geographical distribution and the global mean values with a notable exception of the poor simulation of observed tropical Pacific variability (Figure 8.18). The HadCM2 model substantially overestimated tropical Pacific variability, whereas it was underestimated in the GFDL_R15_a and ECHAM3/LSG models. They also noticed that on the inter-decadal time-scale, the greatest variance in the models was generally located near sea-ice margins close to regions of deep oceanic convection and associated with low-frequency variations of the thermohaline circulation. While the three models generally agreed on the dominant modes of variability, there was substantial inter-model disparity in the magnitude of each mode. The analysis of Stouffer *et al*. (2000) can easily be reconciled with Barnett (1999) by realising that Stouffer *et al*. (2000) examined a subset (GFDL_R15_a, HadCM2, ECHAM3/LSG models) of those CMIP models considered by Barnett (1999) that did not experience climate drift, and that less emphasis was placed on the poor resolution of tropical Pacific variability.

As an extension to the above analysis, Bell *et al*. (2000) compared annual mean surface air temperature variability in sixteen CMIP control simulations to the thermometer record, on time-

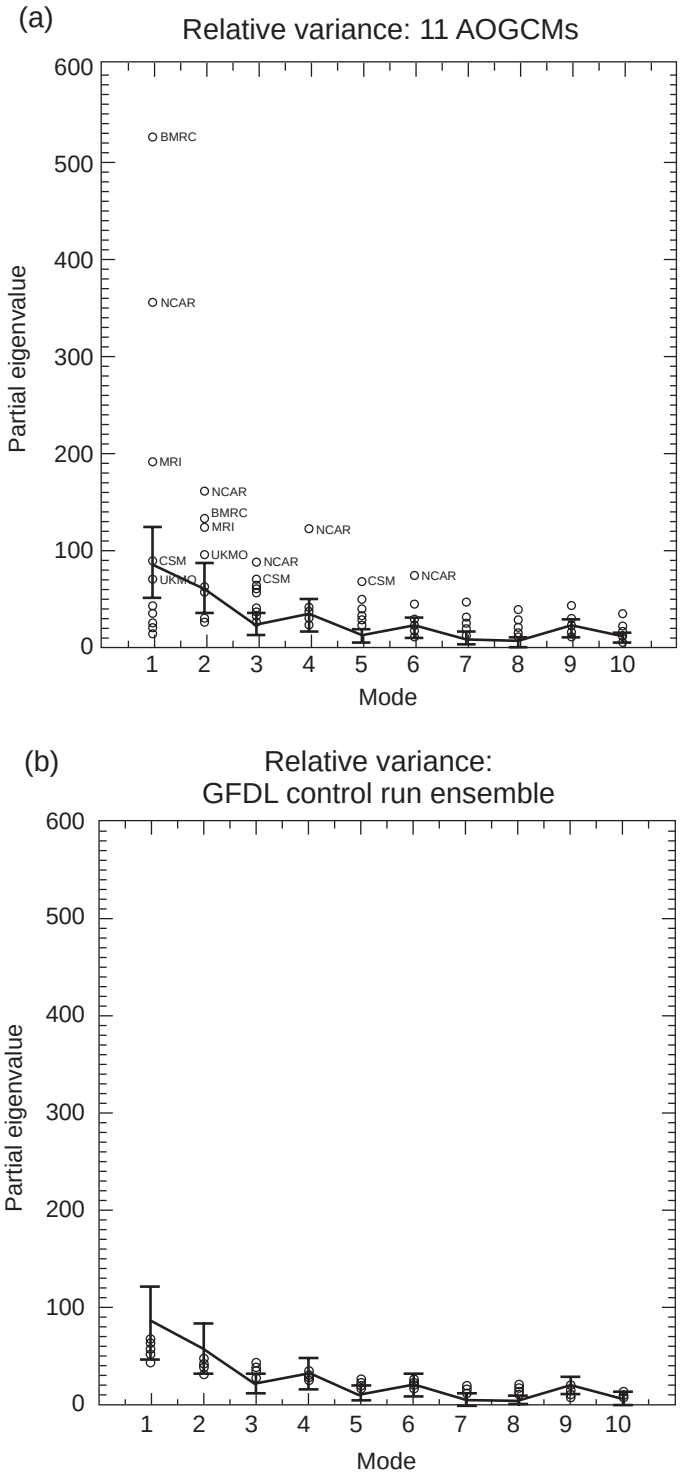

Figure 8.17: (a) Partial eigenvalue spectrum for the EOFs from eleven CMIP AOGCMs. The observations (heavy line), together with their 95% confidence limits (vertical bars), are obtained by projecting the observed surface air temperature (Jones and Briffa, 1992; Rayner *et al*., 1996) onto the common EOFs obtained from eleven CMIP AOGCMs. (b) as in (a) except for ten separate 100-year segments of the GFDL control run. Taken from Barnett (1999).

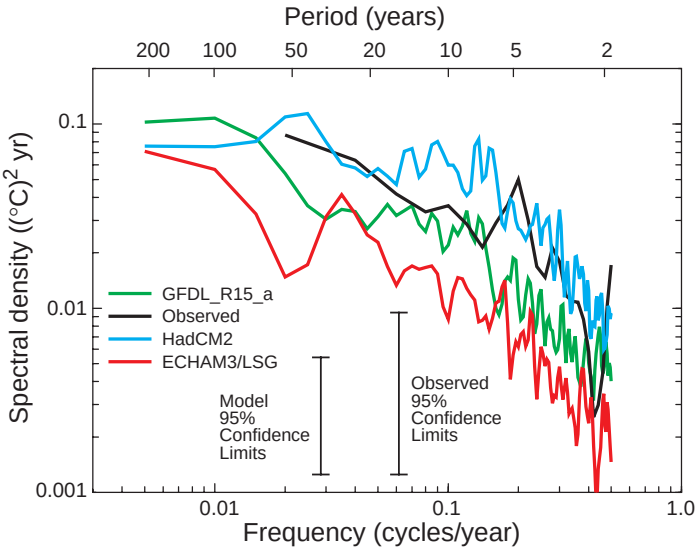

Figure 8.18: Power spectra of the detrended globally averaged annual mean surface air temperature (SAT) anomaly. The curves represent the estimates obtained from HadCM2 (blue), GFDL_R15_a (green) and ECHAM3/LSG (red). The observed (black line) is from the globally averaged annual mean SAT anomalies compiled by Jones and Briffa (1992). The spectra are smoothed Fourier transforms of the autocovariance function using a Tukey window of 100 lags for the models and 30 lags for the observations. The two vertical lines represent the range of 95% confidence in the spectral estimates for the model and the observations. Taken from Stouffer *et al*. (2000).

scales of 1 year to 40 years (Figure 8.19). The authors found that: (1) thirteen of the sixteen CMIP models underestimate variability in surface air temperatures over the global oceans; (2) twelve of the sixteen models overestimate variability over land; (3) all the models overestimate the ratio of air temperature variability over land to variability over oceans. These results likely reflect problems in both the ocean and land-surface components of climate models. In particular, underestimation of variability over oceans may be due, at least in part, to weak or absent representations of El Niño in the models; overestimation of variability over land may be due to poor land surface parametrizations including insufficient soil moisture.

Duffy *et al*. (2000) also partitioned the CMIP models into those that are flux adjusted and those that are not. They defined two measures of temperature variability and applied them to the CMIP control simulations. The simulations differed substantially in the amount of temperature variability they showed. However, on time-scales of 1 year to 20 years, the flux adjusted simulations did not have significantly less variability than the non-flux adjusted simulations; there is some suggestion that they may have *more* variability. Thus it cannot be argued, for example, that the use of flux adjusted models in studies of detection of anthropogenic climate change tends to make observed temperature changes seem more significant than they should be, compared to natural internal climate variability. Nevertheless, it is still an open question as to how coupled model variability depends on internal model parameters and resolution.

8.6.2.2 Comparison with palaeo-data

There have been relatively few studies which have undertaken a systematic comparison of AOGCM variability with variability found in the Holocene proxy temperature record. However, three studies (from the MPI (Max Planck Institute), Hadley Centre and GFDL) that focus on the analysis of long control integrations are available. Barnett *et al*. (1996) demonstrated that the GFDL_R15_a (Stouffer *et al*., 1994) and ECHAM1/LSG (Cubasch *et al*., 1994) models underestimate the levels of decadal-scale variability in summer palaeo-temperature proxies from 1600 to 1950 (expanded version of Bradley and Jones, 1993), with increasing disparity with observations at lower frequencies.

Using annual and decadal mean near-surface palaeo-temperature reconstructions at seventeen locations Jones *et al*. (1998) demonstrated, through a principal component analysis, that the standard deviation of the GFDL_R15_a model (Stouffer *et al*., 1994) and the HadCM2 model (Johns *et al*., 1997; Tett *et al*., 1997) principal component time-series compared favourably with both proxy and observed data. Time-series of the top seven principal components did, however, show much less century time-scale variability than in the proxy time-series. This was especially true in the HadCM2 model that was dominated by tropic-wide decadal variability. Through cross-spectral analysis they concluded that the "GFDL control integration bears a remarkable similarity in its statistical properties to that obtained from the proxy data. In view of this similarity it appears the spatial structures from the control integration can be used to represent the spatial structures of naturally occurring variations in near-surface air temperature". This conclusion was also highlighted by Delworth and Mann (2000) who noted that both palaeo-temperature reconstructions (Mann *et al*., 1998) and the GFDL_R15_a coupled model suggest a distinct oscillatory mode of climate variability (with an approximate time-scale of about 70 years) of hemispheric scale and centred around the North Atlantic.

8.6.3 The Role of Volcanic and Solar Forcing and Changes in Land Use

Coupled model control runs have a general tendency to underestimate the variability found in both the instrumental and palaeo-proxy record, especially over the oceans (the converse is true over land when compared to the instrumental record). With the exception of Santer *et al*. (2000), none of the aforementioned simulations examined the potential climatic effects of stratospheric aerosols associated with volcanic emissions. On the longer time-scales, none of these studies included variability in solar forcing. Crowley (2000) has estimated that changes in solar irradiance and volcanism may account for between 41 and 64% of pre-industrial, decadal-scale surface air temperature variations.

Cubasch *et al*. (1997) demonstrated that when solar variations were included in the ECHAM3/LSG model, their simulation from 1700 through the 20th century showed enhanced low-frequency variability associated with variability in solar irradiance (see also Lean and Rind, 1998). The implication of climate change detection and attribution studies (Chapter 12; Hegerl *et al*., 1997; Tett *et al*., 1999) for the reproduction of 20th century climate by AOGCMs, is that changes in solar irradiance may be important to include if one

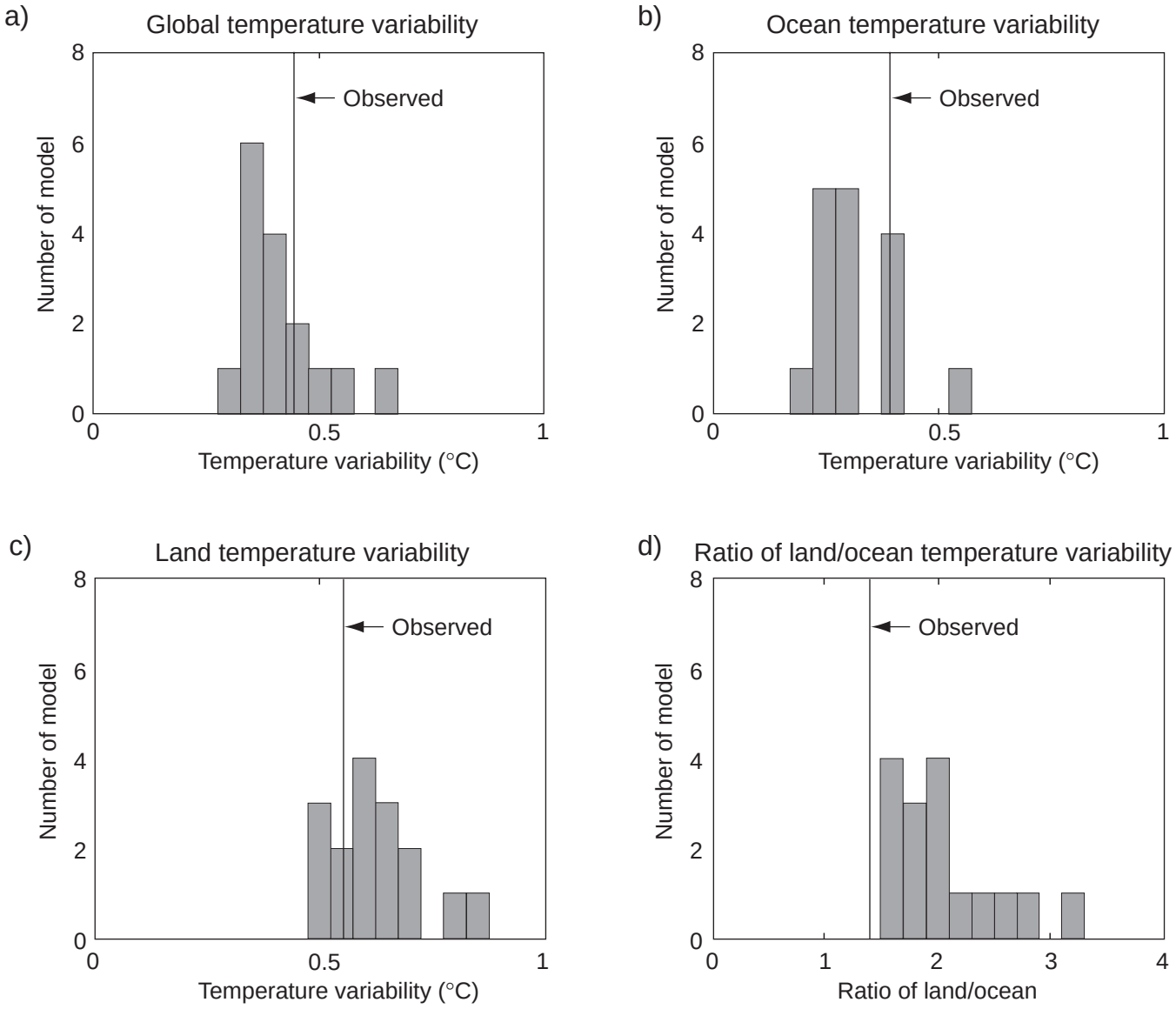

Figure 8.19: Simulated variability of annual mean surface air temperatures over the last 40 years, 1959 to 1998 in sixteen CMIP simulations and in observations (Jones, 1994; Parker *et al*., 1995). (a) Global-mean temperature variability; four models show higher than observed amounts of variability. (b) Mean over-ocean temperature variability; three models show higher than observed amounts of variability. (c) Mean over-land temperature variability; four models show less than observed amounts of variability. (d) Ratio of over-land to over-ocean temperature variability; all models show higher than observed ratios. Taken from Bell *et al*. (2000).

wants to reproduce the warming in the early part of the century. As noted earlier, it is conceivable that this early warming may also be solely a result of natural internal climate variability (Delworth and Knutson, 2000). Energy balance/upwelling diffusion climate models and Earth system models of intermediate complexity, when forced with volcanic and solar variations for the past 400 years, capture the cooling associated with the Little Ice Age (Betrand *et al*., 1999; Crowley and Kim, 1999; Free and Robock, 1999), although they are not capable of assessing regional climatic anomalies associated with local feedbacks or changes in atmospheric dynamics. These same models produce the observed warming of the past century when additionally forced with anthropogenic greenhouse gases and aerosols**.**

Hansen *et al*. (1997) conducted a systematic study of the climate system response to various radiative forcings for the period 1979 to 1995 (over which period Nimbus 7 satellite data were available) using the Goddard Institute for Space Studies (GISS) AGCM coupled to a mixed-layer ocean model. A series of ensemble simulations, with each ensemble consisting of five experiments, were conducted by cumulatively adding, one-by-one, radiative forcing effects due to stratospheric aerosols (associated with volcanic emissions), decreases in upper level ozone, increases in anthropogenic greenhouse gases, and changes in solar irradiance (Figure 8.20). While changes in tropospheric aerosols, either via direct or indirect effects, were not included in their calculations, over the short record a reasonable agreement

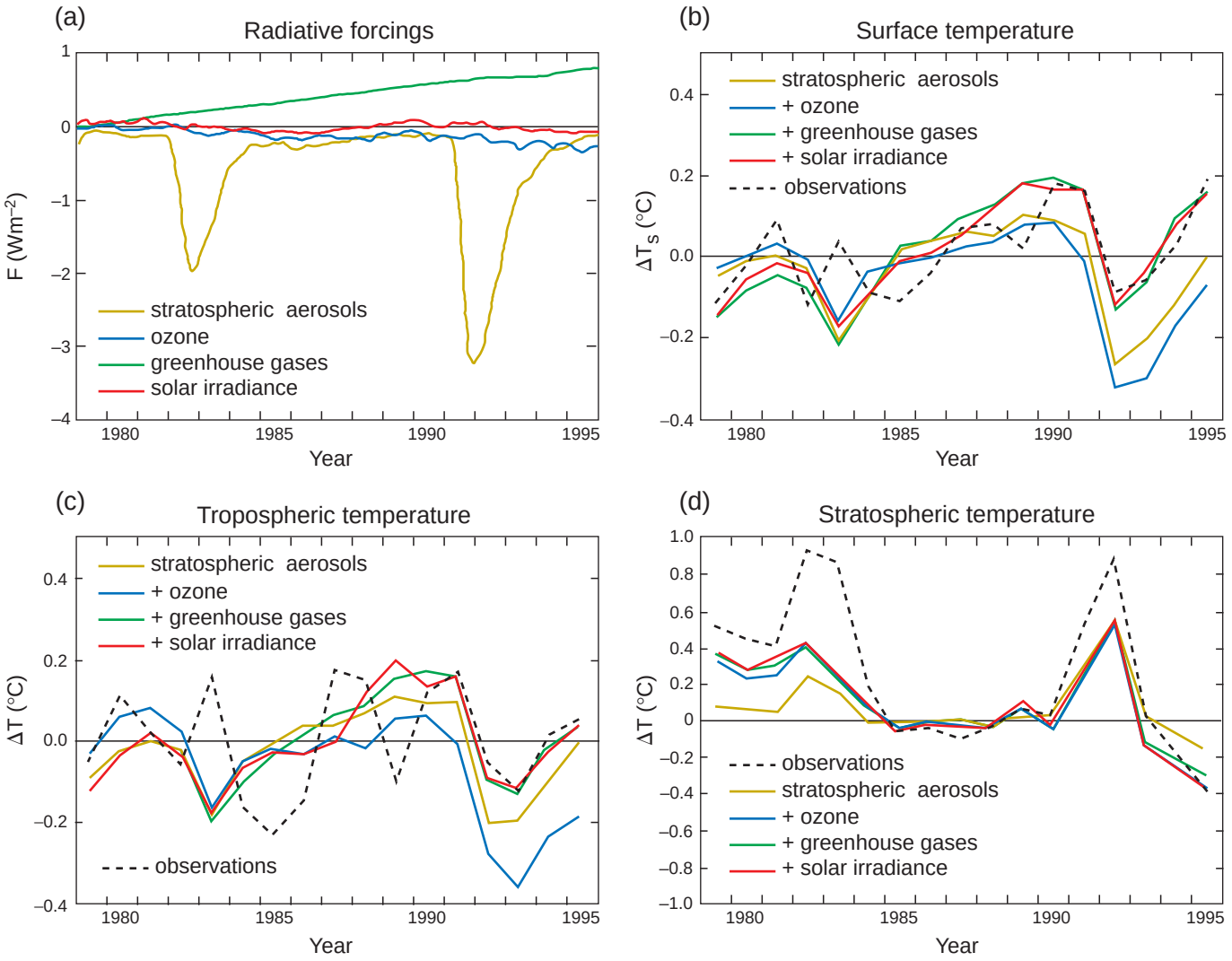

Figure 8.20: (a) Radiative forcing (Wm^{-2}) since 1979 due to changes in stratospheric aerosols, ozone, greenhouse gases and solar irradiance. (b) to (d) Observed global annual mean surface, tropospheric and stratospheric temperature changes and GISS GCM simulations as the successive radiative forcings are cumulatively added one by one. An additional constant 0.65 Wm^{-2} forcing was included in all their simulations, representing the estimated disequilibrium forcing for 1979. The base period defining the zero mean observed temperature was 1979 to 1990 for the surface and the troposphere and 1984 to 1990 for the stratosphere. Taken from Hansen *et al.* (1997).

with observations was obtained. Internal climate variability (e.g., the warming associated with the El Niño of 1983 and the cooling associated with the La Niña of 1989 in Figure 8.20b,c) is not well resolved in the model. These experiments point out that while solar irradiance changes caused minimal changes over the period (consistent with the analysis of Hegerl *et al.*, 1997; Tett *et al.*, 1999), stratospheric aerosols associated with volcanic emissions and changes in upper level ozone are important components which need to be included if one hopes to accurately reproduce the variations in the instrumental record.

Changing land-use patterns affect climate in several ways (see Chapter 6, Section 6.11). While the impact of land-use changes on radiative forcing is small (e.g., Hansen *et al.*, 1998) changes in roughness, soil properties and other quantities may be important (see Chapter 7, Section 7.4). Brovkin *et al.* (1999) demonstrated that CLIMBER (Climate Biosphere Model) was able to capture the long-term trends and slow modulation of the Mann *et al.* (1998) reconstruction of Northern Hemisphere temperatures over the past 300 years provided changes in land-use patterns (as well as changes in atmospheric CO_2 and changing solar forcing) were taken into account. Some recent model results suggest that land cover changes during this century may have caused regional scale warming (Chase *et al.*, 2000; Zhao *et al.*, 2001) but this remains to be examined with a range of climate models.

8.6.4 Climate of 20th Century: Summary

Several coupled models are able to reproduce the major trend in 20th century surface air temperature, when driven by historical radiative forcing scenarios corresponding to the 20th century.

However, in these studies idealised scenarios of only sulphate radiative forcing have been used. One study using the ECHAM4/OPYC model that includes both the indirect and direct effects of sulphate aerosols, as well as changes in tropospheric ozone, suggests that the observed surface and tropospheric air temperature discrepancies since 1979 are reduced when stratospheric ozone depletion and stratospheric aerosols associated with the Pinatubo eruption are included. Systematic evaluation of 20th century AOGCM simulations for other trends found in observational fields, such as the reduction in diurnal temperature range over the 20th century and the associated increase in cloud coverage, have yet to be conducted.

The inclusion of changes in solar irradiance and volcanic aerosols has improved the simulated variability found in several AOGCMs. In addition, some evaluation studies aimed at the reproduction of 20th century climate have suggested that changes in solar irradiance may be important to include in order to reproduce the warming in the early part of the century. Another study has suggested that this early warming can be solely explained as a consequence of natural internal climate variability.

Taken together, we consider that there is an urgent need for a systematic 20th century climate intercomparison project with a standard set of forcings, including volcanic aerosols, changes in solar irradiance and land use, as well as a more realistic treatment of both the direct and indirect effects of a range of aerosols.

8.6.5 Commentary on Land Cover Change

Land-cover change can occur through human intervention (land clearance), via direct effects of changes in CO_2 on vegetation physiology and structure, and via climate changes (Chapter 7). Evidence from observational studies (see Chapter 7, Section 7.4.2) and modelling studies (e.g., Betts *et al.*, 1997, 2000; Chase *et al.*, 2000; Zhao *et al.*, 2001) demonstrate that changes in land cover can have a significant impact on the regional scale climate but suggestions that land clearance has an impact on the global scale climate is currently speculative. Evidence from palaeoclimate (Section 8.5) and modelling work (Section 8.5 and Chapter 7, Section 7.4) indicates that these changes in vegetation may lead to very significant local and regional scale climate changes which, in some cases, may be equivalent to those due to increasing CO_2 (Pitman and Zhao, 2000).

On time-scales of decades the impact of land cover change could significantly influence the rate of atmospheric CO_2 increase (Chapter 3), the nature and extent of the physical climate system response, and ultimately, the response of the biosphere to global change (Chapter 8). Models currently under development that can represent changes in land cover resulting from changes in climate and CO_2 should enable the simulations of these processes in the future. If these models can be coupled with scenarios representing human-induced changes in land cover over the next 50 to 100 years, the important effects of land- cover change can be included in climate models. While the inclusion of these models of the biosphere is not expected to change the global scale response to increasing CO_2, they may significantly effect the simulations of local and regional scale change.

8.7 Coupled Model: Phenomena

The atmosphere-ocean coupled system shows various modes of variability that range widely from intra-seasonal to inter-decadal time-scales (see Chapters 2 and 7). Since the SAR, considerable progress has been achieved in characterising the decadal to inter-decadal variability of the ocean-atmosphere system (Latif, 1998; Navarra, 1999). Successful evaluation of models over a wide range of phenomena increases our confidence.

8.7.1 El Niño-Southern Oscillation (ENSO)

ENSO is a phenomenon resulting from large-scale air-sea interactions (see Chapter 7, Section 7.6.5). ENSO modelling has advanced considerably since the SAR (e.g., Yukimoto *et al.*, 1996; Kimoto and Shen, 1997; Knutson *et al.*, 1997; Timmermann *et al.*, 1998). Some models now use enhanced horizontal resolution in the tropics to better resolve equatorial ocean dynamics. Models show SST variability in the tropical Pacific, which has some similarity to observed ENSO as is shown in upper panels of Figure 8.21. However, some aspects of ENSO are still not well captured by present day coupled models (Delecluse *et al.*, 1998). Latif *et al.* (1999) analysed the SST climatology and interannual variability simulated by twenty four models in the equatorial Pacific. When compared with observations, the models have flaws in reproducing the annual cycle. About half of the models are characterised by too weak interannual variability in the eastern equatorial Pacific, while models generally have larger variability in the central equatorial Pacific (Table 8.2). It was found that the majority of the models show the observed ENSO-monsoon relationship, that is, a weak Indian summer monsoon tends to be associated with El Niño.

Seasonal forecasting with coupled global models has just begun (Barnston *et al.*, 1999; McPhaden, 1999), although few of the models discussed in Chapter 9 are used. While forecast skill of coupled global models is still lower than statistical models (Landsea and Knaff, 2000), coupled global models have better skill than simple models. The 1997 to 1998 El Niño event (Trenberth, 1998b) is a good test of coupled model forecast systems. Figure 8.22 plots the SST anomaly during the 1997 to 1998 El Niño for predictions made with various initial conditions by prediction systems at ECMWF (Stockdale *et al.*, 1998), the Japan Meteorological Agency (JMA) (Ishii *et al.*, 1998), NCEP (Barnston *et al.*, 1999) and for the hindcast made at the Bureau of Meteorology Research Centre (BMRC) (Wang *et al.*, 2000). Those comprehensive models predicted unusually warm tropical Pacific SST for 1997, albeit with underestimation of the strength of the event and the warming speed. A similar conclusion is reached with other global climate models (Oberhuber *et al.*, 1998; Zhou *et al.*, 1998). Unusually strong Madden-Julian Oscillation (MJO, see Section 8.7.4) and westerly wind bursts may have affected not only the timing but also the amplitude of the 1997 to 1998 El Niño (McPhaden, 1999; Moore and Kleeman, 1999), and, in this respect, models may fail to forecast the onset of an El Niño in some circumstances. However, these results suggest an improved ability of coupled models to forecast El Niño if sufficient data to initialise the model are available from a good ocean data assimilation system.

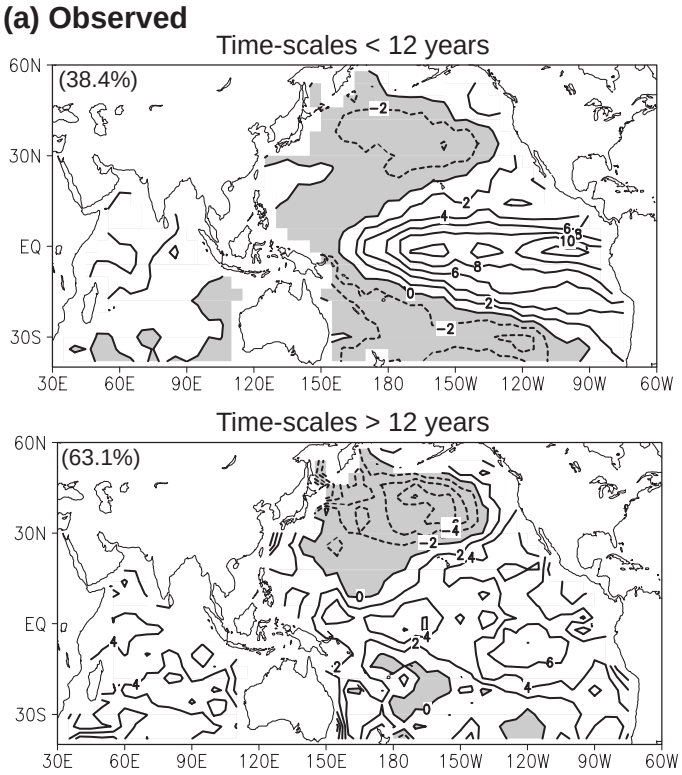

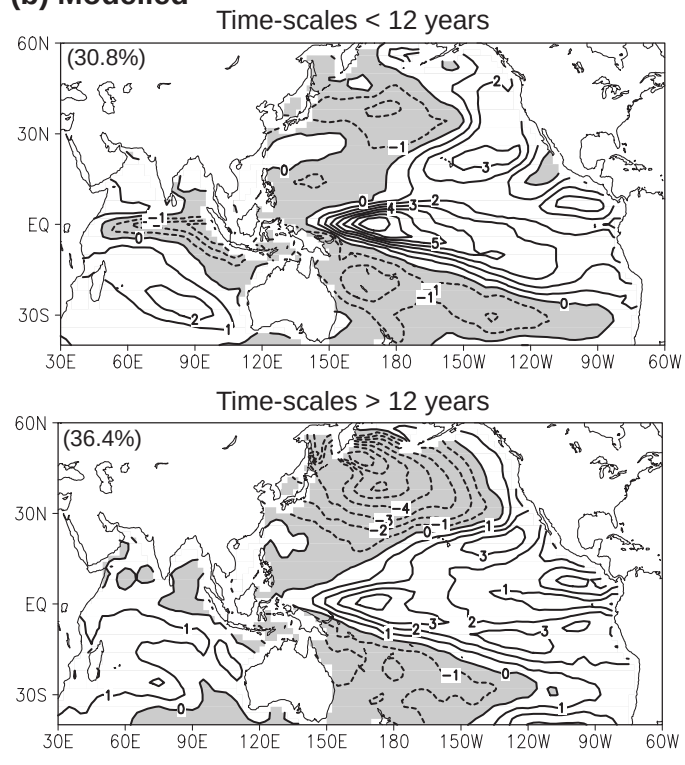

Figure 8.21: Comparison of eigenvectors for the leading EOFs of the SSTs between the ENSO time-scale (<12 years) (upper panels) and the decadal time scale (>12 years) (lower panels) for (a) observation, and (b) the MRI coupled climate model, respectively (Yukimoto, 1999). Numbers in bracket at the upper left show explained variance in each mode.

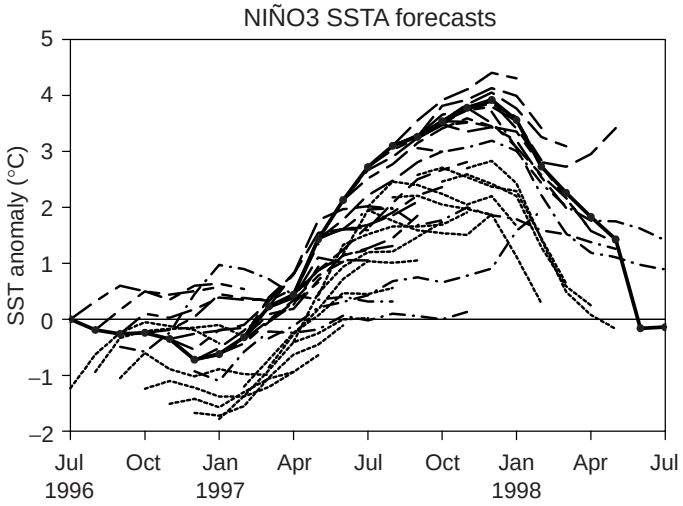

Figure 8.22: Niño-3 SST anomaly predictions and hindcast made at various times during the 1997 to 1998 El Niño event together with the subsequent observed SST anomaly (solid). Predictions made at ECMWF (Stockdale *et al*., 1998, long dash), JMA (Ishii *et al*., 1998, short dash), NCEP (Barnston *et al*., 1999, long short dash) and the hindcast made at BMRC (Wang *et al*., 2000, dot dash) are shown.

In summary, the higher resolution coupled climate models employed since the SAR are better able to simulate El Niño-like SST variability in the tropical Pacific. However, there still remain common model errors such as weaker amplitude of SST anomalies and westward shift of the variability maximum compared to the observations. Current models can predict major El Niño events with some accuracy, suggesting that, as the resolution increases and the model physics improves, El Niño simulation will also improve.

8.7.2 Pacific Decadal Oscillation (PDO)

The leading mode in the Pacific with decadal time-scale is usually called the Pacific Decadal Oscillation (PDO, see Chapter 2, Section 2.6.3). Unlike the well-documented interannual mode (ENSO), the decadal pattern does not have a distinctive equatorial maximum. Several coupled climate models are able to reproduce a pattern of this decadal variability broadly similar to the observed pattern (Latif and Barnett, 1996; Robertson, 1996; Yukimoto *et al*., 1996, 2000; Knutson and Manabe, 1998; Yu *et al*., 2000a). These modelling groups have proposed different mechanisms to explain the observed Pacific decadal variability based on analysis of large samples of simulated decadal variability in their coupled models. An example is shown in Figure 8.21b, where larger SST variability in the North Pacific than in the equatorial region is captured (Yukimoto, 1999). While the geographical location of the mid-latitude poles and the amplitude ratio between the tropical and mid-latitude poles vary slightly from one model to another, pattern correlation between the observed and model leading decadal EOFs are quite high.

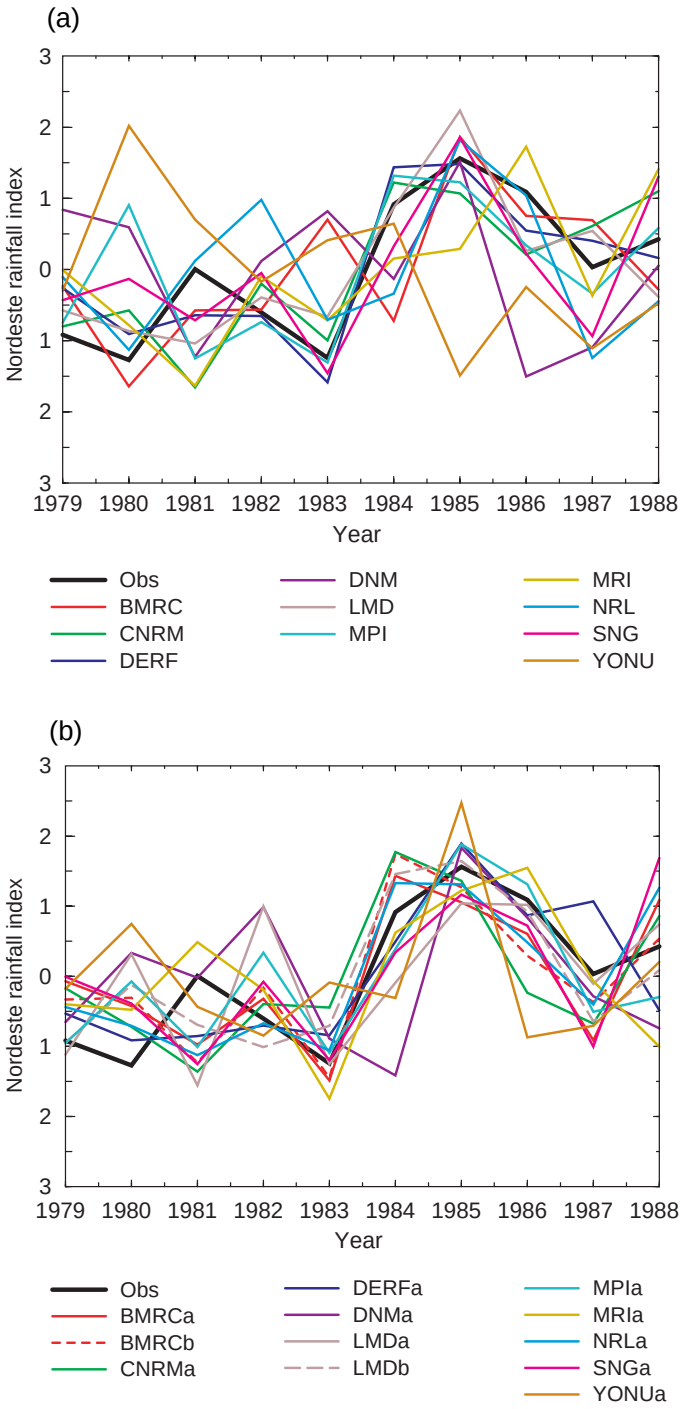

Figure 8.23: Simulated (March-May) and observed (March-April) averaged Nordeste (north-eastern Brazil) rainfall indices for (a) the original AMIP simulations, (b) the revised AMIP simulations (Sperber *et al*., 1999).

8.7.3 Monsoons

Monsoon constitutes an essential phenomenon for a tropical climate (see Chapter 7, Section 7.6.3). The monsoon precipitation simulated by AGCMs has been evaluated in AMIP (Sperber and Palmer, 1996; Zhang *et al*., 1997; Gadgil and Sajani, 1998). The seasonal migration of the major rain belt over the West African region is well simulated by almost all models. However coarse resolution climate models generally fail to give satisfactory simulations of the East Asian, East African and North American monsoons (Stensrud *et al*., 1995; Lau and Yang, 1996; Semazzi and Sun, 1997; Yu *et al*., 2000b). For example, models have excessive precipitation in the eastern periphery of the Tibetan Plateau. Increase of horizontal resolution can improve the precipitation details, but may not be sufficient to remove large-scale model biases (Kar *et al*., 1996; Lal *et al*., 1997; Stephenson *et al*., 1998; Chandrasekar *et al*., 1999; Martin, 1999; also see Section 8.9.1).

Interannual variations of Nordeste (north-eastern Brazil) rainfall are well captured with atmospheric models with prescribed interannually varying SST (Potts *et al*., 1996; Sperber and Palmer, 1996). This is also the case for the South American monsoon (Robertson *et al*., 1999) and the West African monsoon (Rowell *et al*., 1995; Semazzi *et al*., 1996; Rocha and Simmonds, 1997; Goddard and Graham, 1999). The precipitation variation over India is less well simulated. However the models show better skill in reproducing the interannual variability of a wind shear index over the Indian summer monsoon region, indicating that the models exhibit greater fidelity in capturing the large-scale dynamic fluctuations than the regional scale rainfall variations.

More recent atmospheric models with revised physical parametrizations show improved interannual variability of the all-India rainfall, Indian/Asian monsoon wind shear, Sahel and Nordeste rainfall (Figure 8.23) (Sperber *et al*., 1999). Improvement in the simulation of interannual variability is associated with a better simulation of the observed climate by the models (Sperber and Palmer, 1996; Ferranti *et al*., 1999; Martin and Soman, 2000). The observed rainfall/ENSO SST correlation pattern is better simulated by those models that have a rainfall climatology in closer agreement with observations (Gadgil and Sajani, 1998).

Coupled climate models that simulate El Niño-like SST variability in the tropical Pacific indicate a strong connection between ENSO and the strength of the Indian summer monsoon in qualitative agreement with observations (Meehl and Arblaster, 1998; Kitoh *et al*., 1999; Latif *et al*., 1999). Besides the ENSO time-scale, the South Asian monsoon reveals a strong biennial oscillation. Coupled models can reproduce this tropospheric biennial oscillation (TBO) (Meehl, 1997; Ogasawara *et al*., 1999).

8.7.4 Madden and Julian Oscillation (MJO)

MJO is a 30 to 60 day oscillation that moves eastward in the tropical large-scale circulation, and affects both mid-latitude atmospheric circulation and the Asian-Australian monsoon. Slingo *et al*. (1996) showed that nearly all of the AMIP models

have power in the intra-seasonal time-scale of equatorial upper troposphere zonal wind at higher frequencies than the observation. They also show that most models underestimated the strength of the MJO. Slingo *et al*. (1999) show that the HadAM3 model forced by the observed SST displays a decadal time-scale variability of MJO activity as observed, implying a possible link between long-term changes of tropical SST and MJO activity, and also the ability of a current atmospheric model to simulate it.

Recent studies suggest an important role of air-sea interaction on the intra-seasonal time-scale phenomena (Flatau *et al*., 1997; Waliser *et al*., 1999; Li and Yu, 2001), thus a possible improvement in reproducing the MJO by coupled climate models. This warrants a need to evaluate the MJO in coupled climate models, but this is yet to be undertaken.

8.7.5 The North Atlantic Oscillation (NAO) and the Arctic Oscillation (AO)

The North Atlantic Oscillation (NAO) is a regional mode of variability over the North Atlantic, while the Arctic Oscillation (AO) is a hemispheric mode of variability which resembles in many respects the NAO (see Chapter 7, Section 7.6.4). Coupled climate models simulate the NAO quite well, although there are some differences in its amplitude (Delworth, 1996; Laurent *et al*., 1998; Saravanan, 1998; Osborn *et al.*, 1999). Atmospheric models with prescribed SST also simulate the spatial pattern of NAO variability fairly well (Rodwell *et al*., 1999), although coupling to an interactive ocean does seem to produce the most realistic NAO pattern. A realistic AO is simulated in the CCCma (Fyfe *et al*., 1999), GISS (Shindell *et al*., 1999) and GFDL (Broccoli *et al*., 1998) climate models. The AO extends into the mid-troposphere to lower stratosphere where it is associated with variations in westerly wind speed (see Chapter 2, Section 2.6.5 and Chapter 7, Section 7.6.4). This coupled troposphere-stratosphere mode of internal variability has been reproduced in the Meteorological Research Institute (MRI) coupled climate model (Kitoh *et al*., 1996; Kodera *et al*., 1996).

8.7.6 Pacific-North American (PNA) and Western Pacific (WP) Patterns

The Pacific-North American (PNA) and Western Pacific (WP) patterns are low-frequency teleconnection patterns (Wallace and Gutzler, 1981). Observations show that the PNA and WP are sensitive to the frequency distribution of the SST anomalies associated with ENSO. The HadAM3 model correctly reproduces the changes in frequency distribution of the PNA pattern between the El Niño years and the La Niña years (Renshaw *et al*., 1998). However, this model fails to reproduce the WP mode distribution. On the other hand, the JMA atmospheric model showed an ability to simulate the WP with reasonable intensity, responding to SST anomalies (Kobayashi *et al*., 2000). How extra-tropical air-sea interactions affect such weather regimes is not yet clear and an evaluation of the ability of coupled climate models to simulate these modes is yet to be undertaken.

8.7.7 Blocking

Blocking affects the large-scale flow and storm tracks and thus is important for mid-latitude climate. D'Andrea *et al*. (1998) evaluated the statistical behaviour of fifteen AMIP AGCMs in simulating Northern Hemisphere mid-latitude blocking. The AMIP models simulate reasonably well the seasonality and geographical location of blocking, but have a general tendency to underestimate both blocking frequency and the average duration of blocks. Using the ECMWF model, Brankovic and Molteni (1997) obtained a more realistic representation of Pacific blocking. This was due to reduced systematic error of zonal flow over the north-eastern Pacific. However, model deficiencies still remain in the Atlantic region. A link between the mean flow error in a model and blocking was also shown by Stratton (1999). In general, more recent atmospheric models show an improvement in ability to reproduce atmospheric blocking, but a corresponding evaluation of coupled climate models has not yet been undertaken.

8.7.8 Summary

Recent atmospheric models show improved performance in simulating many of the important phenomena, compared with those at the time of the SAR, by using better physical parametrizations and using higher resolutions both in the horizontal and in the vertical domain. A systematic evaluation of the ability of coupled climate models to simulate a full range of the phenomena referred in this section is yet to be undertaken. However, an intercomparison of El Niño simulations, one of the most important phenomena, has revealed the ability of coupled climate models to simulate the El Niño-like SST variability in the tropical Pacific and its associated changes in precipitation in the tropical monsoon regions, although the region of maximum SST variability is displaced further westward than in the observations.

8.8 Extreme Events

Since the SAR, there has been more attention paid to the analysis of extreme events in climate models. Unfortunately, none of the major intercomparison projects such as AMIP and CMIP have had diagnostic sub-projects that concentrated on analyses of extreme events. Very few coupled models have been subjected to any form of systematic extreme event analysis. Intercomparison of extreme events between models is also made very difficult due to the lack of consistent methodologies amongst the various analyses and also to the lack of access to high-frequency (at least daily) model data. Analysis has also been limited by the comparatively low resolution at which most models are run, this presents difficulties since most extreme events are envisaged to occur at the regional scale and have comparatively short lifetimes. However other forms of extreme event analysis have been developed which use the large-scale fields produced by a climate model and produce various indices of extreme events; such indices include maximum potential intensity of tropical cyclones (Holland, 1997) or maps of 20-year return values of variables such as precipitation or maximum temperature (Zwiers and

Table 8.4: *Analyses of extreme events in GCMs since the SAR. Wherever possible the model names have been made consistent with Table 8.1; however, since much of the analysis has been done with AGCMs alone (and often with comparatively old model versions) there often is no correspondence between these two tables. The references given refer to the particular analysis used, and are not necessarily tied to a specific model description.*

Names	References	Characteristics		Extreme events			
		AGCM	OGCM	T	Pr	ETC	TC
ARPEGE-C	Royer *et al*.,1998	T42, L30	no				F,G
CCC2	Zwiers and Kharin, 1998	T32, L10	no	D,L,R	D,L,R	P	P
CCM	Tsutsui and Kasahara, 1996	T42, L18	no				F,G
	Zhang and Wang, 1997	T42, L18	no				F
	Kothavala, 1997	T42L18	no		E		
CGCM1	Kharin and Zwiers, 2000	T32, L10	T64, L29	D,L.R	D,L,R	P	P
CSIRO	Watterson *et al*., 1995	R21, L9	no				F,G
	Walsh and Pittock, 1998	R21, L9	no	E			I,T,W
	Schubert *et al*., 1998	R21, L9	no	D,E			
ECHAM	Bengtsson *et al*., 1995, 1996, 1999	T106, L19	no				F,I,N
	Lunkeit *et al*., 1996	ECHAM2	OPYC			M	
	Beersma *et al*., 1997	ECHAM3	no				F,S
	Christoph *et al*.1997	T42, L19	no				S
	Schubert *et al*., 1998	T42, L19	LSG				F,I,S
FSU	Krishnamurti *et al*., 1998	T42, L16	no				F
GFDL	Vitart *et al*., 1997	T42, L18	no				F
	Haywood *et al*., 1997	R15, L9	GFDL_R15_a		D		
	Knutson *et al*., 1998	R30, L14	no				I
	Delworth *et al*., 1999	R15L9	no	H			
	Wetherald and Manabe, 1999	R15L9	no		D		
HadCM2	Carnell and Senior, 1998	2.5×3.75, L19	2.5×3.75, L20				N,S
HadCM2b	Bhaskaran and Mitchell, 1998	2.5×3.75, L19	2.5×3.75, L20		E		
HadAM2	Thorncroft and Rowell, 1998	2.5×3.75,L19	no				L,W
	Durman *et al*., 2001	2.5×3.75,L19	no		D,E		
JMA	Sugi *et al*., 1997	T106, L21	no				C
	Yoshimura *et al*., 1999	T106, L21	no				C
JMA/NIED	Matsuura *et al*., 1999	T106, L21	0.5×1.0, L37				F
PMIP	Kageyama *et al*., 1999	ECHAM3, LMD, UGAMP, UKMO	no		D		S
UKMO	Gregory and Mitchell1, 1995	2.5×3.75, L11	no	D	D		
	Hulme and Viner, 1998	UKTR	no				T
AGCMs	Hennessy *et al*., 1997	CSIRO, UKHI	no		D		
	Henderson-Sellers *et al.*, 1998	GFDL,ECHAM3	no				F,G,I,N,U
	McGuffie *et al*., 1999	BMRC, CCM	no		E,L,R		E,L,R
	Zhao *et al*., 2000	IAP, NCC	IAP				

Under “Extreme events”, column T denotes extremes in temperature, Pr denotes extremes in precipitation, ETC denotes extra-tropical cyclone, TC denotes tropical cyclone. The model names and characteristics are further explained (where possible) in Table 8.1.
GCM analyses have been with different techniques and methods designated as: C for cyclone centres; D for daily variability of temperature or precipitation; E for extreme temperature or precipitation; F for frequency of cyclones; G for Gray’s yearly genesis parameter; H for heat index; I for intensity of cyclone; L for dry/wet spells or hot/cold spells; M for maximum eddy growth rate; N for numbers of cyclones; P for wind speed; R for return value or return period; S for storm track; T for sea surface temperature; U for maximum potential intensity; W for wave activity.

Kharin, 1998) (a 20-year return value implies that the value given is reached once in every 20 years).

In this chapter we assess the following types of extreme events that can be presented in terms of global patterns; frequency of tropical cyclones, daily maximum and minimum temperature, length of hot or cold spells, and precipitation intensity and frequency (floods and droughts). While it is arguable that extra-tropical cyclones belong to the class of "extreme events" we choose to include them here for consistency with other chapters. Table 8.4 summarises the climate models and the types of extreme events that have been analysed since the SAR. Assessments of extreme events that are purely local or regional are discussed in Chapter 10.

8.8.1 Extreme Temperature

Analysis of extreme temperature in climate model simulations has concentrated on the surface daily maximum and minimum temperature, or on the duration of hot/cold spells on the global scale (Schubert, 1998; Zwiers and Kharin, 1998; McGuffie *et al*., 1999; Kharin and Zwiers, 2000).

Zwiers and Kharin (1998) and Kharin and Zwiers (2000) analysed the 20-year return values for daily maximum and minimum screen temperature simulated by both CCC GCM2 and CGCM1. Comparison with the NCEP reanalyses shows that the model reproduced the return values of both maximum and minimum temperature and warm/cold spells reasonably well.

Intercomparisons among five AGCMs for the return values of extreme temperature of <–20°C and >40°C over the globe show a reasonable level of agreement between the models in terms of global scale variability (McGuffie *et al*., 1999).

8.8.2 Extreme Precipitation

Analysis of extreme precipitation simulated by climate models has included the daily variability of anomalous precipitation (Zwiers and Kharin, 1998; McGuffie *et al*., 1999; Kharin and Zwiers, 2000), patterns of heavy rainfall (Bhaskran and Mitchell, 1998; Zhao *et al*., 2000b), as well as wet and dry spells (Thorncroft and Rowell, 1998; McGuffie *et al*., 1999). The results show some agreement with the available observations but the comparatively low model resolution is an inhibiting factor.

Ideally the simulated extreme rainfall should be compared with grided data calculated from the observed station data; however, observed grided data comparable to those produced by the models are scarce. Therefore, often the NCEP/NCAR reanalysis data are used as an "observed" data set despite the fact that this data set does not appear to reproduce daily variability well (Zwiers and Kharin, 1998). Another issue is the interpretation of precipitation simulated by a climate model, some authors treat simulated precipitation as grid-box averages; others argue that it should be treated as grid-point values (Zwiers and Kharin, 1998). Hennessy *et al*. (1997) compared the daily precipitation by both CSIRO and UKHI (United Kingdom High-Resolution) AGCMs coupled to mixed-layer ocean models. They found that simulated frequencies of daily precipitation were close to those for grid-box average observations.

In summary, in contrast with the simulations of extreme temperature by climate models, extreme precipitation is difficult to reproduce, especially for the intensities and patterns of heavy rainfall which are heavily affected by the local scale (see Chapter 10).

8.8.3 Extra-tropical Storms

Analyses of occurrences and tracks of extra-tropical storms have been performed for some climate models (Lunkeit *et al*., 1996; Beersma *et al*., 1997; Carnell and Senior, 1998; Schubert *et al*., 1998; Zwiers and Kharin, 1998; Kharin and Zwiers, 2000). However, very different methods are used to characterise extra-tropical storms, among the methods used are: mid-latitude storm tracks defined by 1,000 hPa wind speed (Zwiers and Kharin, 1998), maximum eddy growth rate at 350 hPa and 775 hPa (Lunkeit *et al*., 1996), index of storm tracks (such as 500 hPa height variability, sea level pressure, surface wind) (Beersma *et al*., 1997), frequency, intensity and track of 500 hPa transient eddies (Schubert *et al*., 1998), as well as low centres at 500 hPa (Carnell and Senior, 1998).

Kaurola (1997) compared the numbers of the observed extra-tropical storms north of 30°N for five winter seasons and from a 30-year simulation of the ECHAM3 atmospheric model for two periods during the control run. The comparisons indicated that the ratios of total numbers between the simulations and observations were 0.96 and 0.97 for two respective periods. It appears that the ECHAM3 model is able to simulate the numbers of storms north of 30°N in wintertime. The mid-latitude storm tracks over the North Pacific and Atlantic Oceans and over the southern circumpolar ocean were also well simulated by the CCC GCM2 (Zwiers and Kharin, 1998).

Kageyama *et al*. (1999) focused on the storm tracks of the Northern Hemisphere as simulated by several AGCMs. Intercomparisons of the nine AGCMs show that the models reproduce reasonably the storm tracks defined with high-pass second-order transient eddy quantities. These results also indicated that higher resolution models tend to be better at reproducing the storm tracks.

Schubert *et al*. (1998) analysed North Atlantic storms in the ECHAM3/LSG model. Their analysis indicated that the storm frequency, position and density agreed with the observations. Lunkeit *et al*. (1996) analysed storm activity in the ECHAM2/OPYC model. They found that the mean eddy activity and storm tracks in that simulation were in reasonable agreement with observations.

The general ability of models to simulate extra-tropical storms and storm tracks is most encouraging.

8.8.4 Tropical Cyclones

Tropical cyclones can be characterised in models by several measures such as their intensity, track, frequency and location of occurrence (Bengtsson *et al*., 1996; Sugi *et al*., 1997; Tsutsui *et al*., 1999). Other broad-scale fields such as maximum wind speed, maximum potential intensity (Holland, 1997) and high sea surface temperature (Hulme and Viner, 1998) are also used as

indicators of tropical cyclones. Thus it is important to consider the particular characteristics that are used to describe tropical cyclones in a given analysis when results from models are compared (Henderson-Sellers *et al*., 1998; Krishnamurti *et al*., 1998; Royer *et al*., 1998; Walsh and Pittock, 1998).

Many analyses have been based on the physical parameters favourable for cyclogenesis as summarised by Gray (1981). Gray relates the climatological frequency of tropical cyclone genesis to six environmental factors: (1) large values of low-level relative vorticity, (2) Coriolis parameter (at least a few degrees poleward of the equator), (3) weak vertical shear of the horizontal winds, (4) high SST's exceeding 26°C and a deep thermocline, (5) conditional instability through a deep atmospheric layer, and (6) large values of relative humidity in the lower and middle troposphere (Gray, 1981; Henderson-Sellers *et al*., 1998). Following the general concepts outlined by Emanuel (1987), Holland (1997) has derived an alternative thermodynamic approach to estimate maximum potential intensity of tropical cyclones. The approach requires an atmosphere sounding, SST, and surface pressure; it includes the oceanic feedback of increasing moist entropy associated with falling surface pressure over a steady SST, and explicitly incorporates a representation of the cloudy eye wall and a clear eye.

Several climate model simulations in Table 8.4 have been analysed using a variety of the above techniques to determine the frequency of tropical cyclones (Bengtsson *et al*., 1995; Watterson *et al*., 1995; Vitart *et al*., 1997; Royer *et al*., 1998). The ECHAM3 model has by far the highest horizontal resolution amongst these models. The numbers of simulated tropical cyclones are between 70 and 141 per year. The numbers of observed tropical cyclones per year are quite variable; 80 for the period 1958 to 1977 (Gray, 1979), 99 for the period 1952 to 1971 (Gray, 1975) and 86 for the period of 1970 to 1995 (Henderson-Sellers *et al*., 1998). Despite the differing definitions of tropical cyclones used in the different analyses, the range of tropical cyclones numbers simulated by the models are similar to the observed data.

Bengtsson *et al*. (1995; 1996; 1999) have analysed a five-year simulation with ECHAM3 at T106 (100 km) horizontal resolution. They conclude that the model could reproduce some aspects of the characteristic structure of tropical cyclones and some aspects of their geographical distribution and seasonal variability. They also found that in certain areas, in particular in the north-east Pacific, a realistic number of tropical cyclones was only generated by the model when the horizontal resolution was finer than 100 km. Their results showed a reasonably good agreement with the observed distribution, tracks and annual variability of tropical cyclones (Bengtsson *et al*., 1995, 1999). Sugi *et al*. (1997) and Yoshimura *et al*. (1999) used a 100 km version of the JMA AGCM and compared the simulated geographical distribution of tropical cyclones with observations. They obtained reasonably realistic geographical patterns. However, in contrast to the observations, they did not find a significant difference in tropical cyclone frequency when they used the SSTs representing El Niño and La Niña years.

Henderson-Sellers *et al*. (1998) suggested that AOGCMs could provide useful information of the frequency of tropical cyclones, but the models they studied all had coarse resolution (about 500 km), climate drift (or flux adjustment) and unproven skill for present day tropical cyclones. A first attempt of tropical cyclones simulations with a high-resolution coupled climate model was performed by Matsuura *et al*. (1999) with a 100 km JMA atmospheric model coupled with the GFDL modular ocean model (MOM2) (0.5°×1.0°) model (but without sea ice). This model reproduced some aspects of the structure of observed tropical cyclones, although the simulated "tropical cyclones" are weaker and larger in scale than the observed. The model also shows the observed tendency of less (more) frequent tropical cyclones and an eastward (westward) shift of their locations over the northwestern equatorial Pacific during El Niño (La Niña) years. This result gives us some confidence in using a high-resolution coupled climate model in the future to explore the relationship between global warming and the frequency and intensity of tropical cyclones .

In summary, high horizontal resolution AGCMs (or AOGCMs) are able to simulate some aspects of "tropical cyclone-like vortices" with some degree of success, but it is still too computationally expensive to use such models for long experiments. The type of tropical cyclone index chosen in the analysis of low-resolution climate models is important, the use of maximum potential intensity may provide the most robust estimate, but analyses using this index remain infrequent.

8.8.5 Summary and Discussion

Since the SAR, more attention has been paid to the analysis of extreme events in climate model simulations. Evaluations indicate that climate models are more capable of reproducing the variability in maximum and minimum temperature in the global scale than the daily precipitation variability. The ability of climate models to simulate extra-tropical storm tracks and storm frequency is encouraging. When tropical cyclones were analysed, high-resolution models generally produced better results. It is worth noting that some high-resolution operational numerical weather prediction models have demonstrated reasonable ability in forecasting tropical cyclones. This increases our confidence that they may be better reproduced by high-resolution climate models in the future.

The lack of consistent methodologies used in analyses of extreme events prevents a ready intercomparison of results between models; future IPCC assessments would be greatly assisted if common approaches were adopted.

8.9 Coupled Models – Dependence on Resolution

The importance of numerical aspects of climate models continues to be well recognised and new numerical techniques are beginning to be tested for use in climate simulation. However, there has been very little systematic investigation of the impact of improved numerics for climate simulation and many important questions remain unanswered. The degree of interaction between horizontal and vertical resolution in climate models and the interaction of physical parametrizations at differing resolutions has made it extremely difficult to make general statements about the convergence of model solutions and hence the optimum

resolution that should be used. An important question regarding the adequacy of resolution is deciding whether the information produced at finer scales at higher resolution feeds back on the larger scales or do the finer scales simply add to local effects (Williamson, 1999). Insufficient systematic work has been done with coupled models to answer this question. As well as improving numerical accuracy in advection, improved horizontal resolution can also improve the representation of the lower boundary of a model (the mountains) and the land-sea mask; this may improve the regional climate of a model but little systematic work has been carried out to assess this aspect.

8.9.1 Resolution in Atmospheric Models

A series of experiments that explores convergence characteristics has been conducted with the NCAR Community Climate Model (CCM) by Williamson (1999). In these experiments the grid and scale of the physical parametrizations was held fixed while the horizontal resolution of the dynamical core was increased. As the dynamical resolution was increased, but the parametrization resolution held fixed, the local Hadley circulation in the dual-resolution model simulations converged to a state close to that produced by a standard model at the fixed parametrization resolution. The mid-latitude transient aspects did not converge with increasing resolution when the scale of the physics was held fixed. Williamson (1999) concludes that the physical parametrizations used in climate models should explicitly take into account the scale of the grid on which it is applied. That does not seem to be common in parametrizations for global climate models today.

Pope *et al*. (1999) have also illustrated the positive impact of increased horizontal resolution on the climate of HADAM3. A number of systematic errors evident at low resolution are reduced as horizontal resolution is increased from 300 to 100 km. Improvements are considered to be mainly associated with better representation of storms. It is apparent that, for some models at least, neither the regional aspects of a climate simulation nor the processes that produce them converge over the range of horizontal resolutions commonly used (e.g., Déqué and Piedelievre, 1995; Stephenson and Royer, 1995; Williamson *et al*., 1995; Stephenson *et al.*, 1998). As part of a European project (High Resolution Ten-Year Climate Simulations, HIRETYCS, 1998), it was found that increases in horizontal resolution did not produce systematic improvements in model simulations and any improvements found were of modest amplitude.

The need for consistency between horizontal and vertical resolution in atmospheric models was first outlined by Lindzen and Fox-Rabinovitz (1989) but little systematic study has been followed. Experiments with the NCAR CCM3 showed that increased vertical resolution (up to 26 levels) above the standard 18 levels typical of the modest vertical resolutions of climate models is beneficial to the simulations (Williamson *et al.*, 1998). Pope *et al*. (2000) also considered the impact of increased (up to 30 levels) vertical resolution on simulations with HADAM3. In both cases a number of improvements were noted due mostly to the improved representation of the tropopause as the resolution was increased. However, Bossuet *et al*. (1998) reached a somewhat different conclusion when they increased the vertical resolution in the ARPEGE model; they concluded that increasing vertical resolution produced little impact on the simulated mean climate of their model. They also found that the physical parametrizations they employed were resolution independent. Increased vertical resolution in the upper troposphere and stratosphere has generally reduced model systematic errors in that region (Pawson *et al.*, 2000).

Enhanced regional resolution within an AGCM is possible through the global variable-resolution stretched-grid approach that has been further developed since the SAR (e.g., Dèquè and Piedelievre, 1995; Fox-Rabinovitz *et al*., 1997); this is discussed in more detail in Chapter 10.

8.9.2 Resolution in Ocean Models

A number of important oceanic processes are not resolved by the current generation of coupled models, e.g., boundary currents, mesoscale eddy fluxes, sill through flows. Two model studies show an explicit dependence of ocean heat transport on resolution, ranging between 4° and 0.1° (Fanning and Weaver, 1997a; Bryan and Smith, 1998). However, this dependence appears to be much weaker when more advanced sub-grid scale mixing parametrizations are used, at least at resolutions of 0.4° or less (Gent *et al*., 1999). As previously noted, a number of recent non-flux adjusted models produce acceptable large-scale heat transports. The need for ocean resolution finer than 1° is a matter of continuing scientific debate.

Some ocean models have been configured with increased horizontal resolution (usually specifically in the meridional direction) in the tropics in order to provide a better numerical framework to handle tropical ocean dynamics. Unfortunately at this time, there has been little systematic intercomparison of such model configurations.

8.9.3 Summary

The lack of carefully designed systematic intercomparison experiments exploring impacts of resolution is restricting our ability to draw firm conclusions. However, while the horizontal resolution of 2.5° (T42) or better in the atmospheric component of many coupled models is probably adequate to resolve most important features, the typical vertical resolution of around 20 levels is probably too low, particularly in the atmospheric boundary layer and near the tropopause. The potential exists for spurious numerical dispersion, when combined with errors in parametrizations and incompletely modelled processes, to produce erroneous entropy sources. This suggests that further careful investigation of model numerics is required as part of a continuing overall programme of model improvement. The vertical resolution required in the ocean component is still a matter of judgement and tends to be governed by available computing resources. There is still considerable debate on the adequacy of the horizontal resolution in the ocean component of coupled models and it is suggested that some results (those that are reliant on meridional heat transport) from coupled models with coarse (>1°) resolution ocean components should be treated cautiously.

8.10 Sources of Uncertainty and Levels of Confidence in Coupled Models

8.10.1 Uncertainties in Evaluating Coupled Models

Our attempts to evaluate coupled models have been limited by the lack of a more comprehensive and systematic approach to the collection and analysis of model output from well co-ordinated and well designed experiments. Important gaps still remain in our ability to evaluate the natural variability of models over the last several centuries. There are gaps in the specification of the radiative forcing (especially the vertical profile) as well as gaps in proxy palaeo-data necessary for the production of long time series of important variables such as surface air temperature and precipitation.

In order to assist future coupled model evaluation exercises, we would strongly encourage substantially expanded international programmes of systematic evaluation and intercomparison of coupled models under standardised experimental conditions. Such programmes should include a much more comprehensive and systematic system of model analysis and diagnosis, and a Monte Carlo approach to model uncertainties associated with parametrizations and initial conditions. The computing power now available to most major modelling centres is such that an ambitious programme that explores the differing direct responses of parametrizations (as well as some indirect effects) is now quite feasible.

Further systematic and co-ordinated intercomparison of the impact of physical parametrizations both on the ability to simulate the present climate (and its variability) and on the transient climate response (and its variability) is urgently needed.

The systematic analysis of extremes in coupled models remains considerably underdeveloped. Use of systematic analysis techniques would greatly assist future assessments.

It is important that in future model intercomparison projects the experimental design and data management takes heed of the detailed requirements of diagnosticians and the impacts community to ensure the widest possible participation in analysing the performance of coupled models.

8.10.2 Levels of Confidence

We have chosen to use the following process in assigning confidence to our assessment statements; the level of confidence we place in a particular finding reflects both the degree of consensus amongst modellers and the quantity of evidence that is available to support the finding. We prefer to use a qualitative three-level classification system following a proposal by Moss and Schneider (1999), where a finding can be considered:

"*well established*" – nearly all models behave the same way; observations are consistent with nearly all models; systematic experiments conducted with many models support the finding;

"*evolving*" – some models support the finding; different models account for different aspects of the observations; different aspects of key processes can be invoked to support the finding; limited experiments with some models support the finding; parametrizations supporting the finding are incompletely tested;

"*speculative*" – conceptually plausible idea that has only been tried in one model or has very large uncertainties associated with it.

8.10.3 Assessment

In this chapter, we have evaluated a number of climate models of the types used in Chapter 9. The information we have collected gives an indication of the capability of coupled models in general and some details of how individual coupled models have performed.

We regard the following as "well established":

- Incremental improvements in the performance of coupled models have occurred since the SAR, resulting from advances in the modelling of the oceans, atmosphere and land surface, as well as improvements in the coupling of these components.

- Coupled models can provide credible simulations of both the annual mean climate and the climatological seasonal cycle over broad continental scales for most variables of interest for climate change. Clouds and humidity remain sources of significant uncertainty but there have been incremental improvements in simulations of these quantities.

- Some non-flux adjusted models are now able to maintain stable climatologies of comparable quality to flux adjusted models.

- There is no systematic difference between flux adjusted and non-flux adjusted models in the simulation of internal climate variability. This supports the use of both types of model in detection and attribution of climate change.

- Several coupled models are able to reproduce the major trend in surface air temperature, when driven by radiative forcing scenarios corresponding to the 20th century. However, in these studies only idealised scenarios of only sulphate radiative forcing have been used.

- Many atmospheric models are able to simulate an increase of the African summer monsoon in response to insolation forcing for the Holocene but they all underestimate this increase if vegetation feedbacks are ignored.

We regard the following as "evolving":

- Coupled model simulation of phenomena such as monsoons and the NAO has improved since the SAR.

- Analysis of, and confidence in, extreme events simulated within climate models is emerging, particularly for storm tracks and storm frequency.

- The performance of coupled models in simulating ENSO has improved; however, the region of maximum SST variability is displaced westward and its strength is generally underestimated. When suitably initialised, some coupled models have had a degree of success in predicting ENSO events.

- Models tend to underestimate natural climate variability derived from proxy data over the last few centuries. This may be due to missing forcings, but this needs to be explored more systematically, with a wider range of more recent models.

- A reasonable simulation of a limited set of past climate states (over the past 20,000 years) has been achieved using a range of climate models, enhancing our confidence in using models to simulate climates different from the present day.

- Our ability to increase confidence in the simulation of land surface quantities in coupled models is limited by the need for significant advances in the simulation of snow, liquid and frozen soil moisture (and their associated water and energy fluxes).

- Coupled model simulations of the palaeo-monsoons produce better agreement with proxy palaeo-data when vegetation feedbacks are taken into account; this suggests that vegetation changes, both natural and anthropogenic, may need to be incorporated into coupled models used for climate projections.

- Models have some skill in simulating ocean ventilation rates, which are important in transient ocean heat uptake. However these processes are sensitive to choice of ocean mixing parametrizations.

- Some coupled models now include improved sea-ice components, but they do not yield systematic improvements in the sea-ice distributions. This may reflect the impact of errors in the simulated near surface wind fields, which offsets any improvement due to including sea-ice motion.

- Some coupled models produce good simulations of the large-scale heat transport in the coupled atmosphere-ocean system. This appears to be an important factor in achieving good model climatology without flux adjustment.

- The relative importance of increased resolution in coupled models remains to be evaluated systematically but many models show benefits from increased resolution.

- Our ability to make firmer statements regarding the minimum resolution (both horizontal and vertical) required in the components of coupled models is limited by the lack of systematic modelling studies.

We regard the following as "speculative":

- Tropical vortices with some of the characteristics of "tropical cyclones" may be simulated in high resolution atmospheric models but not yet in coupled climate models. Considerable debate remains over their detailed interpretation and behaviour.

- Some modelling studies suggest that adding forcings such as solar variability and volcanic aerosols to greenhouse gases and the direct sulphate aerosol effect improves the simulation of climate variability of the 20th century.

- Emerging modelling studies that add the indirect effect of aerosols and of ozone changes to greenhouse gases and the direct sulphate aerosol effect suggest that the direct aerosol effect may previously have been overestimated.

- Lack of knowledge of the vertical distribution of radiative forcing (especially aerosol and ozone) is contributing to the discrepancies between models and observations of the surface-troposphere temperature record.

Our overall assessment

Coupled models have evolved and improved significantly since the SAR. In general, they provide credible simulations of climate, at least down to sub-continental scales and over temporal scales from seasonal to decadal. The varying sets of strengths and weaknesses that models display lead us to conclude that no single model can be considered "best" and it is important to utilise results from a range of coupled models. We consider coupled models, as a class, to be suitable tools to provide useful projections of future climates.

References

Arking, A., 1996: Absorption of solar energy in the atmosphere: Discrepancy between model and observations. *Science*, **273**, 779-782.

Arking, A., 1999: The influence of clouds and water vapor on atmospheric absorption. *Geophys. Res. Lett.*, **26**, 2729-2732.

Arpe, K., H. Behr and L. Dümenil, 1997: Validation of the ECHAM4 climate model and re-analyses data in the Arctic region. Proc. Workshop on the Implementation of the Arctic Precipitation data Archive (APDA) at the Global Precipitation Climatology Centre (GPCC), Offenbach, Germany, World Climate Research Programme WCRP-98, WMO/TD No.804, 31-40.

Banks, H.T., 2000: Ocean heat transport in the South Atlantic in a coupled climate model. *J. Geophys. Res*. **105**, 1071-1092.

Barnett, T.P., 1999: Comparison of near-surface air temperature variability in 11 coupled global climate models. *J. Climate*, **12**, 511-518.

Barnett, T.P., B.D. Santer, P.D. Jones, R.S. Bradley and K.R. Briffa, 1996: Estimates of low frequency natural variability in near-surface air temperature. *The Holocene*, **6**, 255-263.

Barnston, A.G., Y. He and M.H. Glantz, 1999: Predictive skill of statistical and dynamical climate models in SST forecasts during the 1997-98 El Niño episode and the 1998 La Niña onset. *Bull. Am. Met. Soc*., **80**, 217-243.

Barthelet, P., S. Bony, P. Braconnot, A. Braun, D. Cariolle, E. Cohen-Solal, J.-L. Dufresne, P. Delecluse, M. Déqué, L. Fairhead, M.-A. Filiberti, M. Forichon, J.-Y. Grandpeix, E. Guilyardi, M.-N. Houssais, M. Imbard, H. LeTreut, C. Lévy, Z.-X. Li, G. Madec, P. Marquet, O. Marti, S. Planton, L. Terray, O. Thual and S. Valcke, 1998a: Simulations couplées globales de changements climatiques associés à une augmentation de la teneur atmosphérique en CO_2. C. R. Acad. Sci. Paris, Sciences de la terre et des planètes, 326, 677-684 (in French with English summary).

Barthelet, P., L. Terray and S. Valcke, 1998b: Transient CO_2 experiment using the ARPEGE/OPAICE nonflux corrected coupled model. *Geophys. Res. Lett*., **25**, 2277-2280.

Beersma, J.J., K.M. Rider, G.J. Komen, E. Kaas and V.V. Kharin, 1997: An analysis of extra-tropical storms in the North Atlantic region as simulated in a control and 2×CO_2 time-slice experiment with a high-resolution atmospheric model. *Tellus*, **49A**, 347-361.

Bell, J., P.B. Duffy, C. Covey, L. Sloan and the CMIP investigators, 2000: Comparison of temperature variability in observations and sixteen climate model simulations. *Geophys. Res. Lett.*, **27**, 261-264.

Bengtsson, L., M. Botzet and M. Esch, 1995: Hurricane-type vortices in a general circulation model. *Tellus*, **47A**, 175-196.

Bengtsson, L., M. Botzet and M. Esch, 1996: Will greenhouse gas-induced warming over the next 50 years lead to higher frequency and greater intensity of hurricanes? *Tellus*, **48A**, 57-73.

Bengtsson, L., E. Roeckner and M. Stendel, 1999: Why is global warming proceeding much slower than expected?. *J. Geophys., Res*., **104**, 3865-3876.

Betrand, C., J.-P. Van Ypersele and A. Berger, 1999: Volcanic and solar impacts on climate since 1700. *Clim. Dyn.*, **15**, 355-367.

Betts, A.K., J.H. Ball and A.C.M. Beljaars, 1993: Comparison between the land surface response of the ECMWF model and the FIFE-1987 data. *Quart. J. R. Met. Soc*., **119**, 975-1001.

Betts, R.A., P.M. Cox, S.E. Lee and F.I. Woodward, 1997: Contrasting physiological structural vegetation feedbacks in climate change simulations. *Nature*, **387**, 796-799.

Betts, R.A., P.M. Cox and F.I. Woodward, 2000: Simulated responses of potential vegetation to doubled-CO_2 climate change and feedbacks on near-surface temperature. *Global Ecology and Biogeography*, **9**, 171-180.

Bhaskaran, B. and J.F.B. Mitchell, 1998: Simulated changes in Southeast Asian monsoon precipitation resulting from anthropogenic emissions. *Int. J. Climatol.*, **18**, 1455-1462.

Boer, G.J., G. Flato, M.C. Reader and D. Ramsden, 2000: A transient climate change simulation with greenhouse gas and aerosol forcing: experimental design and comparison with the instrumental record for the 20th century. *Clim. Dyn*., **16**, 405-426.

Bonan, G.B., 1995: Land-atmosphere CO_2 exchange simulated by a land surface process model coupled to an atmospheric general circulation model. *J. Geophys. Res.*, **100**, 2817-2831.

Bossuet, C., M. Déué and D. Cariolle, 1998: Impact of a simple parameterization of convective gravity-wave drag in a stratosphere-troposphere general circulation model and its sensitivity to vertical resolution. *Ann. Geophysicae*, **16**, 238-249.

Boville, B.A. and P.R. Gent, 1998: The NCAR Climate System Model, Version One. *J. Climate*, **11**, 1115-1130.

Boville, B.A. and J.W. Hurrell, 1998: A comparison of the atmospheric circulations simulated by the CCM3 and CSM1. *J. Climate*, **11**, 1327-1341.

Boville, B.A., J.T. Kiehl, P.J. Rasch and F.O. Bryan, 2001: Improvements to the NCAR CSM-1 for transient climate simulations. *J. Climate*, **14**, 164-179.

Braconnot, P. and C. Frankignoul, 1993: Testing model simulations of the thermocline depth variability in the tropical Atlantic from 1982 to 1984. *J. Phys. Oceanogr.*, **23**, 626-647.

Braconnot, P., S. Joussaume, O. Marti and N. de Noblet, 1999: Synergistic feedbacks from ocean and vegetation on the African monsoon response to mid-Holocene insolation. *Geophys. Res. Lett.*, **26**, 2481-2484.

Braconnot, P., O. Marti, S. Joussaume and Y. Leclainche, 2000: Ocean feedback in response to 6 kyr BP insolation. *J. Climate*, **13**, 1537-1553.

Bradley, R.S. and P.D. Jones, 1993: 'Little Ice Age' summer temperature variations: their nature and relevance to recent global warming trends. *Holocene*, **3**, 367-376.

Brankovic, C. and F. Molteni, 1997: Sensitivity of the ECMWF model northern winter climate to model formulation. *Clim. Dyn*., **13**, 75-101.

Broccoli, A.J., 2000: Tropical cooling at the LGM: An atmosphere-mixed layer ocean model simulation, *J. Climate*, **13**, 951-976.

Broccoli, A.J. and E.P. Marciniak, 1996: Comparing simulated glacial climate and paleodata: a reexamination. *Paleoceanogr.*, **11**, 3-14.

Broccoli, A.J., N.-C. Lau and M.J. Nath, 1998: The cold ocean-warm land pattern: Model simulation and relevance to climate change detection. *J. Climate*, **11**, 2743-2763.

Brostrom, A., M. Coe, S.P. Harrison, R. Gallimore, J.E. Kutzbach, J. Foley, I.C. Prentice and P. Behling, 1998: Land Surface feedbacks and palaeomonsoons in Northern Africa. *Geophys. Res. Lett.*, **25**, 3615-3618.

Brovkin , V., A. Ganopolski, M. Claussen, C. Kubatzki and V. Petoukhov, 1999: Modelling climate response to historical land cover change. *Global Ecology and Biogeography*, **8**, 509-517.

Bryan, F.O., 1998: Climate drift in a multi century integration of the NCAR Climate System Model. *J. Climate*, **11**, 1455-1471.

Bryan, F.O. and R.D. Smith, 1998: Modelling the North Atlantic circulation: from eddy-resolving to eddy-permitting. International WOCE Newsletter, **33**, 12-14.

Bryden, H.L., D.H. Roemmich and J.A. Church, 1991: Ocean heat transport across 24N in the Pacific. *Deep Sea Res*., **38**, 297-324.

Carnell, R.E. and C.A. Senior, 1998: Changes in mid-latitude variability due to increasing greenhouse gases and sulphate aerosols. *Clim. Dyn*., **14**, 369-383.

Cess, R., M.H. Zhang, G.L. Potter, V. Alekseev, H.W. Barker, S. Bony, R.A. Colman, D.A. Dazlich, A.D. Del Genio, M. Deque, M.R. Dix, V. Dymnikov, M. Esch, L.D. Fowler, J.R. Fraser, V. Galin, W.L. Gates, J.J. Hack, W.J. Ingram, J.T. Kiehl, Y. Kim, H. Le Treut, K.K.-

W. Lo, B.J. McAvaney, V.P. Meleshko, J.-J. Morcrette, D.A. Randall, E. Roeckner, J.-F. Royer, M.E. Schlesinger, P.V. Sporyshev, B. Timbal, E.M. Volodin, K.E. Taylor, W. Wang, W.C. Wang and R.T. Wetherald, 1997: Comparison of the seasonal change in cloud-radiative forcing from atmospheric general circulation models and satellite observations. *J. Geophys. Res*., **102**, 16593-16603.

Chandrasekar, A., D.V.B. Rao and A. Kitoh, 1999: Effect of horizontal resolution on the simulation of Asian summer monsoon using the MRI GCM-II. *Pap. Met. Geophys*., **50**, 65-80.

Chase, T.N., R.A. Pielke, T.G.F. Kittel, R. Nemani and S.W. Running, 2000: Simulated impacts of historical land cover changes on global climate. *Clim. Dyn.*, **16**, 93-105.

Chassignet, E.P., L.T. Smith, R. Bleck and F.O. Bryan, 1996: A model comparison: numerical simulations of the north and equatorial Atlantic oceanic circulation in depth and isopycnic coordinates. *J. Phys. Oceanogr*., **26**, 1849-1867.

Chen, T.H., A. Henderson-Sellers, P.C.D. Milly, A.J. Pitman, A.C.M. Beljaars, J. Polcher, F. Abramopoulos, A. Boone, S. Chang, F. Chen, Y. Dai, C.E. Desborough, R.E. Dickenson, L. Dumenil, M. Ek, J.R. Garratt, N. Gedney, Y.M. Gusev, J. Kim, R. Koster, E.A. Kowalczyk, K. Laval, J. Lean, D. Lettenmaier, X. Liang, J.-F. Mahfouf, H.-T. Mengelkamp, K. Mitchell, O.N. Nasonova, J. Noilhan, J. Polcher, A. Robock, C. Rosenzweig, J. Schaake, C.A. Schlosser, J.-P. Schulz, A.B. Shmakin, D.L. Verseghy, P. Wetzel, E.F. Wood, Y. Xue, Z.-L. Yang and Q. Zeng, 1997: Cabauw experimental results from the project for intercomparison of land surface parameterization schemes. *J. Climate*, **10**, 1144-1215.

Christoph, M., U. Ulbrich and P. Speth, 1997: Midwinter suppression of Northern Hemisphere storm track activity in the real atmosphere and in GCM experiments. *J. Atmos. Sci.,* **54**, 1589-1599.

Claussen, M. and V. Gayler, 1997: The greening of Sahara during the mid-Holocene: results of an interactive atmosphere-biome model. *Global Ecol Biogeography Letters*, **6**, 369-377.

Claussen, M., C. Kubatzki, V. Brovkin and A. Ganopolski, 1999: Simulation of an abrupt change in Saharan vegetation in the mid-Holocene. *Geophys. Res. Lett.*, **26**, 2037-2040.

CLIMAP, 1981: Seasonal reconstructions of the Earth's surface at the last glacial maximum. Map Series, Technical Report MC-36, Geological Society of America, Boulder, Colorado.

Coe, M.T. and G.B. Bonan, 1997: Feedbacks between climate and surface water in northern Africa during the middle Holocene. *J. Geophys. Res.*, **102**, 11087-11101.

Coe, M.T. and S. Harrison, 2000: A comparison of the simulated surface water area in Northern Africa for the 6000 yr. BP experiments, In "Paleoclimate Modeling Intercomparison Project (PMIP) : proceedings of the third PMIP workshop, Canada, 4-8 October 1999" P. Braconnot (Ed), WCRP-111, WMO/TD-1007, 65-68.

COHMAP-Members, 1988: Climatic changes of the last 18,000 years: observations and model simulations. *Science*, **241**, 1043-1052.

Covey, C., A. Abe-Ouchi, G.J. Boer, G.M. Flato, B.A. Boville, G.A. Meehl, U. Cubasch, E. Roeckner, H. Gordon, E. Guilyardi, L. Terray, X. Jiang, R. Miller, G. Russell, T.C. Johns, H. Le Treut, L. Fairhead, G. Madec, A. Noda, S.B. Power, E.K. Schneider, R.J. Stouffer and J.-S. von Storch, 2000a: The Seasonal Cycle in Coupled Ocean-Atmosphere General Circulation Models, *Clim. Dyn*., **16**, 775-787.

Covey, C., K.M. AchutaRao, S.J. Lambert and K.E. Taylor, 2000b: Intercomparison of Present and Future Climates Simulated by Coupled Ocean-Atmosphere GCMs. *PCMDI Report No 66*. Program for Climate Model Diagnosis and Intercomparison, Lawrence Livermore National Laboratory, University of California, Livermore, CA.

Cowling, S.A., 1999: Simulated effects of low atmospheric CO_2 on structure and composition of North American vegetation at the Last Glacial Maximum. *Global Ecology and Biogeography*, **8**, 81-93.

Cox, M.D., 1989: An idealised model of the world ocean. Part I: the global scale water masses. *J. Phys. Oceanogr*., **19**, 1730-1752.

Crossley, J.F., J. Polcher, P.M. Cox, N. Gedney and S. Planton, 2000: Uncertainties linked to land surface processes in climate change simulations. *Clim. Dyn.* **16**, 949-961.

Crowley, T.J., 2000: Causes of climate change over the past 1000 years. *Science*, **289**, 270–277.

Crowley, T.J. and S.K. Baum, 1997: Effect of vegetation on an ice-age climate model simulation. *J. Geophys. Res.*, **102**, 16463-16480.

Crowley, T.J. and K.-Y. Kim, 1999: Modeling the temperature response to forced climate change over the last six centuries. *Geophys. Res. Lett*., **26**, 1901-1904.

Cubasch, U., K. Hasselmann, H. Höck, E. Maier-Reimer, U. Mikolajewicz, B.D. Santer and R. Sausen, 1992: Time-dependent greenhouse warming computations with a coupled ocean-atmosphere model. *Clim. Dyn*., **8**, 55-69.

Cubasch, U., B.D. Santer, A. Hellbach, G.C. Hegerl, H. Hock, E. Meir Reimer, U. Mikolajewicz , A. Stossel and R. Voss, 1994: Monte Carlo forecasts with a coupled ocean-atmosphere model. *Clim. Dyn*., **10**, 1-19.

Cubasch, U., R. Voss, G.C. Hegerl, J. Waszkewitz and T.J. Crowley, 1997: Simulation of the influence of solar radiation variations on the global climate with an ocean-atmosphere general circulation model. *Clim. Dyn*., **13**, 757-767.

Danabasoglu, G., 1998: On the wind-driven circulation of the uncoupled and coupled NCAR climate system ocean model. *J. Climate*, **11**, 1442-1454.

Danabasoglu, G. and J.C. McWilliams, 1996: Sensitivity of the global ocean circulation to parameterizations of mesoscale tracer transports. *J. Climate*, **8**, 2967-2987.

D'Andrea, F., S. Tibaldi and Co-authors, 1998: Northern Hemisphere atmospheric blocking as simulated by 15 atmospheric general circulation models in the period 1979-1988. *Clim. Dyn*., **14**, 385-407.

de las Heras, M.M. and R. Schlitzer, 1999: On the importance of intermediate water flows for the global ocean overturning. *J. Geophys. Res*., **104**, 15515-15536.

Delecluse, P., M.K. Davey, Y. Kitamura, S.G.H. Philander, M. Suarez and L. Bengtsson, 1998: Coupled general circulation modeling of the tropical Pacific. *J. Geophys. Res.*, **103**, 14357-14373.

Del Genio, A.D., W. Kovari Jr. and M.-S. Yao, 1994:Climatic implications of the seasonal variation of upper troposphere water vapor, *Geophys. Res. Lett*., **21**, 2701-2704.

Delworth, T.L., 1996: North Atlantic interannual variability in a coupled ocean-atmosphere model. *J. Climate*, **9**, 2356-2375.

Delworth, T.L. and M.E. Mann, 2000: Observed and simulated multidecadal variability in the North Atlantic. *Clim. Dyn*., **16**, 661-676.

Delworth, T.L., J.D. Mahlman and T.R. Knutson, 1999, Changes in heat index associated with CO_2-induced global warming. *Clim. Change*, **43**, 369-396.

Delworth, T.L. and T.R. Knutson, 2000: Simulation of the early 20th century global warming. *Science*, **287**, 2246–2250.

De Noblet, N., M. Claussen and C. Prentice, 2000: Mid-Holocene greening of the Sahara: first results of the GAIM 6000 yr BP experiment with two asynchronously coupled atmosphere/biome models. *Clim. Dyn.*, **16**, 643-659.

Déqué, M. and J.P. Piedelievre, 1995: High resolution climate simulation over Europe. *Clim. Dyn*., **11**, 321-339.

Desborough, C.E, 1999: Surface energy balance complexity in GCM land surface models. *Clim. Dyn.*, **15**, 389-403.

Dewitt, D.G. and E.K. Schneider, 1999: The processes determining the annual cycle of equatorial sea surface temperature: A coupled general circulation model perspective. *Mon. Wea. Rev*., **127**, 381-395.

Dijkstra , H.A. and J.D. Neelin, 1999: Imperfections of the thermohaline circulation: multiple equilibria and flux correction. *J. Climate*,

12, 1382-1392.

Dirmeyer, P.A., A.J. Dolman and N. Sato, 1999: The pilot phase of the global soil wetness project. *Bull. Am. Met. Soc.*, **80**, 851-878.

Dixon, K.W. and J.R. Lanzante, 1999: Global mean surface air temperature and North Atlantic overturning in a suite of coupled GCM climate change experiments. *Geophys. Res. Lett*., **26**, 1885-1888.

Dixon, K.W., J.L. Bullister, R.H. Gammon and R.J. Stouffer, 1996: Examining a coupled climate model using CFC-11 as an ocean tracer. *Geophys Res. Lett*., **23**, 1957-1960.

Doherty, R., J. Kutzbach, J. Foley and D. Pollard, 2000: Fully-coupled climate/dynamical vegetation model simulations over Northern Africa during the mid-Holocene. *Clim. Dyn.*, **16**, 561-573.

Doney, S.C., W.G. Large and F.O. Bryan, 1998: Surface ocean fluxes and water-mass transformation rates in the coupled NCAR Climate System Model. *J. Climate*, **11**, 1420-1441.

Ducharne, A., K. Laval and J. Polcher, 1998: Sensitivity of the hydrological cycle to the parameterization of soil hydrology in a GCM. *Clim. Dyn.*, **14**, 307-327.

Duffy, P.B., J. Bell, C. Covey and L. Sloan, 2000: Effect of flux adjustments on temperature variability in climate models. *Geophys. Res. Lett.*, **27**, 763-766.

Dümenil, L., S. Hagemann, and K. Arpe, 1997: Validation of the hydrological cycle in the Arctic using river discharge data. Proc. Workshop on Polar Processes in Global Climate (13-15 November 1996, Cancun, Mexico), AMS, Boston, USA.

Duplessy, J.C., N.J. Shackleton, R.G. Fairbancks, L. Labeyrie, D. Oppo and N. Kallel, 1988: Deepwater source variations during the last climatic cycle and their impact on the global deepwater circulation. *Paleoceanography*, **3**, 343-360.

Durman, C.F., J.M. Gregory, D.C. Hassell, R.G. Jones and J.M. Murphy, 2001: A comparison of extreme European daily precipitation simulated by a global and regional climate model for present and future climates. *Quart. J. R. Met. Soc*., in press.

DYNAMO Group, 1997: Dynamics of North Atlantic Models: simulation and assimilation with high resolution models. Report no. 294, Institut fuer Meereskunde, University of Kiel, Kiel, Germany, 334pp.

Emanuel, K.A., 1987: The dependence of hurricane intensity on climate. *Nature,* **326**, 483-485.

Emori, S., T. Nozawa, A. Abe-Ouchi, A. Numaguti, M. Kimoto and T. Nakajima, 1999: Coupled ocean-atmosphere model experiments of future climate change with an explicit representation of sulfate aerosol scattering. *J. Met. Soc. Japan*, **77**, 1299-1307.

England, M.H. and S. Rahmstorf, 1999: Sensitivity of ventilation rates and radiocarbon uptake to subsurface mixing parameterisation in ocean models. *J. Phys. Oceanogr*., **29**, 2802-2827.

England, M.H. and E. Maier-Reimer, 2001: Using Chemical tracers to Assess Ocean models. *Rev. Geophys.*, **39**, 29-70.

Fanning, A.F. and A.J. Weaver, 1996: An Atmospheric energy-moisture balance model: Climatology, interpentadal climate change, and coupling to an ocean general circulation model. *J. Geophys. Res*., **101**, 15111-15128.

Fanning, A.F. and A.J. Weaver, 1997a: A horizontal resolution and parameter sensitivity analysis of heat transport in an idealized coupled model. *J. Climate*, **10**, 2469-2478.

Fanning, A.F. and A.J. Weaver, 1997b: On the role of flux adjustments in an idealised coupled climate model. *Clim. Dyn*., **13**, 691-701.

Farrera, I., S.P. Harrison, I.C. Prentice, G. Ramstein, J. Guiot, P.J. Bartlein, R. Bonnefille, M. Bush, W. Cramer, U. von Grafenstein, K. Holmgren, H. Hooghiemstra, G. Hope, D. Jolly, S.-E. Lauritzen, Y. Ono, S. Pinot, M. Stute and G. Yu, 1999: Tropical climates at the last glacial maximum: a new synthesis of terrestrial palaeoclimate data. I. Vegetation, lake-levels and geochemistry. *Clim. Dyn.*, **15**, 823-856.

Ferranti, L., J.M. Slingo, T.N. Palmer, B.J. Hoskins, 1999: The effect of land surface feedbacks on the monsoon circulation. *Quart. J. R. Met. Soc.*, **125**, 1527-1550.

Flatau, M., P.J. Flatau, P. Phoebus and P.P. Niiler, 1997: The feedback between equatorial convection and local radiative and evaporative processes: The implications for intra seasonal oscillations. *J. Atmos. Sci*., **54**, 2373-2386.

Flato, G.M. and G.J. Boer, 2001: Warming Asymmetry in Climate Change Experiments. *Geophys. Res. Lett*., **28**, 195-198.

Flato, G., G.J. Boer, W.G. Lee, N.A. McFarlane, D. Ramsden, M.C. Reader and A.J. Weaver, 2000: The Canadian Centre for Climate Modelling and Analysis Global Coupled Model and its Climate. *Clim. Dyn.*, **16**, 451-468.

Foley, J.A., J.E. Kutzbach, M.T. Coe and S. Levis, 1994: Feedbacks between climate and boreal forests during the Holocene epoch. *Nature,* **371**, 52-54.

Folland, C.K., D.E. Parker, A. Colman and R. Washington, 1999: Large scale modes of ocean surface temperature since the late nineteenth century. In: *Beyond El Niño: Decadal and Interdecadal Climate Variability.* Navarra, A., Ed., Springer-Verlag, Berlin, pp 73-102.

Foster, D.J., Jr. and R.D. Davy, 1988: Global snow depth climatology. USAF publication USAFETAC/TN-88/006, Scott Air Force Base, Illinois, 48 pp.

Fox-Rabinovitz, M.S., G.L. Stenchikov, M.J. Suarez and L.L. Takacs, 1997: A Finite-Difference GCM Dynamical Core with a Variable-Resolution Stretched Grid. *Mon. Wea. Rev.*, **125**, 2943–2968.

Frankignoul, C., C. Duchêne and M.A. Cane, 1989: A statistical approach to testing equatorial ocean models with observed data. *Journal of Physical Oceanography*, **19**, 1191-1209.

Free, M. and A. Robock, 1999: Global warming in the context of the Little Ice Age. *J. Geophys. Res.*, **104**, 19057-19070.

Frei, A. and D. Robinson, 1998: Evaluation of snow extent and its variability in the Atmospheric Model Intercomparison Project. *J. Geophys. Res.*, **103**, 8859-8871.

Fyfe, J.C., G.J. Boer and G.M. Flato, 1999: The Arctic and Antarctic oscillations and their projected changes under global warming. *Geophys. Res. Lett*., **26**, 1601-1604.

Gadgil, S. and S. Sajani, 1998: Monsoon precipitation in the AMIP runs. *Clim. Dyn*., **14**, 659-689.

Gallee, H., J.P. van Ypersele, T. Fichefet, C. Tricot and A. Berger, 1991: Simulation of the last glacial cycle by a coupled, sectorially averaged climate-ice sheet model. I. The climate model. *J. Geophys Res*., **96**, 13139-13161.

Ganopolski, A., C. Kubatzki, M. Claussen, V. Brovkin and V. Petoukhov, 1998a: The influence of vegetation-atmosphere-ocean interaction on climate during the mid-Holocene. *Science*, **280**, 1916-1919.

Ganopolski, A., S. Rahmstorf, V. Petoukhov and M. Claussen, 1998b: Simulation of modern and glacial climates with a coupled global model of intermediate complexity. *Nature,* **391**, 351-356.

Garratt, J.R., 1994: Incoming shortwave fluxes at the surface - a comparison of GCM results with observations. *J. Climate*, **7**, 72-80.

Garratt, J.R. and A.J. Prata, 1996: Downwelling Longwave Fluxes at Continental Surfaces - A Comparison of Observations with GCM Simulations and Implications for the Global Land-Surface Radiation Budget. *J. Climate*, **9**, 646-655.

Garratt, J.R., A.J. Prata, L.D. Rotstayn, B.J. McAvaney and S. Cusack, 1998: The Surface Radiation Budget over Oceans and Continents. *J. Climate,* **11**, 951-1968.

Gates, W.L., A. Henderson-Sellers, G.J. Boer, C.K. Folland, A. Kitoh, B.J. McAvaney, F. Semazzi, N. Smith, A.J. Weaver and Q.-C. Zeng, 1996: Climate Models - Evaluation. In: *Climate Change 1995: The Science of Climate Change. Contribution of Working Group I to the Second Assessment Report of the Intergovernmental Panel on Climate Change* [Houghton, J.T., L.G. Meira Filho, B.A. Callander, N. Harris, A. Kattenberg, and K. Maskell (eds.)]. Cambridge University Press, Cambridge, United Kingdom and New York, NY, USA, pp 228-284.

Gates, W.L., J. Boyle, C. Covey, C. Dease, C. Doutriaux, R. Drach, M.

Fiorino, P. Gleckler, J. Hnilo, S. Marlais, T. Phillips, G. Potter, B.D. Santer, K.R. Sperber, K. Taylor and D. Williams, 1999: An Overview of the Results of the Atmospheric Model Intercomparison Project (AMIP I). *Bull. Am. Met. Soc*., **80**, 29-55.

Gedney, N., P.M. Cox, H. Douville, J. Polcher and P.J. Valdes, 2000: Characterising GCM land surface schemes to understand their response to climate change. *J. Climate,* **13**, 3066-3079.

Gent, P.R and J.C. McWilliams, 1990: Isopycnal mixing in ocean circulation models. *J. Phys.Oceanogr*., **20**, 150-155.

Gent, P.R., F.O. Bryan, G. Danabasoglu, S.C. Doney, W.R. Holland, W.G. Large and J.C. McWilliams, 1998: The NCAR Climate System Model Global Ocean Component. *J. Climate,* **11**, 1287-1306.

Gent, P.R., F.O. Bryan, S.C. Doney and W.G. Large, 1999: A perspective on the ocean component of climate models. CLIVAR Exchanges **4**(4).

Gibson, J.K., P. Kallberg, S. Uppala, A. Hernandez, A. Nomura and E. Serrano, 1997: ERA description. ECMWF Reanalysis Project Report Series 1, European Centre for Medium Range Weather Forecasts, Reading, UK, 66 pp.

Gilgen, H., M. Wild and A. Ohmura, 1998: Means and trends of shortwave irradiance at the surface estimated from Global Energy Balance Archive data. *J. Climate,* **11**, 2042-2061.

Gloersen, P., W.J. Campbell, D.J. Cavalieri, J.C. Comiso, C.L. Parkinson and H.J. Zwally, 1992: Arctic and Antarctic sea ice, 1978-1987: Satellite passive-microwave observations and analysis. NASA SP-511, National Aeronautics and Space Administration, Washington, 290 pp.

Goddard, L. and N.E. Graham, 1999: The importance of the Indian Ocean for GCM-based climate forecasts over eastern and southern Africa. *J. Geophys. Res*., **104**, 19099-19116.

Goosse, H., E. Deleersnijder, T. Fichefet and M. England, 1999: Sensitivity of a global coupled ocean-sea ice model to the parameterization of vertical mixing. *J. Geophys. Res*., **104**, 13681-13695.

Gordon, H.B. and S.P. O'Farrell, 1997: Transient climate change in the CSIRO coupled model with dynamic sea ice. *Mon. Wea. Rev*., **125**, 875-907.

Gordon, C., C. Cooper, C.A. Senior, H.T. Banks, J.M. Gregory, T.C. Johns, J.F.B. Mitchell and R.A. Wood, 2000: The simulation of SST, sea ice extents and ocean heat transports in a version of the Hadley Centre coupled model without flux adjustments. *Clim. Dyn.*, **16**, 147-168.

Gray, W.M., 1975: Tropical cyclone genesis. CSU Report No.234, 121 pp.

Gray, W.M., 1979: Hurricanes: their formation, structure and likely role in the tropical circulation, in Shaw, D.B. (ed.), *Meteorology over the tropical oceans*, Royal Meteorological Society, J. Glaisher House, Grenville place, Bracknell, Berks, pp 155-218.

Gray, W.M. 1981: Recent advances in Tropical Cyclone Research from rawinsonde composite analysis. World Meteorological Organisation, 407 pp.

Gregory, J.M. and J.F.B. Mitchell, 1995: Simulation of daily variability of surface temperature and precipitation over Europe in the current and 2×CO_2 climate using the UKMO climate model. *Quart. J. R. Met. Soc.*, **121**, 1451-1476.

Gregory, J.M. and J.F.B. Mitchell, 1997: The climate response to CO_2 of the Hadley Centre coupled AOGCM with and without flux adjustment. *Geophys. Res. Lett*., **24**, 1943-1946.

Guilderson, T., R. Fairbanks and J. Rubenstone, 1994: Tropical temperature variations since 20,000 years ago: modulating interhemispheric climate change. *Science,* **263**, 663-665.

Guilyardi, E., 1997: Role de la physique oceaniqe sur la formation/consummation des masses d'eau dans un modle couplé-atmosphè. Ph.D. thesis, Université Paul Sabatier, 195 pp.

Guilyardi, E. and G. Madec, 1997: Performance of the OPA/ARPEGE-T21 global ocean-atmosphere coupled model. *Clim. Dyn.,* **13**, 149-165.

Guiot, J., J.J. Boreux, P. Braconnot, F. Torre and PMIP participants, 1999: Data-model comparison using fuzzy logic in palaeoclimatology. *Clim. Dyn.*, **15**, 569-581.

Hagemann, S. and L. Dümenil, 1998: A parameterization of the lateral water flow for the global scale. *Clim. Dyn.*, **14**, 17-31.

Hall, M.M. and H.L. Bryden, 1982: Direct estimates of ocean heat transport. *Deep Sea Res*., **29**, 339-359.

Handorf , D., V.K. Petoukhov, K. Dethloff, A.V. Eliseev, A. Weisheimer and I.I. Mokhov, 1999: Decadal climate variability in a coupled atmosphere-ocean climate model of moderate complexity. *J. Geophys. Res.*, **104**, 27253-27275.

Hansen, J., M. Sato, A. Lacis and R. Rueby, 1997: The missing climate forcing. *Phil. Trans. Roy. Soc. Lond*. B, **352**, 231-240.

Hansen, J., M. Sato, A. Lacis, R. Rueby, I. Tegen and E. Matthews, 1998: Climate forcing in the Industrial Era. *Proc. Nat. Acad. Sci*., **95**, 12753-12758.

Harrison, S.P., G. Yu and P.E. Tarasov, 1996: The Late Quaternary lake-level record from northern Eurasia. *Quat. Res.,* **45**, 138-159.

Harrison, S.P., D. Jolly, F. Laarif, A. Abe-Ouchi, B. Dong, K. Herterich, C. Hewitt, S. Joussaume, J.E. Kutzbach, J. Mitchell, N. de Noblet and P. Valdes, 1998: Intercomparison of simulated global vegetation distributions in response to 6 kyr BP orbital forcing. *J. Climate,* **11**, 2721-2742.

Harvey, L.D.D., J. Gregory, M. Hoffert, A. Jain, M. Lal, R. Leemans, S.C.B. Raper, T.M.L. Wigley and J.R. de Wolde, 1997: An introduction to simple climate models used in the IPCC Second Assessment Report. *IPCC Technical Paper 2,* J.T. Houghton, L.G. Meira Filho, D.J. Griggs and K. Maskell (Eds.). IPCC, Geneva, Switzerland, 51 pp.

Hasselmann, K., L. Bengtsson, U. Cubasch, G.C. Hegerl, H. Rodhe, E. Roeckner, H. von Storch, R. Voss and J. Waszkewitz, 1995: Detection of anthropogenic climate change using a fingerprint method. In: *Proceedings of "Modern Dynamical Meteorology", Symposium in honor of Aksel Wiin-Nielsen, 1995*, P. Ditlevsen (ed.), ECMWF press, 1995.

Haywood, J.M., R.J. Stouffer, R.T. Wetherald, S. Manabe and V. Ramaswamy, 1997: Transient response of a coupled model to estimated changes in greenhouse gas and sulfate concentrations. *Geophys. Res. Lett*., **24**, 1335-1338.

Hegerl, G.C., K. Hasselmann, U. Cubasch, J.F.B. Mitchell, E. Roeckner, R. Voss and J. Waszkewitz, 1997: Multi-fingerprint detection and attribution analysis of greenhouse gases, greenhouse gas-plus-aerosol and solar forced climate change. *Clim. Dyn*., **13**, 613-634.

Henderson-Sellers, A., A.J. Pitman, P.K. Love, P. Irannejad and T. Chen, 1995: The project for Intercomparison of land surface parameterisation schemes PILPS) Phases 2 and 3. *Bull. Am. Met. Soc.*, **76**, 489-503.

Henderson-Sellers, A., H. Zhang, G. Berz, K. Emanuel, W. Gray, C. Landsea, G. Holland, J. Lighthill, S.-L. Shieh, P. Webster and K. McGuffie, 1998: Tropical cyclones and global climate change: a post-IPCC assessment. *Bull. Am. Met. Soc*., **79**, 19-38.

Henderson-Sellers, A. and K. McGuffie, 1999: Concepts of good science in climate change modelling: Comments on S. Shackley *et al.* Climatic Change 38, 1998. *Clim. Change*, **42**, 597-610.

Hennessy, K.J., J.M. Gregory and J.F.B. Mitchell, 1997: Changes in daily precipitation under enhanced greenhouse conditions. *Clim. Dyn*., **13**, 667-680.

Hewitt, C.D. and J.F.B. Mitchell, 1997: Radiative forcing and response of a GCM to ice age boundary conditions: cloud feedbacks and climate sensitivity. *Clim. Dyn.*, **13**, 821-834.

Hewitt, C.D. and J.F.B. Mitchell, 1998: A fully coupled GCM simulation of the climate of the mid-Holocene. *Geophys. Res. Lett.*, **25**, 361-364.

HIRETYCS (High Resolution Ten-Year Climate Simulations), 1998: Final Report, Contract No. ENV4-CT95-0184, European

Commission Environment and Climate Program, Brussels.

Hoelzmann, P., D. Jolly, S.P. Harrison, F. Laarif, R. Bonnefille and H.-J. Pachur, 1998: Mid-Holocene land-surface conditions in northern Africa and the Arabian peninsula: a data set for AGCM simulations. *Global Biogeochemical Cycles*, **12**, 35-52.

Hoffert, M.I. and C. Covey, 1992 : Deriving global climate sensitivity from paleoclimate reconstructions. *Nature*, **360**, 573-576.

Hogan, T.F. and T. Li, 1997: Long-term simulations with a coupled global atmosphere-ocean prediction system. *NRL Review*, 183-185.

Hogg, N.G., 1983: A note on the deep circulation of the western North Atlantic: its nature and causes. *Deep Sea Res*., **30**, 945-961.

Holland, G.J., 1997: The maximum potential intensity of tropical cyclones. *J. Atmos. Sci*., **54,** 2519-2541.

Hulme, M., 1992: Global land precipitation climatology for the evaluation of general circulation models. *Clim. Dyn*., **7**, 57–72.

Hulme, M., 1994: Validation of large-scale precipitation fields in general circulation models. In*: Global Precipitation and Climate Change*. Desbois, M., and F. Desalmand, Eds., NATO ASI Series, Springer Verlag, Berlin.

Hulme, M. and D. Viner, 1998: A climate change scenario for the tropics. *Clim. Change*, **39**, 145-176.

IPCC, 1996: Climate Change 1995: The Science of Climate Change. Contribution of Working Group I to the Second Assessment Report of the Intergovernmental Panel on Climate Change [Houghton, J.T., L.G. Meira Filho, B.A. Callander, N. Harris, A. Kattenberg, and K. Maskell (eds.)]. Cambridge University Press, Cambridge, United Kingdom and New York, NY, USA, 572 pp.

Ishii, M., N. Hasegawa, S. Sugimoto, I. Ishikawa, I. Yoshikawa and M. Kimoto, 1998: An El Niño prediction experiment with a JMA ocean-atmosphere coupled model, "Kookai". Proceedings of WMO International Workshop on Dynamical Extended Range Forecasting, Toulouse, France, 17-21 November 1997, WMO/TD-No. 881, 105-108.

Jia, Y., 2000: The ocean heat transport and meridional overturning near 25N in the Atlantic in the CMIP models. *CLIVAR Exchanges*, **5**(3), 23-26.

Johns, T.C., 1996: A description of the Second Hadley Centre Coupled Model (HadCM2). *Climate Research Technical Note 71*, Hadley Centre, United Kingdom Meteorological Office, Bracknell Berkshire RG12 2SY, United Kingdom, 19 pp.

Johns, T.C., R.E. Carnell, J.F. Crossley, J.M. Gregory, J.F.B. Mitchell, C.A. Senior, S.F.B. Tett and R.A. Wood, 1997: The second Hadley Centre coupled atmosphere-ocean GCM: model description, spinup and validation. *Clim. Dyn*., **13**, 103-134.

Jolly, D. and A. Haxeltine, 1997: Effect of low glacial atmospheric CO_2 on tropical African montane vegetation. *Science*, **276**, 786-788.

Jolly, D., S.P. Harrison, B. Damnati and R. Bonnefille, 1998a: Simulated climate and biomes of Africa during the Late Quaternary: comparison with pollen and lake status data. *Quat. Sci. Rev.*, **17**, 629-657.

Jolly, D., I.C. Prentice, R. Bonnefille, A. Ballouche, M. Bengo, P. Brenac, G. Buchet, D. Burney, J.-P. Cazet, R. Cheddadi, T. Edorh, H. Elenga, S. Elmoutaki, J. Guiot, F. Laarif, H. Lamb, A.-M. Lezine, J. Maley, M. Mbenza, O. Peyron, M. Reille, I. Reynaud-Ferrera, G. Riollet, J. C. Ritchie, E. Roche, L. Scott, I. Ssemmanda, H. Straka, M. Umer, E. Van Campo, S. Vilimumbala, A. Vincens and M. Waller, 1998b: Biome reconstruction from pollen and plant macrofossil data for Africa and the Arabian peninsula at 0 and 6 ka. *J. Biogeogr.,* **25**, 1007-1027.

Jones, P.D., 1994: Hemispheric surface air temperature variations: a reanalysis and an update to 1993. *J. Climate,* **7**, 1794-1802.

Jones, P.D. and K. Briffa, 1992: Global surface air temperature variations over the twentieth century. Part 1: Spatial, temporal, and seasonal details. *Holocene*, **2**, 165–179.

Jones, P.D., K.R. Briffa, T.P. Barnett and S.F.B. Tett, 1998: High-resolution palaeoclimatic records for the last millennium: interpretation, integration and comparison with general circulation model control-run temperatures. *The Holocene*, **8**, 455-471.

Jones, P.D., N. New, D.E. Parker, S. Martin and I.G. Rigor, 1999: Surface air temperature and its change over the past 150 years. *Rev. Geophys.*, **37**, 173-199.

Joussaume, S. and K.E. Taylor, 1995: Status of the Paleoclimate Modeling Intercomparison Project (PMIP). *Proceedings of the first international AMIP scientific conference*. WCRP Report, 425-430.

Joussaume, S., K.E. Taylor, P. Braconnot, J.F.B. Mitchell, J.E. Kutzbach, S.P. Harrison, I.C. Prentice, A.J. Broccoli, A. Abe-Ouchi, P.J. Bartlein, C. Bonfils, B. Dong, J. Guiot, K. Herterich, C.D. Hewitt, D. Jolly, J.W. Kim, A. Kislov, A. Kitoh, M.F. Loutre, V. Masson, B. McAvaney, N. McFarlane, N. de Noblet, W.R. Peltier, J.Y. Peterschmitt, D. Pollard, D. Rind, J.F. Royer, M.E. Schlesinger, J. Syktus, S. Thompson, P. Valdes, G. Vettoretti, R.S. Webb and U. Wyputta, 1999: Monsoon changes for 6000 years ago: results of 18 simulations from the Paleoclimate Modeling Intercomparison Project (PMIP). *Geophys. Res. Lett.,* **26**, 859-862.

Kageyama, M., P.J. Valdes, G. Ramstein, C. Hewitt and U. Wyputta, 1999: Northern Hemisphere storm tracks in present day and last glacial maximum climate simulations: a comparison of the European PMIP models. *J. Climate*, **12**, 742-760.

Kageyama, M., O. Peyron, S. Pinot, P. Tarasov, J. Guiot, S. Joussaume and G. Ramstein, 2001: The Last Glacial Maximum climate over Europe and western Siberia: a PMIP comparison between models and data. *Clim. Dyn.*, **17**, 23-43.

Kalnay, E. and Coauthors, 1996: The NCEP/NCAR 40-year Reanalysis Project. *Bull. Am. Met. Soc.,* **77**, 437-471.

Kar, S.C., M. Sugi and N. Sato, 1996: Simulation of the Indian summer monsoon and its variability using the JMA Global Model. *Pap. Met. Geophys*., **47**, 65-101.

Kattenberg, A., F. Giorgi, H. Grassl, G.A. Meehl, J.F.B. Mitchell, R.J. Stouffer, T. Tokioka, A.J. Weaver and T.M.L. Wigley, 1996: Climate models — projections of future climate. In: *Climate Change 1995 – The Science of Climate Change: Contribution of Working Group I to the Second Assessment Report of the Intergovernmental Panel on Climate Change.* Houghton, J.T., L.G. Meira Filho, B.A. Callander, N. Harris, A. Kattenburg and K. Maskell, Eds., Cambridge University Press, Cambridge, England, pp. 285-357.

Kattsov, V.M., J.E. Walsh, A. Rinke, K. Dethloff, 2000: Atmospheric climate models: simulation of the Arctic Ocean fresh water budget components. In *The Freshwater Budget of the Arctic Ocean* (E.L. Lewis, ed.) Kluwer Academic Publishers, Dordrecht, The Netherlands, pp 209-247.

Kaurola, J., 1997: Some diagnostics of the northern wintertime climate simulated by the ECHAM3 model. *J. Climate*, **10**, 201-222.

Kharin, V.V. and F.W. Zwiers, 2000: Changes in the extremes in an ensemble of transient climate simulations with a coupled atmosphere-ocean GCM. *J. Climate*, **13**, 3760-3780.

Kiehl, J.T., J.J. Hack, M.H. Zhang and R.D. Cess, 1995: Sensitivity of a GCM climate to enhanced shortwave cloud absorption. *J. Climate*, **8**, 2200-2212.

Kimoto, M. and X. Shen, 1997: Climate variability study by GCM - monsoon and El Niño - Center for Climate System Research Series, No. 2, 91-116, CCSR, University of Tokyo (in Japanese).

Kitoh, A., H. Koide, K. Kodera, S. Yukimoto and A. Noda, 1996: Interannual variability in the stratosphere-troposphere circulation in a coupled ocean-atmosphere GCM. *Geophys. Res. Lett.*, **23**, 543-546.

Kitoh, A., S. Yukimoto and A. Noda, 1999: ENSO-monsoon relationship in the MRI coupled GCM. *J. Met. Soc. Japan*, **77**, 1221-1245.

Knutson, T.R. and S. Manabe, 1998: Model assessment of decadal variability and trends in the tropical Pacific Ocean. *J. Climate*, **11**, 2273-2296.

Knutson, T.R., S. Manabe and D. Gu, 1997: Simulated ENSO in a global coupled ocean-atmosphere model: Multidecadal amplitude modula-

tion and CO_2 sensitivity. *J. Climate*, **10**, 138-161.

Knutson, R., R.E. Tuleya and Y. Kurihara, 1998: Simulated increase of hurricane intensities in a CO_2-warmed climate. *Science*, **279**, 1018-1020.

Knutson, T.R., T.L. Delworh, K.W. Dixon and R.J. Stouffer, 1999: Model assessment of regional surface temperature trends (1949-1997). *J. Geophys. Res.*, **104**, 30981-30996.

Kobayashi, C., K. Takano, S. Kusunoki, M. Sugi and A. Kitoh, 2000: Seasonal predictability in winter over eastern Asia using the JMA global model. *Quart. J. R. Met. Soc*., **126**, 2111-2123.

Kodera, K., M. Chiba, H. Koide, A. Kitoh and Y. Nikaidou, 1996: Interannual variability of the winter stratosphere and troposphere in the Northern Hemisphere. *J. Met. Soc. Japan*, **74**, 365-382.

Koster, R.D. and P.C. Milly, 1997: The interplay between transpiration and runoff formulations in land surface schemes used with atmospheric models. *J. Climate*, **10**, 1578-1591.

Kothavala, Z., 1997: Extreme precipitation events and the applicability of global climate models to study floods and droughts. *Math. and Comp. in Simulation*, **43**, 261-268.

Krishnamurti, T.N., R. Correa-Torres, M. Latif and G. Daughenbaugh, 1998: The impact of current and possibly future sea surface temperature anomalies on the frequency of Atlantic hurricanes. *Tellus*, **50A**, 186-210.

Kubatzki, C. and M. Claussen, 1998: Simulation of the global biogeophysical interactions during the last glacial maximum. *Clim. Dyn.*, **14**, 461-471.

Kutzbach, J.E. and Z. Liu, 1997: Response of the African monsoon to orbital forcing and ocean feedbacks in the Middle Holocene. *Science*, **278**, 440-443.

Kutzbach, J.E., G. Bonan, J. Foley and S. Harrison , 1996a: Vegetation and soil feedbacks on the response of the African monsoon to forcing in the early to middle Holocene. *Nature*, **384**, 623-626.

Kutzbach, J.E., P.J. Bartlein, J.A. Foley, S.P. Harrison, S.W. Hostetler, Z. Liu, I.C. Prentice and T. Webb III, 1996b: Potential role of vegetation feedback in the climate sensitivity of high-latitude regions: A case study at 6000 years B.P. *Global Biogeochemical Cycles*, **10**, 727-736.

Lal, M., U. Cubasch, J. Perlwitz and J. Waszkewitz, 1997: Simulation of the Indian monsoon climatology in ECHAM3 climate model: Sensitivity to horizontal resolution. *Int. J. Climatol.*, **17**, 847-858.

Lambert, S.J. and G.J. Boer, 2001: CMIP1 evaluation and intercomparison of coupled climate models. *Clim. Dyn.*, **17**, 2/3, 83-106.

Landsea, C.W. and J.A. Knaff, 2000: How much skill was there in forecasting the very strong 1997-98 El Niño? *Bull. Am. Met. Soc.*, **81**, 2107-2120.

Latif, M., 1998: Dynamics of interdecadal variability in coupled ocean-atmosphere models. *J. Climate*, **11**, 602-624.

Latif, M. and T.P. Barnett, 1996: Decadal climate variability over the North Pacific and North America: Dynamics and predictability. *J. Climate*, **9**, 2407-2423.

Latif, M., K. Sperber and Co-authors, 1999: ENSIP: The El Niño simulation intercomparison project. CLIVAR Report.

Lau, W.K.-M. and S. Yang, 1996: Seasonal variation, abrupt transition, and intra seasonal variability associated with the Asian summer monsoon in the GLA GCM. *J. Climate*, **9**, 965-985.

Laurent, C., H. Le Treut, Z.X. Li, L. Fairhead and J.L. Dufresne, 1998: The influence of resolution in simulating inter-annual and inter-decadal variability in a coupled ocean-atmosphere GCM with emphasis over the North Atlantic. IPSL report N8.

Lean, J. and D. Rind, 1998: Climate forcing by changes in solar radiation. *J. Climate*, **11**, 3069-3094.

Legutke, S. and R. Voss, 1999: The Hamburg Atmosphere-Ocean Coupled Circulation Model ECHO-G. Deutches Klimarechenzentrum Tech. Rep. No.18, Hamburg.

Lemke, P., W.D. Hibler, G. Flato, M. Harder and M. Kreyscher, 1997: On the improvement of sea ice models for climate simulations: the Sea Ice Model Intercomparison Project. *Ann. Glaciol*., **25**, 183-187.

Levis, S., J.A. Foley and D. Pollard, 1999: Climate-vegetation feedbacks at the Last Glacial Maximum. *J. Geophys. Res.*, **104**, 31191-31198.

Li, T. and T.F. Hogan, 1999: The role of the annual mean climate on seasonal and interannual variability of the tropical Pacific in a coupled GCM. *J. Climate*, **12**, 780-792.

Li, W. and Y.-Q. Yu, 2001: Intraseasonal oscillation in coupled general circulation model. *Scientia Atmospherica Sinica* (in Chinese with English abstract), **25**, 118-132.

Li, Z., L. Moreau and A. Arking, 1997: On solar energy disposition: A perspective from observation and modeling. *Bull. Am. Met. Soc*., **78**, 53-70.

Lindzen, R.S. and M.S. Fox-Rabinovitz, 1989: Consistent Vertical and Horizontal Resolution. *Mon. Wea. Rev*., **117**, 2575-2583.

Liu, Z., R.G. Gallimore, J.E. Kutzbach, W. Xu, Y. Golubev, P. Behling and R. Selin, 1999: Modeling long-term climate changes with equilibrium asynchronous coupling. *Clim. Dyn.*, **15**, 324-340.

Lunkeit, F., M. Ponater, R. Sausen, M. Sogalla, U. Ulbrich and M. Windelband, 1996: Cyclonic activity in a warmer climate. *Contribution to Atmospheric Physics*, **69**, 393-407.

Macdonald, A.M., 1998: The global ocean circulation: a hydrographic estimate and regional analysis. *Progr. Oceanogr*., **41**, 281-382.

Mahowald, N., K.E. Kohfeld, M. Hansson, Y. Balkanski, S.P. Harrison, I.C. Prentice, M. Schulz and H. Rodhe, 1999: Dust sources and deposition in the Last Glacial Maximum and current climate. *J. Geophys. Res*., **104**(D13), 15895-15916.

Malevsky-Malevich, S.P., E.D. Nadyozhina, V.V. Simonov, O.B. Shklyarevich and E.K. Molkentin, 1999: The evaluation of climate change influence on the permafrost season soil thawing regime. *Contemporary Investigation at Main Geophysical Observatory*, **1**, 33-50 (in Russian).

Manabe, S.J. and R.J. Stouffer, 1996: Low-frequency variability of surface air temperature in a 1000-year integration of a coupled atmosphere-ocean-land model. *J. Climate*, **9**, 376-393.

Manabe , S. and R.J. Stouffer, 1997: Coupled ocean-atmosphere response to freshwater input: comparison to Younger Dryas event. *Palaeooceanography*, **12**, 321-336.

Manabe, S., R.J. Stouffer, M.J. Spelman and K. Bryan, 1991: Transient responses of a coupled ocean-atmosphere model to gradual changes of atmospheric CO_2. Part I: Annual mean response. *J. Climate*, **4**, 785-818.

Mann, M.E., R.S. Bradley and M.K. Hughes, 1998: Global-scale temperature patterns and climate forcing over the past six centuries. *Nature*, **392**, 779-787.

Manne, A.S. and R.G. Richels, 1999: The Kyoto Protocol: A Cost-Effective Strategy for Meeting Environmental Objectives? *Energy Journal Special Issue on the Costs of the Kyoto Protocol: A Multi-Model Evaluation*, 1-24.

Manzini , E. and N.A. McFarlane, 1998, The effect of varying the source spectrum of a gravity wave parameterization in a middle atmosphere general circulation model, *J. Geophys. Res.* **103**, 31523-31539.

Manzini and McFarlane, 1998: The effect of varying the source spectrum of a gravity wave parametrization in a middle atmosphere general circulation model. *J. Geophys. Res.*, **103**, 31523-31539.

Marchal, O., T.F. Stocker and F. Joos, 1998: A latitude-depth, circulation-biogeochemical ocean model for paleoclimate studies: Model development and sensitivities. *Tellus*, **50B**, 290-316.

Marotzke, J., 1997: Boundary mixing and the dynamics of three-dimensional thermohaline circulations. *J. Phys. Oceanogr.*, **27**, 1713-1728.

Marotzke, J. and P.H. Stone, 1995: Atmospheric transports, the thermohaline circulation, and flux adjustments in a simple coupled model. *J. Phys. Oceanogr*., **25**, 1350-1364

Martin, G.M., 1999: The simulation of the Asian summer monsoon, and its sensitivity to horizontal resolution, in the UK Meteorological

Office Unified Model. *Quart. J. R. Met. Soc*., **125**, 1499-1525.

Martin, G.M. and M.K. Soman, 2000: Effects of changing physical parametrisations on the simulation of the Asian summer monsoon in the UK Meteorological Office Unified Model. *Hadley Centre Technical Note No. 17*, Met Office, London Road, Bracknell, RG12 2SY, UK.

Matsuura, T., M. Yumoto, S. Lizuka and R. Kawamura, 1999: Typhoon and ENSO simulation using a high-resolution coupled GCM. *Geophys. Res. Lett.*, **26**, 1755-1758.

McGuffie, K., A. Henderson-Sellers, N. Holbrook, Z. Kothavala, O. Balachova and J. Hoestra, 1999: Assessing simulations of daily temperature and precipitation variability with global climate models for present and enhanced greenhouse climates. *Int. J. Climatol.*, **19**, 1-26.

McPhaden, M., 1999: Genesis and evolution of the 1997-98 El Niño. *Science*, **283**, 950-954.

Medvedev, A.S., G.P. Klassen and S.R. Beagley, 1998: On the role of an anisotropic gravity wave spectrum in maintaining the circulation of the middle atmosphere. *Geophys. Res. Lett*., **25**, 509-512.

Meehl, G.A., 1997: The south Asian monsoon and the tropospheric biennial oscillation. *J. Climate*, **10**, 1921-1943.

Meehl, G.A. and W.M. Washington, 1995: Cloud albedo feedback and the super greenhouse effect in a global coupled GCM. *Clim. Dyn*., **11**, 399-411.

Meehl, G.A. and J.M. Arblaster, 1998: The Asian-Australian monsoon and El Niño-Southern Oscillation in the NCAR Climate System Model. *J. Climate*, **11**, 1356-1385.

Meehl, G.A., G.J. Boer, C. Covey, M. Latif and R.J. Stouffer, 2000a: The Coupled Model Intercomparison Project (CMIP). *Bull. Am. Met. Soc*., **81**, 313-318.

Meehl, G.A., W.M. Washington, J.M. Arblaster, T.W. Bettge and W.G. Strand Jr., 2000b: Anthropogenic forcing and decadal climate variability in sensitivity experiments of 20th and 21st century climate. *J. Climate*, **13**, (in press).

Miller, R.L. and X. Jiang, 1996: Surface energy fluxes and coupled variability in the Tropics of a coupled general circulation model. *J. Climate*, **9**, 1599-1620.

Milly, P.C.D., 1997: Sensitivity of greenhouse summer dryness to changes in plan rooting characteristics. *Geophys. Res. Lett.*, **24**, 269-271

Mitchell, J.F.B., T.J. Johns, J.M. Gregory and S.B.F Tett, 1995: Climate response to increasing levels of greenhouse gases and sulphate aerosols. *Nature*, **376**, 501-504.

Mokhov, I.I. and P.K. Love, 1995: Diagnostics of cloudiness evolution in the annual cycle and interannual variability in the AMIP. *Proc. First Int. AMIP Sci. Conf.*, WMO/TD-No.732, 49-53.

Moore, A.M. and R. Kleeman, 1999: Stochastic forcing of ENSO by the intra seasonal oscillation. *J. Climate*, **12**, 1199-1220.

Moss, D. and Schneider, 1999: Uncertainties in the IPCC TAR: Recommendations to lead authors for more consistent assessment and Reporting. (Available from IPCC WGI Technical Support Unit)

Munk, W. and C. Wunsch, 1998: Abyssal Recipes II. *Deep Sea Res*., **45**, 1976-2009.

Murphy, A.H., 1988: Skill scores based on the mean square error and their relationships to the correlation coefficient. *Mon. Wea. Rev*., **116**, 2417-2424.

National Research Council, 2000: Reconciling Observations of Global Temperature Change. National Academy Press, Washington, D.C., 85 pp.

Navarra, A. (ed.), 1999: Beyond El Niño: Decadal and Interdecadal Climate Variability. Springer-Verlag, Berlin, 374 pp.

Neelin, J.D. and H.A. Dijkstra, 1995: Ocean-atmosphere interaction and the tropical climatology. Part I: the dangers of flux correction. *J. Climate*, **8**, 1343-1359.

Nordhaus, W.D., 1994: Managing the Global Commons: The Economics of Climate Change. The MIT Press, Cambridge.

Nozawa, T., S. Emori, T. Takemura, T. Nakajima, A. Numaguti, A. Abe-Ouchi and M. Kimoto, 2000: Coupled ocean-atmosphere model experiments of future climate change based on IPCC SRES scenarios. *Preprints of the 11th Symposium on Global Change Studies*, 9-14 January 2000, Long Beach, USA, 352-355.

Oberhuber, J.M., E. Roeckner, M. Christoph, M. Esch and M. Latif, 1998: Predicting the '97 El Niño event with a global climate model. *Geophys. Res. Lett.*, **25**, 2273-2276.

Ogasawara, N., A. Kitoh, T. Yasunari and A. Noda, 1999: Tropospheric biennial oscillation of ENSO monsoon system in the MRI coupled GCM. *J. Met. Soc. Japan*, ***77***, 1247-1270.

Opsteegh, J.D., R.J. Haarsma, F.M. Selten and A. Kattenberg, 1998: ECBILT: A dynamic alternative to mixed boundary conditions in ocean models. *Tellus*, **50A**, 348-367.

Orr, J.C., E. Maier-Reimer, U. Mikolajewicz, P. Monfray, J.L. Sarmiento, J.R. Toggweiler, N.K. Taylor, J. Palmer, N. Gruber, C.L. Sabine, C. Le Quéré, R.M. Key and J. Boutin, 2001: Estimates of anthropogenic carbon uptake from four 3-D global ocean models. *Global Biogeochem. Cycles*, **15**(1), 43-60.

Osborn, T.J., K.R. Briffa, S.F.B. Tett, P.D. Jones and R.M. Trigo, 1999: Evaluation of the North Atlantic Oscillation as simulated by a coupled climate model. *Clim. Dyn*., **15**, 685-702.

Otto-Bliesner, B.L., 1999: El Niño/La Niña and Sahel precipitation during the middle Holocene. *Geophys. Res. Lett.*, **26**, 87-90.

Parker, D.E., C.K . Folland and M. Jackson, 1995: Marine surface temperature: observed variations and data requirements. *Clim. Change*, **31**, 559-600.

Pawson, S., K. Kodera and Coauthors, 2000: The GCM-Reality Intercomparison Project for SPARC (GRIPS): Scientific issues and initial results. *Bull. Am. Met. Soc*., **81**, 781-796.

Peck, S.C. and T.J. Teisberg, 1996: International CO_2 Emissions Targets and Timetables: An Analysis of the AOSIS Proposal. *Environmental Modeling and Assessment*, **1**(4), 219-227.

Petersen, A.C., 2000: Philosophy of Climate Science. *Bull. Am. Met. Soc*., **81**, 265-271.

Petoukhov, V.K., I.I. Mokhov, A.V. Eliseev and V.A. Semenov, 1998: The IAP RAS global climate model. *Dialogue-MSU*, Moscow, 110 pp.

Petoukhov, V., A. Ganapolski, V. Brovkin, M. Claussen, A. Eliseev, C. Kubatzki and S. Rahmstorf, 2000: CLIMBER-2: A Climate system model of intermediate complexity, Part I: Model description and performance for present climate. *Clim. Dyn*., **16**, 1-17.

Peyron, O., J. Guiot, R. Cheddadi, P. Tarasov, M. Reille, J.L. de Beaulieu, S. Bottema and V. Andrieu, 1998: Climatic reconstruction in Europe for 18,000 years B.P. from pollen data. *Quat. Res.*, **49**, 183-196.

Pinot, S., G. Ramstein, S.P. Harrison, I.C. Prentice, J. Guiot, M. Stute, S. Joussaume and PMIP-participating-groups, 1999: Tropical paleoclimates at the Last Glacial Maximum: comparison of Paleoclimate Modeling Intercomparison Project (PMIP) simulations and paleodata. *Clim. Dyn.*, **15**, 857-874.

Pitman, A.J. and M. Zhao, 2000: The relative Impact of observed change in land cover and carbon dioxide as simulated by a climate model. *Geophys. Res. Lett.*, **27**, 1267-1270.

Pitman, A.J., A.G. Slater, C.E. Desborough and M. Zhao, 1999: Uncertainty in the simulation of runoff due to the parameterization of frozen soil moisture using the GSWP methodology. *J. Geophys. Res.*, **104**, 16879-16888.

PMIP, 2000: Paleoclimate Modeling Intercomparison Project (PMIP): *Proceedings of the third PMIP workshop*, Canada, 4-8 October 1999, P. Braconnot (Ed), WCRP-111, WMO/TD-1007, 271 pp.

Polanyi, M, 1958: Personal Knowledge, Routledge and Kegan Paul, London, 428 pp.

Polcher, J., K. Laval, L. Dümenil, J. Lean and P.R. Rowntree, 1996: Comparing three land surface schemes used in GCMs. *J. Hydrology*,

180, 373-394.

Polcher, J., J. Crossley, C. Bunton, H. Douville, N. Gedney, K. Laval, S. Planton, P.R. Rowntree and P. Valdes, 1998a: Importance of land-surface processes for the uncertainties of climate change: A European Project. *GEWEX News*, **8**(2), 11-13.

Polcher, J., B. McAvaney, P. Viterbo, M.-A. Gaertner, A. Hahmann, J.-F. Mahfouf, J. Noilhan, T. Phillips, A.J. Pitman, C.A. Schlosser, J.-P. Schulz, B. Timbal, D. Verseghy and Y. Xue, 1998b: A proposal for a general interface between land-surface schemes and general circulation models. *Global Planet. Change*, **19**, 263-278.

Pollard, D., J.C. Bergengren, L.M. Stillwell-Soller, B. Felzer and S.L. Thompson, 1998: Climate simulations for 10000 and 6000 years BP using the GENESIS global climate model. *Paleoclimates - Data and Modelling*, **2**, 183-218.

Polzin, K.L., J.M. Toole, J.R. Ledwell and R.W. Schmitt, 1997: Spatial variability of turbulent mixing in the ocean. *Science*, **276**, 93-96.

Pope, V.D., A. Pamment and R.A. Stratton, 1999: Resolution sensitivity of the UKMO climate model. *Research Activities in Atmospheric and Oceanic Modelling, No. 28*, WCRP CAS/JSC working group on numerical experimentation, WMO, Geneva.

Pope, V.D., M. Gallani, P.R. Rowntree and R.A. Stratton, 2000: The impact of new physical parametrisations in the Hadley Centre climate model - HadAM3. *Clim. Dyn.*, **16**, 123-146.

Popper, K., 1982: The Open Universe, Hutchinson, London.

Potts, J.M., C.K. Folland, I.T. Jolliffe and D. Sexton, 1996: Revised "LEPS" scores for assessing climate model simulations and long-range forecasts. *J. Climate*, **9**, 34-53.

Power, S.B., R.A. Colman, B.J. McAvaney, R.R. Dahni, A.M. Moore and N.R. Smith, 1993: The BMRC Coupled atmosphere/ocean/sea-ice model. *BMRC Research Report No. 37*, Bureau of Meteorology Research Centre, Melbourne, Australia, 58 pp.

Power, S.B., F. Tseitkin, R.A. Colman and A. Sulaiman, 1998: A coupled general circulation model for seasonal prediction and climate change research. *BMRC Research Report No 66*, Bureau of Meteorology, Australia.

Prentice, I.C. and T. Webb III, 1998: BIOME 6000: reconstructing global mid-Holocene vegetation patterns from palaeoecological records. *J. Biogeogr.*, **25**, 997-1005.

Prentice, I.C., D. Jolly and BIOME-6000-participants, 1998: Mid-Holocene and glacial-maximum vegetation geography of the northern continents and Africa. *J. Biogeogr.*, **25**, 997-1005.

Rahmstorf, S. and Ganopolski, 1999: Long-term warming scenarios computed with an efficient coupled climate model. *Clim. Change*, **43**, 353-367.

Randall, D.A. and B.A. Wielicki, 1997: Measurements, models and hypotheses in the atmospheric sciences. *Bull. Am. Met. Soc.*, **78**, 399-406.

Raper, S.C.B., T.M.L Wigley and R.A. Warrick, 1996: Global sea-level rise: Past and Future. In: Sea-Level rise and Coastal subsidence, Causes, Consequences and Strategies. Kluwer Academic Publishers, Dordrecht, 369 pp.

Rayner, N.A., E.B. Horton, D.E. Parker, C.K. Folland and R.B. Hackett, 1996: Version 2.2 of the Global Sea-Ice and Sea Surface Temperature dataset, 1903–1994. *CRTN Rep. 74*. HCCPR, Bracknell, United Kingdom.

Renshaw, A.C., D.P. Rowell and C.K. Folland, 1998: Wintertime low-frequency weather variability in the North Pacific-American sector 1949-93. *J. Climate*, **11**, 1073-1093.

Renssen H., R.F.B. Isarin, J. Vandenberghe, M. Lautenschlager and U. Schlese, 2000: Permafrost as a critical factor in palaeoclimate modelling: the Younger Dryas case in Europe. *Earth and Planetary Science Letters*, **176**, 1-5.

Rind, D., 1999: Complexity and climate. *Science*, **284**, 105-107.

Rind, D. and D. Peteet, 1985: Terrestrial conditions at the Last Glacial Maximum and CLIMAP sea-surface temperature estimates: Are they consistent? *Quat. Res.*, **24**, 1-22.

Roberts, M.J., R. Marsh, A.L. New and R.A. Wood, 1996: An intercomparison of a Bryan-Cox-type ocean model and an isopycnic ocean model. Part I: The subpolar gyre and high latitude processes. *J. Phys. Oceanogr.*, **26**, 1495-1527.

Robertson, A.W., 1996: Interdecadal variability over the North Pacific in a multi-century climate simulation. *Clim. Dyn.*, **12**, 227-241.

Robertson, A.W., C.R. Mechoso and Y.-J. Kim, 1999: Interannual variations in the South American monsoon and their teleconnection with the North Atlantic Oscillation. Preprints of 10th Symposium on Global Change Studies, 10-15 January 1999, Dallas, Texas, American Meteorological Society, 434-437.

Robitaille, D.Y. and A.J. Weaver, 1995: Validation of sub-grid-scale mixing schemes using CFCs in a global ocean model. *Geophys. Res. Lett.*, **22**, 2917-2920.

Robock, A., C.A. Schlosser, K.Y. Vinnikov, N.A. Speranskaya, J.K. Entin and S. Qiu, 1998: Evaluation of the AMIP soil moisture simulations. *Global Planet. Change*, **19**, 181-208.

Rocha, A. and I. Simmonds, 1997: Interannual variability of south-eastern African summer rainfall. Part II: Modelling the impact of sea-surface temperatures on rainfall and circulation. *Int. J. Climatol.*, **17**, 267-290.

Rodbell, D.T., 1999: An 15,000 year record of El Niño-driven alluviation in southwestern Ecuador. *Science*, **283**, 516-520.

Rodwell, M.J., D.P. Rowell and C.K. Folland, 1999: Oceanic forcing of the wintertime North Atlantic Oscillation and European climate. *Nature*, **398**, 320-323.

Roeckner, E., J.M. Oberhuber, A. Bacher, M. Christoph and I. Kirchner, 1996: ENSO variability and atmospheric response in a global coupled atmosphere-ocean GCM. *Clim. Dyn.*, **12**, 737-754.

Roeckner, E., L. Bengtsson, J. Feichter, J. Lelieveld and H. Rodhe, 1999: Transient climate change simulations with a coupled atmosphere-ocean GCM including the tropospheric sulfur cycle. *J. Climate*, **12**, 3004-3012.

Rosell-Melé, A., E. Bard, K.C. Emeis, P. Farrimond, J. Grimalt, P.J. MŸller and R.R. Schneider, 1998: Project takes a new look at past sea surface temperatures. *EOS*, **79**, 393-394.

Rowell, D.P., C.K. Folland, K. Maskell and M.N. Ward, 1995: Variability of summer rainfall over tropical North Africa 1906-1992, Observations and modelling. *Quart. J. R. Met. Soc.*, **121**, 669-704.

Royer J.-F., F. Chauvin, B. Timbal, P. Araspin and D. Grimal, 1998: A GCM study of the impact of greenhouse gas increase on the frequency of occurrence of tropical cyclones. *Clim. Change*, **38,** 307-343.

Russell, G.L., J.R. Miller and D. Rind, 1995: A coupled atmosphere-ocean model for transient climate change studies. *Atmos.-Ocean*, **33**, 683-730.

Sandweiss, D., J.B. Richardson, E.J. Rieitz, H.B. Rollins and K.A. Maasch, 1996: Geoarchaeological evidence from Peru for a 5000 years B.P. onset of El Niño. *Science*, **273**, 1531-1533.

Santer, B.D., T.M.L. Wigley, D.J. Gaffen, L. Bengtsson, C. Doutriaux, J.S. Boyle, M. Esch, J.J. Hnilo, P.D. Jones, G. A. Meehl, E. Roeckner, K.E. Taylor and M.F. Wehner, 2000: Interpreting differential temperature trends at the surface and in the lower troposphere. *Science*, **287**, 1227-1232.

SAR, see IPCC, 1996.

Saravanan, R., 1998: Atmospheric low-frequency variability and its relationship to midlatitude SST variability: Studies using the NCAR climate system model. *J. Climate*, **11**, 1386-1404.

Sarmiento, J.L., P. Monfray, E. Maier-Reimer, O. Aumont, R. Murnane and J.C. Orr, 2000: Sea-air CO_2 fluxes and carbon transport: a comparison of three ocean general circulation models. *Global Biogeochem. Cycles*, 14(4), 1267-1281.

Sausen, R., S. Schubert and L. Dumenil, 1994: A model of the river-runoff for use in coupled atmosphere-ocean models. *Journal of*

Hydrology, **155**, 337-352.

Schlosser, C.A., A.G. Slater, A. Robock, A.J. Pitman, K.Y. Vinnikov, A. Henderson-Sellers, N.A. Speranskaya, K. Mitchell, A. Boone, H. Braden, F. Chen, P. Cox, P. de Rosnay, C.E. Desborough, R.E. Dickinson, Y.-J. Dai, Q. Duan, J. Entin, P. Etchevers, N. Gedney, Y.M. Gusev, F. Habets, J. Kim, V. Koren, E. Kowalczyk, O.N. Nasonova, J. Noilhan, J. Schaake, A.B. Shmakin, T.G. Smirnova, D. Verseghy, P. Wetzel, Y. Xue and Z.-L. Yang, 2000: Simulations of a boreal grassland hydrology at Valdai, Russia: PILPS Phase 2(d). *Mon. Wea. Rev.*, **128**, 301-321.

Schmittner, A. and T.F. Stocker, 1999: The stability of the thermohaline circulation in global warming experiments. *J. Climate*, **12**, 1117-1133.

Schneider, E.K. and Z. Zhu, 1998: Sensitivity of the simulated annual cycle of sea surface temperature in the Equatorial Pacific to sunlight penetration. *J. Climate*, **11**, 1932-1950.

Schneider, E.K., Z. Zhu, B.S. Giese, B. Huang, B.P. Kirtman, J. Shukla and J.A. Carton, 1997: Annual cycle and ENSO in a coupled ocean-atmosphere general circulation model. *Mon. Wea. Rev*., **125**, 680-702.

Schubert, S., 1998: Downscaling local extreme temperature changes in South-Eastern Australia from the CSIRO MARK2 GCM. *Int. J. Climatol.*, **18**, 1419-1438.

Schubert, M., J. Perlwitz, R. Blender, K. Fraedrich and F. Lunkeit, 1998: North Atlantic cyclones in CO_2-induced warm climate simulations: frequency, intensity, and tracks. *Clim. Dyn.*, **14**, 827-837.

Sellers, P.J., D.A. Randall, C.J. Collatz, J.A. Berry, C.B. Field, D.A. Dazlich, C. Zhang, G. Collelo and L. Bounoua, 1996: A revised land-surface parameterization (SiB2) for atmospheric GCMs. Part 1: Model formulation. *J. Climate*, **9**, 676-705.

Semazzi, F.H.M. and L. Sun, 1997: The role of orography in determining the Sahelian climate. *Int. J. Climatol.*, **17**, 581-596.

Semazzi, F.H.M., B. Burns, N.-H. Lin and J.-K. Schemm, 1996: A GCM study of the teleconnections between the continental climate of Africa and global sea surface temperature anomalies. *J. Climate*, **9**, 2480-2497.

Shackley, S., P. Young, S. Parkinson and B. Wynne, 1998: Uncertainty, complexity and concepts of good science in climate change modelling: Are GCMs the best tools? *Clim. Change*, **38**, 159-205.

Shackley, S., P. Young and S. Parkinson, 1999: Response to A. Henderson-Sellers and K. McGuffie. *Clim. Change*, **42**, 611-617.

Shindell, D.T., R.L. Miller, G. Schmidt and L. Pandolfo, 1999: Simulation of recent northern winter climate trends by greenhouse-gas forcing. *Nature*, **399**, 452-455.

Slingo, J.M., K.R. Sperber and Co-authors, 1996: Intra seasonal oscillations in 15 atmospheric general circulation models: results from an AMIP diagnostic subproject. *Clim. Dyn*., **12,** 325-357.

Slingo, J.M., D.P. Rowell, K.R. Sperber and F. Nortley, 1999: On the predictability of the interannual behaviour of the Madden-Julian Oscillation and its relationship with El Niño. *Quart. J. R. Met. Soc*., **125**, 583-609.

Sperber, K.R. and T. Palmer, 1996: Interannual tropical rainfall variability in general circulation model simulations associated with the Atmospheric Model Intercomparison Project. *J. Climate*, **9**, 2727-2750.

Sperber, K.R. and Participating AMIP Modelling Groups, 1999: Are revised models better models? A skill score assessment of regional interannual variability. *Geophys. Res. Lett*., **26**, 1267-1270.

Stensrud, D.J., R.L. Gall, S.L. Mullen and K.W. Howard, 1995: Model climatology of the Mexican monsoon. *J. Climate*, **8**, 1775-1794.

Stephenson, D.B. and J.-F. Royer, 1995: GCM simulation of the Southern Oscillation from 1979-1988. *Clim. Dyn*., **11**, 115-128.

Stephenson, D.B., F. Chauvin and J.-F. Royer, 1998: Simulation of the Asian summer monsoon and its dependence on model horizontal resolution. *J. Met. Soc. Japan*, **76**, 237-265.

Stewart, R.E., K.K. Szeto, R.F. Reinking, S.A. Clough and S.P. Ballard, 1998: Midlatitude cyclonic cloud systems and their features affecting large scales and climate. *Rev. Geophys*., **36**, 245-268.

Stockdale, T.N., D.L.T. Anderson, J.O.S. Alves and M.A. Balmaseda, 1998: Global seasonal rainfall forecasts using a coupled ocean-atmosphere model. *Nature*, **392**, 370-373.

Stocker, T.F., D.G. Wright and L.A. Mysak, 1992: A zonally-averaged, coupled ocean-atmosphere model for paleoclimatic studies. *J. Climate*, **5**, 773-797.

Stocker, T.F. and A. Schmittner, 1997: Influence of CO_2 emission rates on the stability of the thermohaline circulation. *Nature*, **388**, 862-865.

Stouffer , R.J. and K.W. Dixon, 1998: Initialization of coupled models for use in climate studies: A review. In Research Activities in Atmospheric and Oceanic Modelling. Report No. 27, WMO/TD-No. 865, World Meteorological Organization, Geneva, Switzerland, I.1-I.8.

Stouffer, R.J., S. Manabe and K.Y. Yinnikov, 1994: Model assessment of the role of natural variability in recent global warming. *Nature*, **367**, 634–636.

Stouffer, R.J., G. Hegerl and S. Tett, 2000: A comparison of surface air temperature variability in three 1000-year coupled ocean-atmosphere model integrations. *J. Climate*, **13**, 513-537.

Stratton, R.A., 1999: A high resolution AMIP integration using the Hadley Centre model HadAM2b. *Clim. Dyn*., **15**, 9-28.

Street-Perrott, F.A. and R.A. Perrott, 1993: Holocene vegetation, lake levels and climate of Africa. *Global Climates since the Last Glacial Maximum*. H.E.J. Wright, J.E. Kutzbach, T. Webb III, W.F. Ruddiman, F.A. Street-Perrott and P.J. Bartlein, Eds., University of Minnesota Press, 318-356.

Street-Perrot, F.A. *et al*., 1997: Impact of lower atmospheric carbon dioxide on tropical mountain ecosystems. *Science*, **278**, 1422-1426.

Sugi, M., A. Noda and N. Sato, 1997: Influence of global warming on tropical cyclone climatology- an experiment with the JMA global model, Research Activities in Atmospheric and Oceanic Modelling. Report No. 25, WMO/TD-No.792, 7.69-7.70.

Tarasov, P.E., T.I. Webb, A.A. Andreev, N.B. Afanas'eva, N.A. Berezina, L.G. Bezusko, T.A. Blyakharchuk, N.S. Bolikhovskaya, R. Cheddadi, M.M. Chernavskaya, G.M. Chernova, N.I. Dorofeyuk, V.G. Dirksen, G.A. Elina, L.V. Filimonova, F.Z. Glebov, J. Guiot, V.S. Gunova, S.P. Harrison, D. Jolly, V.I. Khomutova, E.V. Kvavadze, I.R. Osipova, N.K. Panova, I.C. Prentice, L. Saarse, D.V. Sevastyanov, V.S. Volkova and V.P. Zernitskaya, 1998: Present-day and mid-Holocene biomes reconstructed from pollen and plant macrofossil data from the former Soviet Union and Mongolia. *J. Biogeogr.*, **25**, 1029-1053.

Taylor, K.E., 2000: Summarizing Multiple aspects of model performance in a single diagram. *PCMDI Report No 65*., Program for Climate Model Diagnosis and Intercomparison, Lawrence Livermore National Laboratory, University of California, Livermore CA, 24 pp.

Taylor, K.E., C.D. Hewitt, P. Braconnot, A.J. Broccoli, C. Doutriaux, J.F.B. Mitchell and PMIP-Participating-Groups, 2000: Analysis of forcing, response and feedbacks in a paleoclimate modeling experiment. In "Paleoclimate Modeling Intercomparison Project (PMIP) : proceedings of the third PMIP workshop, Canada, 4-8 October 1999", P. Braconnot (Ed), WCRP-111, WMO/TD-1007, pp 43-50.

Tett, S.F.B., T.C. Johns and J.F.B. Mitchell, 1997: Global and regional variability in a coupled AOGCM. *Clim. Dyn*., **13**, 303–323.

Tett, S.F.B., P.A. Stott, M.R. Allen, W.J. Ingram and J.F.B. Mitchell, 1999: Causes of twentieth century temperature change. *Nature*, **399**, 569-572.

Texier, D., N. de Noblet, S.P. Harrison, A. Haxeltine, D. Jolly, S. Joussaume, F. Laarif, I.C. Prentice and P. Tarasov, 1997: Quantifying the role of biosphere-atmosphere feedbacks in climate change: coupled model simulations for 6000 years BP and comparison with paleodata for northern Eurasia and northern Africa. *Clim. Dyn.*, **13**, 865-882.

Texier, D., N. de Noblet and P. Braconnot, 2000: Sensitivity of the African and Asian monsoons to mid-Holocene insolation and data-inferred surface changes. *J. Climate*, **13**, 164-191.

Thorncroft C.D. and D.P. Rowell, 1998: Interannual variability of African wave activities in a general circulation model. *Int. J. Climatol.*, **18**, 1305-1323.

Timmermann, A., J. Oberhuber, A. Bacher, M. Esch, M. Latif and E. Roeckner, 1998: ENSO response to greenhouse warming. Max-Planck-Institut fur Meteorologie, Report No. 251, 13 pp.

Tokioka, T., A. Noda, A. Kitoh, Y. Nikaidou, S. Nakagawa, T. Motoi, S. Yukimoto and K. Takata, 1996: A transient CO_2 experiment with the MRI CGCM: Annual mean response. *CGER's Supercomputer Monograph Report Vol. 2*, CGER-IO22-96, ISSN 1341-4356, Center for Global Environmental Research, National Institute for Environmental Studies, Environment Agency of Japan, Ibaraki, Japan, 86 pp.

Tol, R.S.J., 1999: 'Spatial and Temporal Efficiency in Climate Change: Applications of FUND'. *Environmental and Resource Economics*, **14** (1), 33-49.

Trenberth, K.E, 1998a: The heat budget of the atmosphere and ocean. *Proceedings of the First International Conference on Reanalysis*. pp 17-20. WCRP 104, WMO/TD-No. 876.

Trenberth, K.E., 1998b: Development and forecasts of the 1997/98 El Niño: CLIVAR scientific issues. *CLIVAR – Exchanges*, **3**(2/3), 4-14.

Tsutsui, J.I. and A. Kasahara, 1996: Simulated tropical cyclones using the National Center for Atmospheric Research Community climate model. *J. Geophys. Res*., **101**(D10), 15013-15032.

Tsutsui, J., A. Kasahara and H. Hirakuchi, 1999: The impacts of global warming on tropical cyclones- a numerical experiment with the T42 version of NCAR CCM2, Preprint volume of the 10th Symposium on Global Change Studies, J16B.310-15 January 1999, Dallas, Texas.

Vinnikov, K.Y., A. Robock, R.J. Stouffer, J.E. Walsh, C.L. Parkinson, D.J. Cavalieri, J.F.B. Mitchell, D. Garrett and V.F. Zakharov, 1999: Global Warming and Northern Hemisphere Sea Ice Extent. *Science*, **286**, 1934-1937.

Visbeck, M., J. Marshall, T. Haine and M. Spall, 1997: On the specification of eddy transfer coefficients in coarse resolution ocean circulation models. *J. Phys. Oceanogr*., **27**, 381-402.

Vitart, F., J.L. Anderson and W.E. Stern, 1997: Simulation of interannual variability of tropical storm frequency in an ensemble of GCM integrations, *J. Climate*, **10**, 745-760.

Volodin, E.M. and V.N. Lykosov, 1998: Parameterization of heat and moisture transfer in the soil-vegetation system for use in atmospheric general circulation models: 2. Numerical experiments on climate modelling. *Izv. RAS, Physics of Atmosphere and Ocean*, **34**, 622-633.

von Storch, J-S., 1994: Interdecadal variability in a global coupled model. *Tellus*, **46A**, 419-432.

von Storch, J-S., V.V. Kharin, U. Cubasch, G.C. Hegerl, D. Schriever, H. von Storch and E. Zorita, 1997: A description of a 1260-year control integration with the coupled ECHAM1/LSG general circulation model. *J. Climate*, **10**, 1525-1543.

Voss, R., R. Sausen, and U. Cubasch, 1998: Periodically synchronously coupled integrations with the atmosphere-ocean general circulation model ECHAM3/LSG. *Climate Dyn.* **14**, 249-266.

Waliser, D.E., K.M. Lau and J.-H. Kim, 1999: The influence of coupled sea surface temperatures on the Madden-Julian oscillation: a model perturbation experiment. *J. Atmos. Sci*., **56**, 333-358.

Wallace, J.M. and D.S. Gutzler, 1981: Teleconnections in the geopotential height field during the Northern Hemisphere winter. *Mon. Wea. Rev*., **109**, 784-812.

Walsh, K. and A.B. Pittock, 1998: Potential changes in tropical storms, hurricanes, and extreme rainfall events as a result of climate change. *Clim. Change*, **39**, 199-213.

Wang, G., R. Kleeman, N. Smith and F. Tseitkin, 2000: Seasonal predictions with a coupled global ocean-atmosphere model. *BMRC Res. Rep. No.77*.

Washington, W.M. and G.A. Meehl, 1996: High-latitude climate change in a global coupled ocean-atmosphere-sea ice model with increased atmospheric CO_2. *J. Geophys. Res*., **101**(D8), 12795-12801.

Washington, W.M. and 10 others, 2000: Parallel Climate Model (PCM): Control and Transient simulations. *Clim. Dyn*., **16**, 755-774.

Watterson, I.G. 1996: Non-dimensional measures of climate model performance. *Int. J. Climatol.*, **16**, 379-391.

Watterson, I.G., 1997, The diurnal cycle of surface air temperature in simulated present and doubled CO_2 climates, *Climate Dynamics*, **13**, 533-545.

Watterson, I.G., J.L. Evans and B.F. Ryan, 1995: Seasonal and interannual variability of tropical cyclogenesis: Diagnostics from large-scale fields. *J. Climate*, **8**, 3052-3066.

Weare, B.C., 2000a: Insights into the importance of cloud vertical structure in climate. *Geophys. Res. Lett.*, **27**, 907-910.

Weare, B.C., 2000b: Near-global observations of low clouds. *J. Climate*, **13**, 1255-1268.

Weare, B.C., I.I. Mokhov and Project Members, 1995: Evaluation of cloudiness and its variability in global climate models. *J. Climate*, **8**, 2224-2238.

Weare, B.C. and AMIP Modeling Groups, 1996: Evaluation of the vertical structure of zonally averaged cloudiness and its variability in the Atmospheric Model Intercomparison Project. *J. Climate*, **9**, 3419-3431.

Weaver, A.J. and T.M.C. Hughes, 1996: On the incompatibility of ocean and atmosphere models and the need for flux adjustments. *Clim. Dyn.*, **12**, 141-170.

Weaver, A.J., M. Eby, A.F. Fanning and E.C.C Wiebe, 1998: Simulated influence of carbon dioxide, orbital forcing and ice sheets on the climate of the Last Glacial Maximum. *Nature*, **394**, 847-853.

Webb, T.I., P.J. Bartlein, S.P. Harrison and K.H. Anderson, 1993: Vegetation lake-levels, and climate in Western North America since 12,000 years. *Global Climates since the Last Glacial Maximum*. H.E.J. Wright, J.E. Kutzbach, T. Webb III, W.F. Ruddiman, F.A. Street-Perrott and P.J. Bartlein, Eds., University of Minnesota Press, 415-467.

Wetherald, R.T. and S. Manabe, 1999: Detectability of summer dryness caused by greenhouse warming. *Clim. Change*, **43**, 495-511.

Whitworth, T. and R.G. Petersen, 1985: Volume transport of the Antarctic Circumpolar Current from bottom pressure measurements. *J. Phys. Oeanogr*., **15**, 810-816.

Wiebe, E.C. and A.J. Weaver, 1999: On the sensitivity of global warming experiments to the parameterisation of sub-grid-scale ocean mixing. *Clim. Dyn*., **15**, 875-893.

Wigley, T.M.L., 1998: The Kyoto Protocol: CO_2, CH_4, and climate implications. *Geophys. Res. Lett*., **25**, 2285-2288.

Wigley, T.M.L. and S.C.B. Raper, 1987: Thermal expansion of sea water associated with global warming. *Nature*, **330**, 127-131.

Wigley, T.M.L. and B.D. Santer, 1990: Statistical comparison of spatial fields in model validation, perturbation and predictability experiments. *J. Geophys. Res.*, **95**, 851-865.

Wigley, T.M.L. and S.C.B. Raper, 1992: Implication for climate and sea level of revised IPCC emissions scenarios. *Nature*, **357**, 293-300.

Wijffels, S.E., R.W. Schmitt, H.L. Bryden and A. Stigebrandt, 1992: Transport of freshwater by the oceans. *J. Phys. Oceanogr.*, **22**, 155-162.

Wild, M., A. Ohmura and U. Cubasch, 1997: GCM-simulated surface energy fluxes in climate change experiments. *J. Climate*, **10**, 3093-3110.

Wild, M., A. Ohmura, H. Gilgen, E. Roeckner, M. Giorgetta and J.-J. Morcrette, 1998: The disposition of radiative energy in the global climate system: GCM-calculated versus observational estimates. *Clim. Dyn.*, **14**, 853-869.

Williamson, D.L., 1995: Skill scores from the AMIP Simulations. *Proc AMIP Scientific Conference* Monterey CA. World Climate Research Program, 253-258.

Williamson, D.L. 1999: Convergence of atmospheric simulations with increasing horizontal resolution and fixed forcing scales. *Tellus*, **51A**, 663-673.

Williamson, D.L. J.J. Hack and J.T. Kiehl, 1995: Climate sensitivity of the NCAR Community Climate Model (CCM2) to horizontal resolution. *Clim. Dyn*., **11**, 377-397.

Williamson, D.L., J.G. Olson and B.A. Boville, 1998: A comparison of semi-Lagrangian and Eulerian tropical climate simulations. *Mon. Wea. Rev*., **126**, 1001-1012.

Wood, R.A., A.B. Keen, J.F.B. Mitchell and J.M. Gregory, 1999: Changing spatial structure of the thermohaline circulation in response to atmospheric CO_2 forcing in a climate model. *Nature*, **399**, 572-575.

Wu, G.-X., X.-H. Zhang, H. Liu, Y.-Q. Yu, X.-Z. Jin, Y.-F. Guo, S.-F. Sun and W.-P. Li, 1997: Global ocean-atmosphere-land system model of LASG (GOALS/LASG) and its performance in simulation study. *Quart. J. of Appl. Meteor.*, **8**, Supplement, 15-28 (in Chinese).

Wunsch, C. and D. Roemmich, 1985: Is the North Atlantic in Sverdrup Balance? *J. Phys. Oceanogr*., **15**, 1876-1883.

Xie, P. and P.A. Arkin, 1996: Analyses of Global Monthly Precipitation Using Gauge Observations, Satellite Estimates, and Numerical Model Predictions. *J. Climate*, **9**, 840-858.

Yoshimura, J., M. Sugi and A. Noda, 1999: Influence of greenhouse warming on tropical cyclone frequency simulated by a high-resolution AGCM, Preprints of 10th Symposium on Global Change Studies, 10-15 January 1999, Dallas, USA, 555-558.

Yu, G. and S.P. Harrison, 1996: An evaluation of the simulated water balance of northern Eurasia at 6000 yr B.P. using lake status data. *Clim. Dyn.*, **12**, 723-735.

Yu, Y.-Q., Y.-F. Guo and X.-H. Zhang, 2000a: Interdecadal climate variability. In*: IAP Global Ocean-Atmosphere-Land System Model* [Zhang, X.-H. (ed)]. Science Press, Beijing, New York, pp 155-170.

Yu, R., W. Li, X. Zhang, Y. Liu, Y. Yu, H. Liu and T. Zhou, 2000b: Climatic features related to Eastern China summer rainfalls in the NCAR CCM3. *Advances in Atmospheric Sciences*, **17**, 503-518.

Yukimoto, S., 1999: The decadal variability of the Pacific with the MRI coupled models. In: Beyond El Niño: Decadal and Interdecadal Climate Variability [Navarra, A. (ed)]. Springer-Verlag, Berlin, pp 205-220.

Yukimoto, S., M. Endoh, Y. Kitamura, A. Kitoh, T. Motoi, A. Noda and T. Tokioka, 1996: Interannual and interdecadal variabilities in the Pacific in a MRI coupled GCM. *Clim. Dyn*., **12**, 667-683.

Yukimoto, S., M. Endoh, Y. Kitamura, A. Kitoh, T. Motoi and A. Noda, 2000: ENSO-like interdecadal variability in the Pacific Ocean as simulated in a coupled GCM. *J. Geophys. Res.*, **105**, 13945-13963.

Zhang, X.-H., G.-Y. Shi, H. Liu and Y.-Q. Yu (eds), 2000: IAP Global Atmosphere-Land System Model. Science Press, Beijing, China, 259 pp.

Zhang, Y. and W.-C. Wang, 1997: Model simulated northern winter cyclone and anti-cyclone activity under a greenhouse warming scenario. *J. Climate*, **10**, 1616-1634.

Zhang, Y., K.R. Sperber, J.S. Boyle, M. Dix, L. Ferranti, A. Kitoh, K.M. Lau, K. Miyakoda, D. Randall, L. Takacs and R. Wetherald, 1997: East Asian winter monsoon: results from eight AMIP models. *Clim. Dyn*., **13**, 797-820.

Zhao, Z.-C., X. Gao and Y. Luo, 2000: Investigations on short-term climate prediction by GCMs in China. *Acta Meteorologica Sinica -English Version*, **14**, 108-119.

Zhao, M., A.J. Pitman and T. Chase, 2001: The Impact of Land Cover Change on the Atmospheric Circulation. *Clim. Dyn.*, **17**, 467-477.

Zhou, G.Q., X. Li and Q.C. Zeng, 1998: A coupled ocean-atmosphere general circulation model for ENSO prediction and 1997/98 ENSO forecast. *Climatic and Environmental Research*, **3**, 349-357 (In Chinese with English abstract).

Zwiers, F.W. and V.V. Kharin, 1998: Changes in the extremes of the climate simulated by CCC GCM2 under CO_2 doubling. *J. Climate*, **11**, 2200-2222.